“O que não tem remédio, remediado está.”

Portuguese proverb

Acknowledgements

First and foremost, I would like to express my gratitude towards both my supervisors, who provided me the trust and freedom to accomplish this very dear project. I would like to thank Professor Christina Vogt for the constant kind words and much needed support, throughout the whole year. I also wish to thank Professor Jostein Halgunset for the patient and kind assistance, and without who this project would be have never become true.

I am also very grateful to Irina Eide, who collected the analysed samples and without whom this study would have not been possible.

Equally important was the contribution of my "partner-in-the-lab", Anne Hedvig Morgenstierne Sundet. I am very thankful for the crazy fun help and good spirits she provided.

This year would not have been the same without the Kavli gang. I wish to thank Maria Mørreaunet, Paulo Jorge Bettencourt Girão, Rabiya Anjem, Torgeir "Togo" Wåga, Vania Cuellar Terceros, and everyone else, with whom I shared good laughs and many many many coffee breaks.

If I survived this year, it is due to a very special person who believes in me more than I do. I am very grateful to have you in my life, Bjørn Erik Juel, and I hope you can be there for many years to come. I thank you for your patience, your friendship, your love, and for reminding me of what is important in life.

Finally, I am very thankful for the people who are truly responsible for me being here: my family. Even though we are many kilometres apart, you have given me the strength to keep going, never doubting my success for a second, and putting in me all your faith. I especially would like to thank my parents, Lita and Luís, for the never-ending love, for teaching me my most important lessons and for making me the hard-working woman I am today.

Abstract

Objective: The aim of this project was to clarify if there is an alteration in the expression profiles of five miRNAs (miR-1, miR-181a, miR-195, miR-210 and miR-584) in preeclamptic placentas *versus* normal placentas.

Experimental design: Formalin-fixed and paraffin-embedded placental samples from pregnancies complicated with preeclampsia (n=12) and from healthy pregnancies (n=10) were used in this study. The preeclampsia cases were all considered to be of early-onset (≤34 weeks of gestation) and five were considered to be severe. The assessment of relative miRNA quantities was performed by two-step quantitative reverse transcription polymerase chain reaction.

Results: Three of the analysed placental miRNAs were revealed to be significantly under-expressed in preeclampsia (miR-1, miR-210 and miR-584). miR-195 did not show any significant change and miR-181a was not successfully assessed. Notably, the significance probability obtained for miR-1 when removing the severe cases from the statistical analysis dropped radically (from p-value=0.036 to p-value=0.002), in spite of the reduction in sample size. The result obtained for miR-210 contrasts with most published studies, performed in severe preeclampsia cases; but it is in concordance with the one study that performed this analysis in mild cases. miR-584 remained very significantly under-expressed whether severe samples were included or excluded from the analysis.

Conclusion: The results lead us to conclude that miR-1, miR-210 and miR-584 are under-expressed in preeclamptic placentas. While some mechanisms appear to be common to preeclampsia as a whole (in this case, reflected by miR-584), some molecules seem to be specific for given subtypes of the syndrome (namely, miR-1 and miR-210). In addition, the widespread assumption that early preeclampsia is more severe is challenged by these results, which indicate different miRNA profiles within early cases of the syndrome. All in all, it seems that miRNA analysis can provide indication about the preeclamptic phenotype, and may provide further insight into the pathophysiology of preeclampsia and its distinct varieties.

Abbreviations

AGO – Argonaute proteins
ActRIIA – Activin receptor type-2A
ACYP2 – Acylphosphatase-2
ADAMTS1 – A disintegrin and metalloproteinase with thrombospondin motifs 1
ARCN1 - Archain 1
ARL13B – ADP-ribosylation factor-like protein 13B
CACNA2D4 – Voltage-dependent calcium channel subunit alpha-2/delta-4
CASK – Peripheral plasma membrane protein
CD163 – Scavenger receptor cysteine-rich type 1 protein M130
CORO1C – Coronin-1C
cDNA – Complementary DNA
ceRNAs – Competing endogenous RNAs
CS – Caesarean section
DNA – Deoxyribonucleic acid
EFNA3 – Ephrin-A3
eIF4F – Eukaryotic Initiation Factor-4F
ER – Endoplasmic reticulum
FFPE – Formalin-fixed paraffin-embedded
FGF2 – Fibroblast growth factor 2
GATA4 – GATA binding protein 4
GJA1 – Gap junction alpha-1 protein
GPD1L – Glycerol-3-phosphate dehydrogenase 1-like protein
HES – hematoxylin, eosin and saffron staining
HIF1A – Hypoxia-inducible factor 1-alpha
HIF3A – Hypoxia-inducible factor 3-alpha
HOXA9 – Homeobox protein Hox-A9
IFN – Interferon
IL – Interleukin
ISCU – Iron-sulfur cluster assembly enzyme
LfR – Intelectin 1/ intestinal lactoferrin receptor
MEF2A – Myocyte enhancer factor 2A
mRNA – Messenger RNA
miRNA – Micro RNA
MHC - Major histocompatibility complex
NF-kB –Tumour necrosis factor receptor superfamily member 11A
NTC – No template control
Nts – Nucleotides
PABPC –Poly(A)-binding protein
PAPPA – Pappalysin-1
PCR – Polymerase chain reaction
PE – Preeclampsia
PISD – Phosphatidylserine decarboxylase proenzyme

Poli(A) – Poliadenilation
PPAP2A – Lipid phosphate phosphohydrolase 1
Pre-miRNA – Precursor micro RNA
Pri-miRNA – Primary micro RNA
PRRX1 – Paired mesoderm homeobox protein 1
qRT-PCR – Quantitative reverse transcription polymerase chain reaction
RNA – Ribonucleic acid
RISC – RNA-induced silencing complexes
RT – Reverse transcriptase
RT-PCR – Reverse transcription polymerase chain reaction
STBM – Syncytiotrophoblast microparticles
***Taq* pol** – *Thermus aquaticus* polymerase
TGF – Transforming growth factor
THSD7A – Thrombospondin type-1 domain-containing protein 7A
UTR – Untranslated region
VEGFA – Vascular endothelial growth factor A

Contents

Introduction

1. The biomedical problem: preeclampsia

1.1. Epidemiology of preeclampsia

Preeclampsia is the most frequent pregnancy-associated disorder, affecting 8.5 million women around the world and being responsible for, at least, 12-18% of maternal and 40% of foetal deaths (1-3). These figures place preeclampsia as one of the top worldwide causes of maternal morbidity and mortality (2, 3).

Additionally, women who experience preeclamptic pregnancies have a higher risk of critical conditions later in life, such as hypertension, micro-albuminuria, ischemic heart disease, stroke and venous thromboembolism, indirectly amplifying the number of casualties associated to the pathology (2).

However, the onset and outcomes of preeclampsia vary greatly and depend on numerous factors. For instance, its frequency fluctuates with race, being greater in African Americans than in Caucasians (2). Furthermore, in developing countries, the mortality associated to preeclampsia is higher, aggravated by the absence of prenatal care and access to proper health facilities and equipment (2). In Norway, as of 2002, preeclampsia presented a prevalence of 4.44% (4).

Also, preeclampsia severity increases with identified risk factors that include: arterial disease, anti-phospholipid antibody syndrome, chronic hypertension, chronic renal disease, rheumatic disease, elevated body mass index, advanced maternal age, restricted sperm exposure, maternal genetic predisposition, multiple gestation, maternal infections, nulliparity, molar pregnancy, hyper-homocysteinemia, pre-existing thrombophilia, pre-gestational diabetes mellitus, previous history of preeclampsia and familial preeclampsia (5-9).

These data illustrate preeclampsia's severity and unpredictability, indicating its underlying epidemiological diversity and supporting the need for further research in this pathologic condition.

1.2. Clinical Information

Preeclampsia is characterized by *de novo* maternal hypertension and proteinuria after 20 weeks of gestation (6, 9). It is diagnosed when maternal blood pressure is ≥140/90 mm Hg on at least two occasions, six hours apart; and there is ≥300 mg/L of protein (≥1+ on a dipstick) in at least two urine samples, four or more hours apart, during a 24-hour period (6, 9, 10). Oedema, particularly in the face and hands, can also be frequently observed in these patients (6).

When no action is taken to manage the condition, preeclampsia may eventually lead to placental failure, with foetal respiratory and nutritional insufficiency, maternal organ dysfunction and, ultimately, death of the mother, of the foetus or both (5, 8, 11).

Preeclampsia is considered severe when, in bed rest, blood pressure exceeds 160/110 mmHg, in addition to proteinuria ≥5 g, in a 24 h specimen, and accessory complications such as maternal pulmonary oedema, liver failure, oliguria (<500 mL/day), thrombocytopenia (<10000 platelets/L), persistent epigastric/right upper-quadrant pain and/or central nervous system symptoms (such as headaches, blurred vision and/or blindness) (6, 9). This severe type of preeclampsia is associated with an early onset of the disease, usually with manifestations before 34 weeks of gestation, with higher severity and additional problematic outcomes (12, 13). Furthermore, it may lead to preeclampsia-related complications that include *abrupto placentae*, HELLP syndrome, aspiration pneumonia, acute renal failure, disseminated intravascular coagulation and stroke (2, 6). Severe preeclampsia may also evolve into eclampsia, characterized by seizures that may take place antepartum, intrapartum or postpartum, during which the patients lose consciousness and do not perform any respiratory effort (6). Preeclampsia may ultimately lead to foetal complications such as neurologic damage, cardiovascular disorders and growth restriction (9).

Some authors claim that preeclampsia comprises, at least, two different pathophysiologies (14). They hold the view that severe preeclampsia, with an early onset during gestation, is a separate entity from late preeclampsia, which develops closer to term. These claims are based on observable phenotypical differences between the different case groups, with early preeclampsia often correlating to uterine growth restriction, low birth weight, maternal gestational diabetes, higher levels of maternal serum liver enzyme, preeclampsia reoccurrences, and maternal high risk of developing hypertension and other cardiovascular diseases. In contrast, late-onset preeclampsia does not seem to be so serious, with mothers being less likely to develop gestational diabetes and thrombophilia, infants being born within normal or high birth weight percentiles, and the mortality risk being considerably lower (9, 14, 15). These different features have lead some authors to believe that separate etiologies and pathophysiological processes are involved in the development of the different forms of the syndrome (14).

Most attempts to prevent preeclampsia have shown little to no benefit, with calcium supplementation and low doses of acetylsalicylic acid being the most effective recommendations (9).

Once it arises, the only known cure for preeclampsia is delivery or pregnancy termination (8, 10). Therefore, a careful deliberation must be made, taking into account the risks of continuing the pregnancy, of delivering a premature baby or of abortion (6).

If prolongation of the pregnancy is decided after risk assessment, the management of the situation may include bed rest, antioxidant vitamins C and E supplementation, magnesium sulfate in combination with other anti-convulsants, anti-hypertensives, and control of fluid balance (5, 6, 11).

Generally, fast improvements are observed as a result of delivery of the placenta, including blood pressure decrease (6).

In general, the outcomes of preeclampsia are variable, highly depending on gestational age at diagnosis, severity of the syndrome, management techniques and presence of risk factors (9).

All these elements influence the clinical manifestations and outcomes of the disease, and reflect its high heterogeneity, which explains the limited prevention and pre-symptomatic diagnostic tools (9).

1.3. Biology of preeclampsia

The lack of preventive and therapeutic tools against preeclampsia reflects the lack of understanding of the disease, its origin, progression and underlying mechanisms.

Even though preeclampsia is thought to be caused by a multitude of factors, it seems consensual that the placenta plays a critical role in its pathophysiology (9, 16, 17). During gestation, this temporary organ is responsible for providing the foetus with oxygen, nutrients and hormones, also removing excretion products. These placental functions are critically based on the maternal blood flow (18). Therefore, it is reasonable to suspect that preeclampsia, a pregnancy-related hypertensive disorder, is connected to disturbed placental behaviour.

1.3.1. The Placenta: Genesis and structure

Indeed, preeclampsia symptoms seem to reflect poor placental development and function, with the main events that lead to its formation being of importance in the etiology of the disorder (19).

Seven days after fertilization, the cells of the blastocyst are organized in an outer and an inner cell mass (17, 20). The external cells, known as trophoblasts, form a thin outer layer that will, eventually, be responsible for the formation of the placenta (21).

Within a two-day period, the blastocyst arrives the uterine cavity, implantation occurs and trophoblasts differentiate into two different cell types: syncytiotrophoblasts and cytotrophoblasts (17, 20). While cytotrophoblasts are cuboid, mononucleated cells that envelop the whole blastocyst, syncytiotrophoblasts are invasive multinucleated cells that create a syncytial layer, aided by the protein syncytin.

As seen in Figure 1, cytotrophoblasts engulf the blastocyst in a thin layer, while syncytiotrophoblasts invade the uterine wall. By the ninth day after fertilization, the formation of lacunae, fluid-filled areas, by the syncytiotrophoblastic mass can be detected, as proliferation continues. By the eleventh day of gestation, syncytiotrophoblasts have reached uterine vessels, which will allow the uteroplacental circulation to start, with blood filling the lacunae that further develop into intervillous spaces (17, 18, 22).

On the molecular level, this invasion of the endometrium is only possible due to adhesion molecules that guarantee structure integrity (such as integrins and selectines), extracellular matrix proteases that promote weakened endometrial intercellular junctions (specifically, serine-proteases and matrix metalloproteinases) and cytokines that modulate the maternal immune response (namely glycodelin A) (23). This latter function is of major importance, for it contributes to maternal immunological tolerance to the embryo (23).

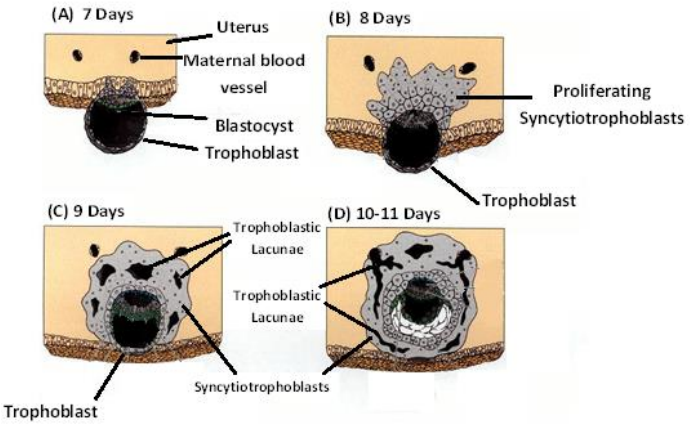

Figure 1 – Early implantation. Once the blastocyst reaches the uterus, implantation begins, with the trophoblasts differentiating in syncytiotrophoblasts and cytotrophoblasts (A). Soon, the cytotrophoblasts are disposed around the blastocyst in a thin layer, as the syncytiotrophoblasts start invading the endometrium (B). Their proliferation gives rise to occasional trophoblastic lacunae (C). As syncytiotrophoblasts reach maternal vessels, the uteroplacental circulation starts (D) [Adapted from Gilbert *et al*, 2000 (21)].

Subsequently, when the maternal spiral arteries are within reach, their invasion by syncytiotrophoblasts is initiated. These cells are incorporated into the vessel walls and replace their endothelial lining, ensuring they become dilated, flaccid, with low resistance and high capacity (5, 8, 9, 18, 24). This remodelling confers to the arteries a tolerance to the increased uterine blood flow that is driven exclusively by the maternal blood pressure, crucial for adequate placental blood perfusion (18). The formation of these foetal-maternal hybrid structures is only possible because trophoblasts do not express major histocompatibility antigens, these being suppressed during the first trimester of gestation (25).

The remodelling of the maternal spiral arteries is completed by the sixteenth week of gestation (20).

Consequently, maternal capillaries are formed to better connect the arteries and veins to the trophoblastic lacunae, assisted by products such as vascular endothelial growth factor, placental growth factor, angiopoietins and interferon-γ (9, 26). This phenomenon results in the transformation of the endometrium into the decidua (9, 21).

The decidua has mainly a nutritional function, with its cells containing high levels of glycogen. However, about forty percent of the early decidua cellular population is composed of leukocytes, mostly natural killers (NKs), but also macrophages, T-cells and B-cells. The NK population is responsible for producing cytokines, growth factors and angiogenic factors, being important for trophoblast proliferation and spiral artery remodelling. The macrophages are considered responsible for trophoblast apoptoptic clearance and subsequent control of their invasion (27, 28).

Additional transformations are required in the trophoblastic lacunae before placentation is complete. In these spaces, chorionic villi, columns of cytotrophoblasts lined by a syncytiotrophoblast layer and enclosing foetal vessels, are formed (20, 29). Eventually, these villi constitute villous trees, extending from the foetal to the maternal placental surface (see Figure 2) (30).

The villous surface is also covered by microvilli that further contribute to a larger exchange surface between mother and foetus (20). As term approaches, accumulated degenerated syncytiotrophoblast nuclei start protruding from the villous surface, constituting syncytial knots. (31).

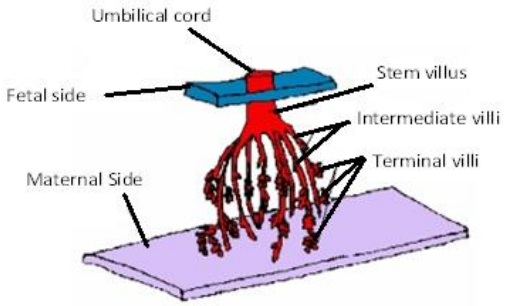

Figure 2 – Structure of a fully developed villous tree. Stem villi sprout from the foetal surface of the placenta, branching into intermediate villi, which further ramify and end in terminal villi [Adapted from Wang *et al*, 2010 (30)].

Upon complete formation of the placenta, by the seventieth day of gestation, maternal blood from the spiral arteries bathes the intervillous spaces, where it is in contact with the chorionic villi, promoting product exchange by diffusion, between the maternal blood and the foetal vessels (18, 20). The waste products are flushed away through maternal veins and the essential molecules are taken to the foetus through the umbilical cord, as displayed in Figure 3 (18).

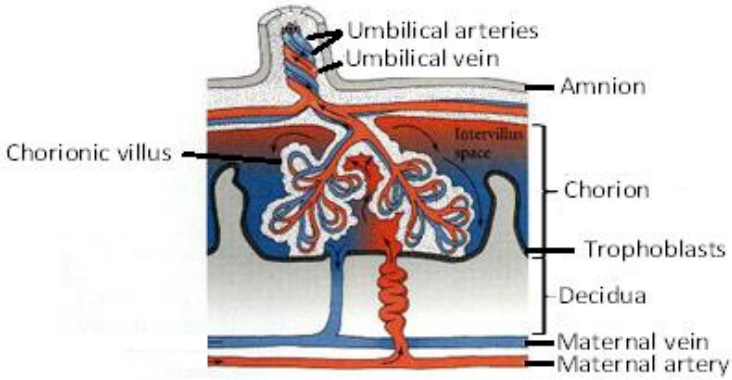

Figure 3 – Fully developed functioning placenta. The maternal oxygenated blood flows from the spiral arteries into the intervillous space through capillaries. It bathes the chorionic villi, where gas and nutrient exchange is performed by diffusion - the waste products are transferred to the maternal blood and the essential ones to the foetal vessels. The discarded products are flushed away with the blood, through capillaries that lead to maternal veins. On the other hand, the essential molecules are taken to the foetus through the umbilical arteries [Adapted from Gilbert *et al*, 2000 (21)].

As the pregnancy continues, the placenta keeps maturing, further developing terminal villi and increasing in capillaries to better respond to the increasing demands of the foetus (32).

1.3.2. The Placenta and Preeclampsia

The appearance of preeclamptic placentas is, generally, different from that of healthy placentas, further confirming the importance of this organ in preeclampsia.

Concerning their macroscopical characteristics, preeclamptic placentas are lighter and thinner than average, with frequent infarctions on the maternal surface (33).

Microscopically, their villi may be necrotic, with a hypoplasic appearance, reduced branching and augmented syncytial knots (24, 30, 33). Reduced syncytiotrophoblast microvilli formation is also found (24).

On a cellular level, preeclamptic trophoblasts generally display condensed chromatin, dilated endoplasmic reticulum (ER) and swollen mitochondria with ruptured membranes, indicating their dysfunction (24, 34). A high level of trophoblastic apoptosis is also characteristic of the preeclamptic placenta (12).

On an immunological level, increased quantities of a number of interleukines (such as IL-1β, IL-6, IL-8 and IL-16), growth factors (namely TGF-β1 and TGF-β3) and other substances (like TNF-α and IFN-γ) are detected in preeclamptic placentas. In contrast, the levels of other specific interleukines, IL-4 and IL-10, are reduced. An increase in $CD68^+$ leukocytes in the decidua and persistence of macrophages at the implantation site is also observed. Moreover, there is no maternal immune shift to a Th2 phenotype, unlike in healthy pregnancies (27).

Biochemically, preeclampsia has been associated with abnormal calcium metabolism, with increased levels of intracellular calcium and reduced calcium-dependent ATPase activity in erythrocytes, and hypocalciuria (35).

As seen previously, a successful pregnancy depends on proper trophoblast invasion and maternal spiral artery remodelling (36). The morphological and histological modifications observed in diseased placentas are signs that these events are deeply affected. These findings have been hypothesized to derive from abnormal differentiation of trophoblasts into cytotrophoblasts and syncytiotrophoblasts (8, 16, 37). As a result, the anomalous cells display reduced invasive properties into the endometrium and the spiral arteries (8, 29). They do not seem to be able to regulate adhesion molecules correctly, to express an endothelial phenotype upon maternal artery invasion, or to give the correct signals to decidual natural killer lymphocytes (8, 9).

All in all, the observations in diseased placentas are consistent with inhibited or superficial endometrium invasion, reduced spiral artery transformation and vascular remodelling, resulting in the placental hypoxia and insufficiency, which are characteristics of preeclampsia (5, 8, 16, 24).

1.3.3. Preeclampsia models

Based on epidemiological data, microscopic and molecular findings, models have been elaborated in an attempt to explain the chain of events that lead to preeclampsia.

The two-stage model of preeclampsia proposes that reduced trophoblast invasion of the endometrium is triggered by the interaction of maternal genetic, behavioural, constitutional, obstetrical and environmental factors with physiological pregnancy changes, constituting the first stage of the syndrome, that results in poor placentation (5, 7, 37).

This has been proposed to lead to the production of (a) placenta-derived debris, such as cytokines, anti-angiogenic factors, deported trophoblasts, syncytiotrophoblast microvesicles (STBM), keratin fragments, free foetal RNA and/or DNA; and (b) oxidative stress, with reactive oxygen species (ROS) generated by the reduced spiral artery perfusion, activating monocytes and neutrophils, further stimulating the release of the placental debris and leading to hypoxic conditions and, consequently, increased apoptotic activity (9, 24, 37).

The release of placental debris and oxidative stress products stimulate an exacerbated maternal systemic inflammatory response, along with systemic dysfunction, with hypoxic placenta and the already mentioned clinical manifestations of the pathology (5, 7).

This chain of cause-effect events known as the two-stage model of preeclampsia is illustrated in Schematic 1.

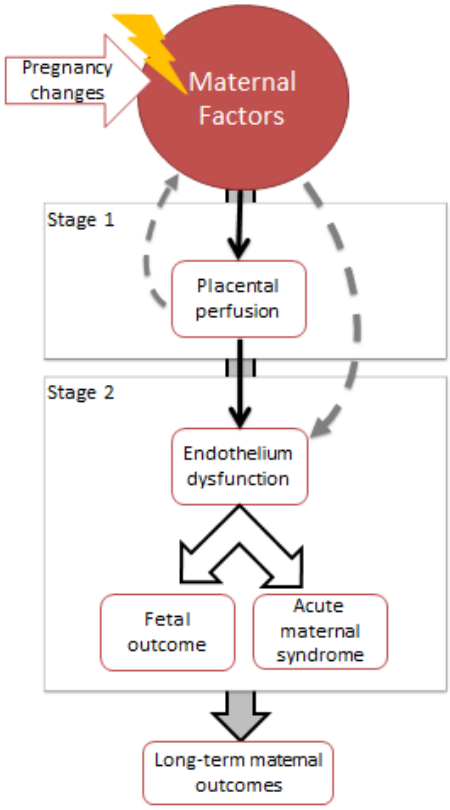

Schematic 1 - The two-stage preeclampsia model. It is proposed that, in the first stage of preeclampsia, the usual pregnancy modifications interact with inherent maternal factors, affecting placental perfusion and the maternal/foetal endothelium. This disturbance leads to the second stage of the disease, affecting both mother and foetus. The maternal factors are also key for long-term maternal outcomes [Based on Roberts *et al*, 2009 (37)].

Unfortunately, the model does not accommodate all clinical observations, with maternal factors possibly playing a role earlier than the model proposes (37). Thus, poor placentation may not constitute the fundamental cause of preeclampsia, but rather a predisposing and pivotal factor (9).

Other proposed hypotheses to explain preeclampsia have been constructed on an immunological basis.

Pregnancy is a state of heightened systemic inflammation, with preeclamptic cases displaying further aggravated reactions (9). It has been suggested that preeclampsia starts with the activation of immunologic cells, modifying the secreted cytokine profiles. This may involve invasive trophoblasts aberrantly expressing the MHC class I molecule HLA-G and its isoforms, making them a target for immune cells. This imbalance of signalling molecules, most notably interferon-γ, is thought to influence the phenotype of the trophoblasts: they become less invasive, leading to poor placentation and placental hypoxia. These events eventually result in the release of inflammatory factors that damage the maternal endothelium and lead to the clinical manifestations of preeclampsia (as depicted in Schematic 2) (27).

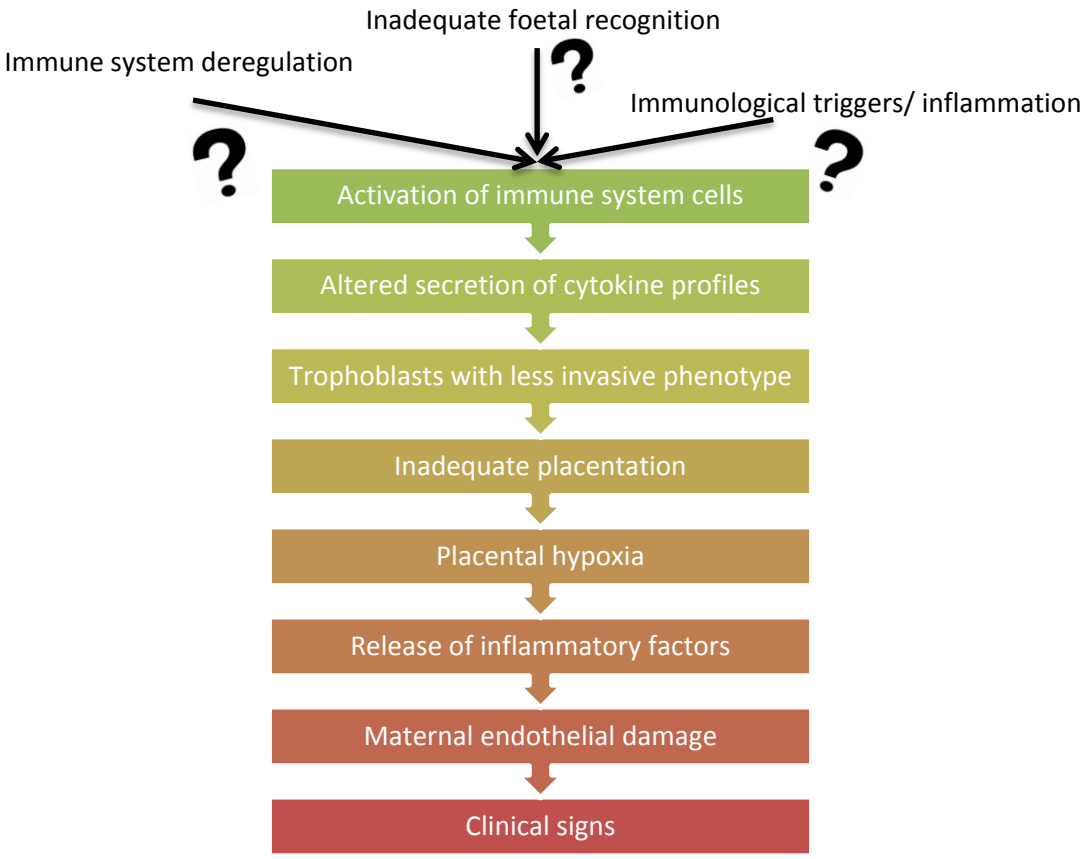

Schematic 2 – A proposed immunological model. It is hypothesized that the immune system is activated, resulting in altered cytokine profiles that confer the trophoblasts a less invasive phenotype. This cascade of events continues, with inadequate placentation leading to hypoxia and further inflammation. As a result, the maternal endothelium is damaged and the clinical manifestations of the disease arise [Based on Laresgoiti-Servitje *et al*, 2010 (27)].

In general, all the proposed theories revolve around four aspects that may or may not interact with each other to contribute to the described clinical symptoms: abnormal trophoblast invasion, angiogenic factors, oxygen deregulation and altered immune response (27, 38).

With the variety of concepts that have been involved in explaining the etiology of the disease, it would seem that preeclampsia is a highly heterogenous entity, from its origin to its outcomes (39). However, the confusing picture also reflects directly our profound lack of knowledge about the mechanisms of the disease, making further research imperative (40).

2. Micro RNAs

Micro ribonucleic acids (miRNAs) are small, single-stranded and non-coding RNA molecules responsible for regulating post-transcriptional gene expression (41-43). Found in a diversity of organisms including plants, algae, viruses and animals, these molecules are widespread in nature and evolutionarily old, controlling processes like proliferation, differentiation, apoptosis and metabolism (44-46).

At least a thousand miRNAs are present in humans, with over half of the transcriptome being regulated by their action (43, 47). Even though there is a limited number of miRNAs compared to the number of possible messenger RNAs (mRNAs) and proteins, one of these small molecules can regulate different targets, and various miRNAs can regulate the same target, meaning that these regulatory pathways are highly complex (44, 47).

Similarly, the mechanisms through which miRNAs control cellular processes are intricate, with their action ranging from gene silencing through translation repression and induced instability to activation of gene expression (48-51). Quite expectedly, miRNA levels are not constant throughout time and are variable across tissue types. Altered expression of these molecules can, therefore, be involved in deregulation of cellular processes and development of pathologic conditions, possibly playing crucial roles in various disease states (41-43, 45).

2.1. Biogenesis

The miRNA genes are organized as independent transcription units, located in either introns or exons of protein-coding gene sequences (48, 52). Auto-regulated by either negative or positive feedback loops, these genes are transcribed by RNA polymerase II, giving rise to long RNA molecules known as primary miRNAs (pri-miRNAs) (44, 47, 48).

Afterwards, still in the nucleus, the extremities of these pri-miRNAs are trimmed by an RNase III, the Drosha protein. This process results in precursor miRNAs (pre-miRNAs), characterized by their imperfectly folded double stranded RNA hairpin structure (42-44, 48).

These molecules are then exported by exportin5 (XPO5) to the cytoplasm, where another enzyme from the RNase III family, Dicer, removes pre-miRNAs' loop region (43, 44). The molecules are cleaved into a duplex miRNA moiety of twenty to twenty-four nucleotides, with protruding 3' ends (42, 44, 49).

Traditionally, the strand with the least stable 5' end (formerly known as miRNA*) has been reported to be degraded, while the remaining strand functions as the mature miRNA (43, 44, 49). However, recently, both strands have been shown to be functional, even if one is dominant over the other, leading to a change of nomenclature to "miRNA-5p" and "miRNA-3p", according to the arm of the hairpin precursor from which they are excised (53).

This long course of maturation is highly dependent on the processing by the involved enzymes, with a slight change in their activity leading a certain pre-miRNA to give rise to a different miRNA (47).

The miRNA biogenesis process, from gene transcription to mature miRNA establishment, is illustrated in Figure 4.

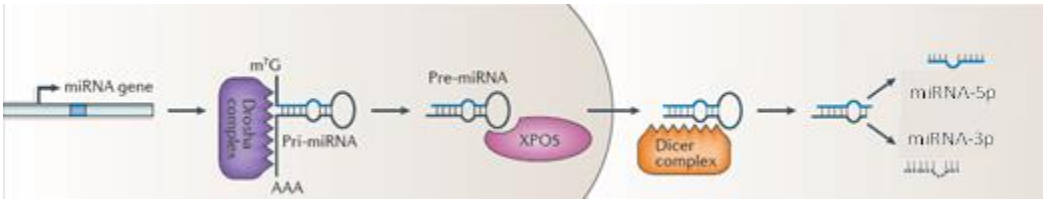

Figure 4 – Biogenesis of miRNAs. After transcription, pri-miRNAs is processed by Drosha into pre-miRNA. The protein XPO5 is responsible for transporting this intermediary into the cytoplasm. Here, Dicer removes the pre-miRNA loop, giving rise to miRNA-5p and miRNA-3p [Adapted from Pasquinelli *et al*, 2012 (49)].

An alternative pathway for miRNA synthesis has been identified in a diversity of organisms, including mammals. In this so-called miRtron pathway, RNA molecules with intronic origin are processed into pre-miRNAs with the help of the splicing machinery, not Drosha (54).

Taking into account all the stages involved in miRNA biogenesis, from transcription to processing and final product formation, the complexity of the miRNA genesis is evident and foresees the intricacy of their mechanisms of action.

2.2. Regulation of other molecules

In the cytoplasm, mature miRNAs mainly induce translational repression or deadenylation and degradation of target mRNAs (48).

However, miRNAs do not act on their own and, in order to perform their function, they are incorporated in RNA-induced silencing complexes (RISCs), giving rise to miRISCs. These large complexes are composed of several proteins, with different functional properties (such as assembly and regulation), the most noteworthy being the Argonaute proteins (AGO), vital for the gene silencing process (42, 43, 46, 49).

Mammals possess four proteins of this family, AGO1-4, but the most prominent for silencing, AGO2, is the only one with RNase function, having the ability to cleave mRNAs at the centre of miRNA-mRNA duplexes (43).

Once miRISC is assembled, miRNAs pair with highly repeated sequences in the target mRNAs' 3' untranslated (UTR) region (43). Nucleotides 2 to 8 of the miRNA compose the seed region that nucleates miRNA-mRNA association; the level of complementarity in this region is decisive to the outcome of the interaction and it is dependable on the organism and the conditions the cell is under (43, 46, 49, 50).

Predominantly in plants, if this complementarity is nearly complete, cleavage is promoted by AGO2 (in the miRISC), in the middle of the pairing sequence (43, 46, 49, 50). In animals, it is more common for miRNAs to destabilize the target mRNAs, as indicated by reduced protein levels and constant mRNA levels. When miRISC binds to the 3'UTR target region, deadenylation factors are recruited to remove the mRNAs' poly(A) tail. Usually, this results in rapid 5' decapping and in an enhanced mRNA susceptibility to exonucleolytic degradation. Though, there have also been reports of storage of deadenylated mRNAs in translationally repressed states (50).

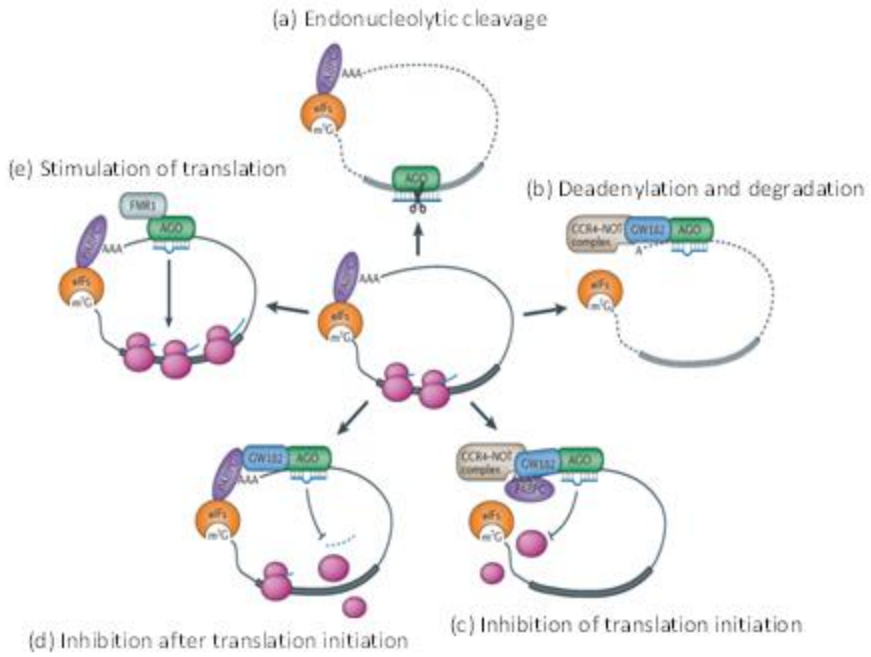

Figure 5 – Different ways of action of miRISC. Endonucleolytic cleavage is triggered mainly in plants (a), while deadenylation and consequent degradation is typical of animal cells (b). Inhibition of translation can occur upon its initiation (c). Even though there have been reports of inhibition during translation elongation, these results are not consistent across studies (50) (d). Translation may also be stimulated by miRNAs (e) [Adapted from Pasquinelli *et al*, 2012 (49)].

Furthermore, there is growing evidence that animal miRNAs may interfere with translational initiation proteins (the eIF4F complex) and the poly(A)-binding protein (PABP), destabilizing, blocking initiation, promoting decapping or proteolysis of the nascent peptide (49, 50, 55).

However, it has also been shown that miRNAs can have a positive regulation on mRNA translation, enhancing it, when the interaction occurs with the 5'UTR region (55).

This unexpected function of miRNAs proves that these molecules may have other functions that are not yet known (43).

The mentioned ways of action of the miRISC complex are summarized in Figure 5.

Even though miRNAs have the capacity to regulate different molecules, they are also regulated themselves, in a variety of ways: their targets can protect miRNA stability or promote their degradation; miRNAs can auto-regulate, when regulating the proteins they interact with; and any molecule complementary to miRNA sequences can sequester and regulate them, being known as competing endogenous RNAs (ceRNAs). All in all, these complex interactions and their implications play an important role in understanding miRNAs' roles and functions (49).

The identification of the targets for each miRNA may also provide valuable information, uncovering how cell processes are regulated (52).

miRNAs are thought to play a part controlling important bioprocesses such as development, differentiation, apoptosis and proliferation, and alterations in their genes or numbers may, therefore, play a part in pathogenesis. In diseased states, miRNA expression and role may be affected by chromosomal abnormalities, mutations, polymorphisms and epigenetic changes (methylations, acetylations, etc) that affect their sequences, biosynthesis or transcription (49, 54). Indeed, abnormal miRNA expression patterns are commonly detected in pathological phenotypes, being involved in cellular deregulation, with the altered function of a single miRNA leading to widespread modifications in the transcriptome and proteome (56).

2.3. Role in Preeclampsia

Given the importance of miRNAs as regulatory molecules, their involvement with preeclampsia pathophysiology is to be anticipated.

In fact, the connection between miRNA expression levels and preeclampsia was documented for the first time in 2007, establishing a new approach in preeclampsia research (57). Ever since, publications have shown a different expression of certain miRNAs in preeclamptic placentas compared to their healthy counterparts.

In general, these studies are based on miRNA isolation from placental chorionic villi that are subjected to three main techniques: quantitative reverse transcription polymerase chain reaction, microarrays and/or sequencing (57-59). Others have taken a different approach, studying the content of circulating miRNAs in maternal blood and how they relate to the diseased state, constituting the promise of a less invasive future option for research and clinical purposes (1).

Furthermore, in some studies, the detected anomalous miRNA profiles were subjected to target prediction analysis in order to uncover the biological meaning of these altered values. For instance, miR-182* was related to faulty angiogenesis by Pineles *et* al, 2007; miR-16 has been related to functions such as cell proliferation and development, as well as immune response, by Hu *et al*, 2009; miR-155 was reported as important for proliferation, migration, differentiation and adhesion, by Zhang *et al*, 2010 (57, 60, 61).

Nevertheless, studies relating miRNAs and preeclampsia have shown inconsistent results: some report the presence of different sets of miRNA; others indicate over-expression of a given miRNA contrarily to some that report its under-expression. The table presented in Appendix A illustrates these divergences among published studies, compiling all the different miRNAs that, in the various studies, have been related to preeclampsia, as of May 2013. The uncertainty of the findings emphasises the need for further research on the topic.

3. Technical Possibilities

Quantitative reverse transcription polymerase chain reaction (qRT-PCR) is one of the techniques that allow analysis of miRNA expression (62).

The polymerase chain reaction (PCR) involves the exponential amplification of a specific nucleic acid sequence (63, 64). The enzyme responsible for this process, the polymerase, mandatorily thermostable (e.g. *Thermus aquaticus* polymerase, *Taq* pol), recognizes the template sequence and, matching complementary nucleotides, builds the new strand (63). Furthermore, to start this polymerization process, the enzyme demands primer molecules, complementary to each end of the fragment to amplify, with exposed 3'-OH groups (63, 65). The rest of the reaction mix consists of template and nucleotides, along with other chemical agents (65).

The PCR process is organized in thermic cycles, as seen in Figure 6, in order for the amplifications to succeed (63).

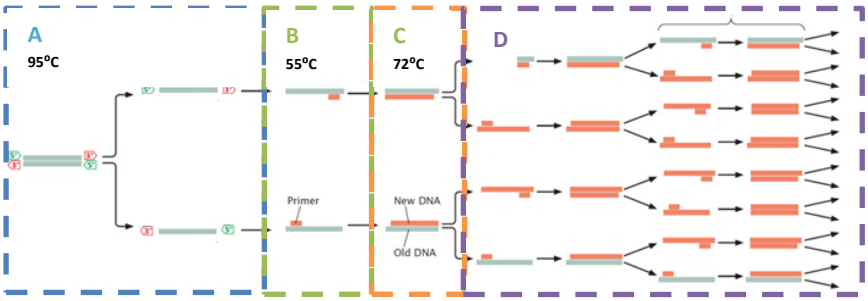

Figure 6 – PCR process. First, high temperatures denature the double stranded DNA template (A). Next, the primers anneal with complementary sequences in the template, as temperature drops (B). The polymerase synthetises new strands as its optimal functioning temperature is reached (C). These cycles are repeated, typically, between thirty and forty times (D) [Adapted from W.H. Freeman and Company, 2005 (65)].

Initially, the reaction mix undergoes a temperature rise to denature, unwind and separate the template molecules into single-stranded chains. Afterwards, the primers anneal with the template molecules, as temperature decreases (T_a, annealing temperature). Subsequently, the polymerase can proceed and synthesize the new products. This cycle is repeated numerous times, producing millions of copies of the original molecule (63).

qRT-PCR is based on the reverse transcription process, followed by an automated quantitative real-time PCR (qPCR), in order to detect RNA molecules.

In a first step, the miRNAs are subjected to the action of a reverse transcriptase (RT). This RNA-dependent DNA-polymerase utilizes the RNA molecules as a template, synthesizing its complementary DNA (cDNA), given specific primers (66). When the target sequences for reverse transcription are relatively short, the use of stem-loop RT primers is advised. These oligonucleotides are complementary to part of the 3' sequence of the RNA target, and insert an adaptor to the newly synthesised cDNA, which will be essential for the hybridization of the reverse primer, during the next step (67).

In the second stage of this technique, a qPCR takes place for automatic detection of the amplification (64). There are several methods qPCR may be based on; one of them relies on a polymerase that also has a 5' nuclease activity and on the use of probes with a fluorescent reporter dye on the 5' end and a quencher dye on the 3' inextensible end (64, 68). When in close proximity, the quencher prevents the emission of the fluorophore light by fluorescence resonance energy transfer (FRET) (64, 68). The probe hybridizes with the complementary template fragment and, during extension, the polymerase cleaves it, separating the two dyes and leading to fluorescent emission (see Figure 7) (64). The radiated light is automatically detected in real time by the thermocycler and this signal increases as amplifications occur and more probes are cleaved (64, 68). The thermocycler then detects the crossing point (Cp) for each sample, the cycle number at which the emitted fluorescence is considered to be significantly above the baseline. This Cp value can be correlated with the quantities of cDNA in each sample, with less cDNA requiring more cycles in order to reach maximum fluorescence, compared to higher amounts of template, which require less thermal cycles (69).

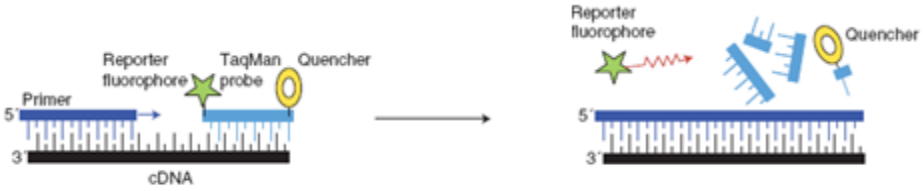

Figure 7 – **Principle of probe-based qPCR.** The probe is constituted by a reporter fluorescent dye on its 5' end and a quencher on its 3' end. Upon annealing, the probes hybridize with the template cDNA. In the extension phase, the polymerase encounters the probe, cleaves it and the fluorophore is free to emit fluorescence. If the fragment is not to be amplified, the probe remains intact and no fluorescent light is radiated [Adapted from Arya *et al*, 2005 (64)].

Another qPCR method makes use of a dsDNA-intercalating agent known as SYBR Green I. This dye emits strong fluorescence when bound to dsDNA, but not when free in solution. Consequently, synthesis of new DNA strands is translated into an increased emitted fluorescence.

Afterwards, the qPCR products can be subjected to a temperature rise, resulting in the denaturation of the previously produced double-chains, and decrease in the emitted fluorescence. This process allows the melting profiles of the PCR products to be obtained, which are especially useful for detection of products with different lengths and/or compositions that display distinct profiles (62, 70). An example of these cases is depicted in Figure 8.

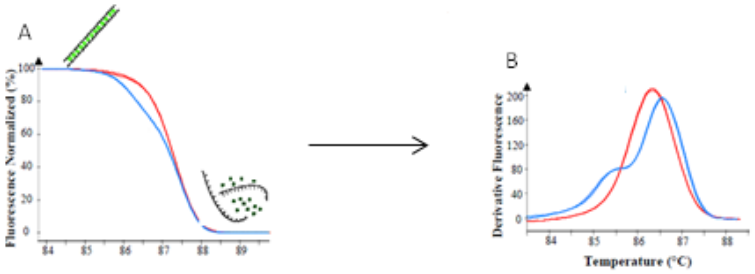

Figure 8 – Example of typical amplification and consequent melting peaks obtained when using SYBR Green I. (A) displays the curves obtained when a melting programme is run; slight differences can be seen between the blue and the red sample. When the change in fluorescence divided by the change in temperature (-ΔF/ΔT) is plotted against the temperature, the melting peaks are obtained (B). These provide a visual aid to detect different amplification products. The smaller amplicons are melted at lower temperatures and the larger amplicons denature at higher temperatures; the sample in blue shows a "shoulder" on its melting peak, denoting the amplification of more than one PCR product (70) [Adapted from Meistertzheim *et al*, 2012 (71)].

qRT-PCR is typically very reproducible, when performed in small, highly stable miRNAs extracted from formalin-fixed, paraffin-embed (FFPE) tissue blocks (62, 64). It makes this technique an effective method to detect these molecules, benefiting from the vast and standardized clinical pathology archives existent all around the world (62).

4. Objectives

Given the severe impact of preeclampsia on mother and child health around the world and our lack of understanding of the underlying mechanisms, the possibility of miRNAs holding clues to its pathogenesis makes further research on this topic a matter of utmost importance.

However, due to the novelty of this approach and the discrepant reports, confirmation or rebuttal of published results is required, in order for new knowledge to be generated, built upon sound data.

Thus, the goal of this thesis is to clarify whether some of those miRNAs which have been claimed to be linked to preeclampsia, really do show an expression pattern which differs between preeclamptic and healthy placentas.

The results of this study will have an impact on the understanding of preeclampsia, possibly uncovering molecules which may be connected to its development, hopefully holding clues to a better management of the condition.

Materials and Methods

A series of diverse methodologies were undertaken in order to fulfil the goal of this project. These procedures were carried out as illustrated in the workflow below.

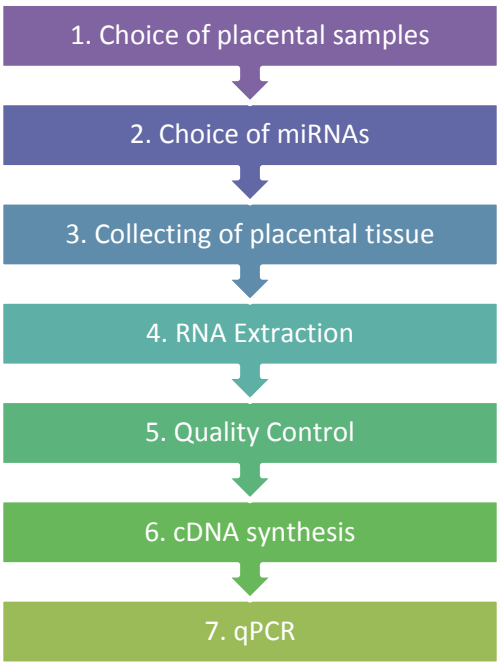

Schematic 3 – Procedures used in this project. Firstly, the placental samples were chosen; followed by choice of miRNAs interesting to analyse. The placental tissue was then collected and total RNA extracted. Following a quality control step, cDNA was synthesized and the quantitative PCR took place.

1. Study population and placental samples

All used placental material was collected at St. Olavs University Hospital (Trondheim, Norway), between 2002 and 2006 (72). The material from this biobank has been approved for research by the Regional Committee for Medical Research Ethics (REK number 2012/1040).

The placentas used in this study originated from women who underwent caesarean section (CS), having had no labour activity. Patients with a history of cardiovascular disease, diabetes and/or perinatal infections were excluded.

The study population was divided into two groups: controls and preeclampsia cases.

Preeclampsia was identified as persistent hypertension (≥140/90 mm Hg, ≥2 measurements, ≥6 hours apart) and sustained proteinuria (≥300 mg/L or ≥1+ on dipstick, ≥2 measurements, ≥4 hours apart), after 20 weeks of gestation. Severe preeclampsia was defined as severe hypertension (≥160/110 mm Hg) and/or severe proteinuria (≥5 g in a 24 h specimen).

Healthy patients, who did not present hypertension or proteinuria during the course of the pregnancy, underwent CS for reasons considered irrelevant to the aim of the study (e.g. breech presentation and previous CS) and delivered healthy foetuses above 2500g, served as controls.

A total of forty-two samples (twenty-one healthy and twenty-one diseased) was chosen for total RNA extraction, according to these criteria. Table 1 displays the demographic characteristics of the study population.

Table 1 – Study population characteristics. None of the participants smoked; all were of Scandinavian nationality. Gestational age at delivery, birth weight and placental weight are different, between the control and preeclampsia group, with the healthy group showing higher figures in all these parameters.

Demographic	Control Samples (n=21)	Preeclampsia Samples (n=21)
Maternal Age (y) (median)	30 (22-37)	28 (20-40)
Nulliparity (n)	6 (28.57%)	14 (66.67%)
Smoking (n)	0 (0%)	0 (0%)
Weight in beginning of pregnancy (kg) (median)	71 (51-104)	70 (54-116)
Body mass index in beginning of pregnancy (kg/m^2) (median)	24,91 (18.47-40.63)	24,42 (19.75-40.14)*
Scandinavian nationality (n)	21 (100%)	21 (100%)
Gestational age at delivery (d) (median)	271 (259-293)	221 (186-255)
Birth weight (g) (median)	3610 (2720-4490)	1393 (680-2610)
Placental weight (g) (median)	600 (450-1050)	280 (145-550)

*Two missing values.

2. miRNA choice

After searching the scientific search engine "PubMed" for the keywords "preeclampsia" and "miRNA", several papers were analysed in order to check which miRNAs had been correlated to preeclampsia, as of October 2012. The resulting table of this extensive search can be found in Appendix A (last updated May 2013).

Among the studies performed on chorionic villi, it was observed that the relative expression of certain miRNAs was divergently classified by some authors. Furthermore, other research groups agreed on the expression levels of some miRNAs and disagreed on others.

Therefore, a group of specific molecules, including questionable and less disputable miRNAs, were selected: miR-1, miR-181a, miR-195, miR-210 and miR-584, as seen in Table 2.

Table 2 – miRNAs in preeclampsia, according to three different studies (58, 73, 74). (-) signifies the miRNA is under-expressed in PE, compared to healthy cases; when the miRNA was considered over-expressed in the diseased cases, the symbol (+) is used.
The study by Enquobahrie *et al*, 2010 indicates an under-expression of miR-1 and miR-584, and an over-expression of miR-210. Noack *et al*, 2011 reported an over-expression of miR-181a, miR-195 and miR-210. Zhu *et al*, 2009 shows an over-expression of miR-181a and miR-584, and an under-expression of miR-1 and miR-195. This study also reported an over-expression of miR-210 in severe cases of preeclampsia and its under-expression in the mild cases. This signifies most authors agreed on the over-expression of miR-210; Zhu *et al*, 2009 and Enquobahrie *et al*, 2010 believe miR-1 is under-expressed; Zhu *et al*, 2009 and Noack *et al*, 2011 agree on the over-expression of miR-181a. The reports concerning the expression of the remaining miRNAs (miR-195 and miR-584) yielded diverging results.

miRNA	Enquobahrie *et al*, 2010 (58)	Noack *et al*, 2011 (73)	Zhu *et al*, 2009 (74)
miR-1	-		- (severe PE)
miR-181a		+	+ (severe PE)
miR-195		+	- (severe PE)
miR-210	+	+	+ (severe PE) - (mild PE)
miR-584	-		+ (severe PE)

3. Placental sample collection

After performance of the caesarean section, the placentas were allowed to detach spontaneously from the uterine wall. They were fixed in buffered formalin and sent for histological examination at the Department of Pathology and Medical Genetics, St. Olavs University Hospital. Routine placental slices were paraffin-embedded, cut in 4 µm sections, stained with hematoxylin, eosin and saffron (HES) and examined by a pathologist, according to the standard routines established at the hospital (72).

Areas rich in villi were marked on the HES sections from the central parts of the placenta, and the corresponding areas in the paraffin blocks were sampled as cylinders (1.2 x 90 mm). Three cylinders were extracted per block. This described workflow is illustrated in Schematic 4, below.

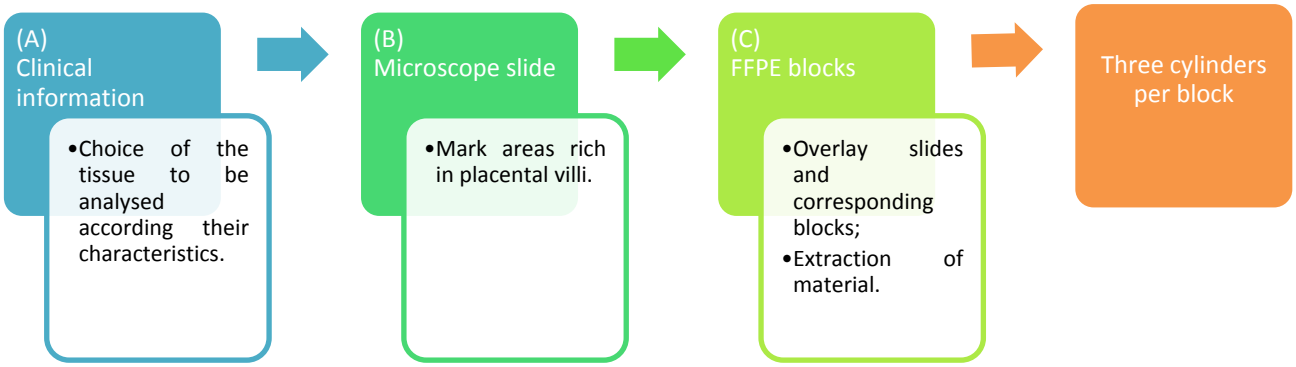

Schematic 4 - Sampling areas of interest from placental tissue. According to the clinical information available, the material with the needed characteristics to make it eligible to be analysed was chosen (A). Microscopic slides from each selected placental section were analysed and the areas more abundant in villi were marked (B). These particular areas were identified in the corresponding FFPE blocks, from which cylinders were later extracted (C).

4. RNA extraction

Subsequently, total RNA was extracted from the tissue cylinders with an optimized RecoverAll™ Total Nucleic Acid Isolation Kit protocol, which can be found in Appendix B (75).

This process consists of four main steps, as shown in Schematic 5. Firstly, the sample cylinders are deparaffinised with xylene and high temperature. Following a wash to remove any remaining organic solvent, the samples are subjected to protease digestion to hydrolyse proteins, including those nucleic acid-bound. Next, the nucleic acids are isolated on a glass fibre filter, with tissue and cellular residues being washed away. Finally, a DNase treatment ensures only RNA remains, which is subsequently eluted from the filter (76).

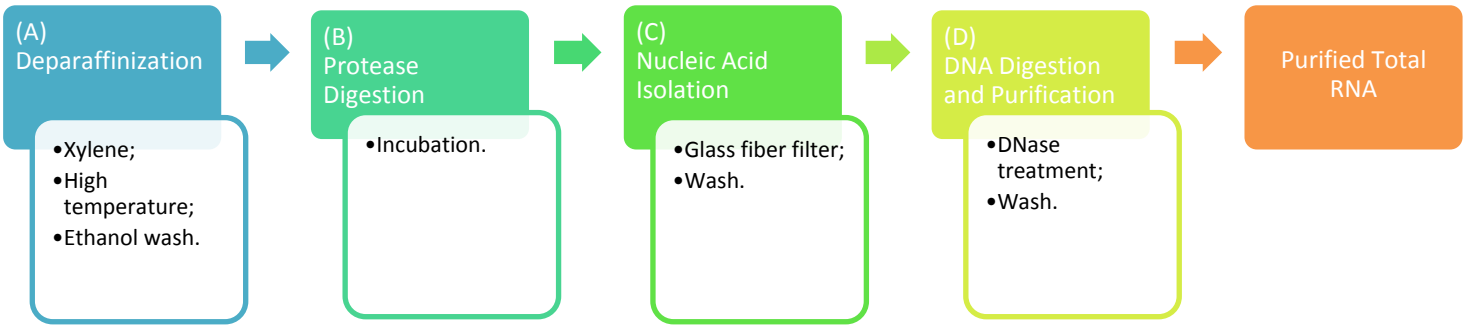

Schematic 5 – RNA extraction process. Firstly, the paraffin is removed from the tissue cylinders, by xylene incubation at high temperature; this organic solvent is then washed away with ethanol (A). Next, the proteins in the sample are degraded in the incubation with protease (B). The nucleic acids are then withheld in a filter, while other cellular components are washed away (C). Finally, the DNA is digested and the total RNA is eluted and isolated (D).

Aliquots of total RNA (10 µL) were prepared, in order to undergo the quality control processes, avoiding excessive freezing and thawing of the samples to be analysed.

5. Quality Control

After its extraction, the obtained RNA underwent two stages of quality control.

First, the Thermo Scientific NanoDrop 1000 Spectrophotometer was used. This spectrophotometer measures the UV absorbance of 1 µL of sample, at different wavelengths (77). After performing the readings, the instrument automatically calculates the sample concentration, and corresponding A_{260}/A_{230} and A_{260}/A_{280} ratios. Each sample was read a minimum of three times.

A supplementary analysis was performed with the Agilent 2100 Bioanalyzer, with two different kits: RNA 6000 Pico and RNA 6000 Nano. This platform provides the possibility to perform an electrophoretic assessment of a maximum of eleven (with the Pico Kit) or twelve samples (using the Nano kit) simultaneously, in a chip format.

It allows sizing, quantification and quality control of total RNA, with a concentration between $5x10^{-2}$ and 5 ng/µl (with the Pico kit) and 5 and 500 ng/µl (with the Nano kit), providing gel images, electropherograms, and an RNA integrity number (RIN) for each sample (78). According to the NanoDrop measurements, the concentrations of the samples exceeded the values indicated above, to carry out the Pico kit assay (78). Therefore, they were diluted, according to the calculations exhibited in Appendix C.

Subsequently to the described quality control steps, ten samples from the healthy group and twelve from the diseased group were chosen, from the forty-two originally selected samples, according to satisfactory purity values. They were identified with the prefix C, for controls (C1-C10), and P, for preeclampsia (P1-P12). Table 3 shows the demographics of these samples, which were later subjected to analysis by qRT-PCR. In Appendix D, more detailed clinical information about each sample can be found.

Table 3 - Demographics of the analysed samples. None of the women smoked and all were of Scandinavian nationality. 70% of the women in the control group were nulliparous, in contrast with 33% in the diseased group. The overall values of gestational age at delivery, birth weight and placental weight were higher in the controls than in the preeclampsia samples.

Demographic	Control Samples (n=10)	Preeclampsia Samples (n=12)
Maternal Age (y) (median)	28.5 (22-37)	28 (20-39)
Nulliparity (n)	3 (30%)	8 (75%)
Smoking (n)	0 (0%)	0 (0%)
Weight in beginning of pregnancy (kg) (median)	71,5 (53-89)	77 (54-96)
Body mass index in beginning of pregnancy (kg/m^2) (median)	24.74 (18.47-34.77)	25.00 (19.75-35.69)
Scandinavian nationality (n)	10 (100%)	12 (100%)
Gestational age at delivery (d) (median)	285 (273-285)	216 (186-251)
Birth weight (g) (median)	3560 (2800-4490)	1340 (685-2610)
Placental weight (g) (median)	600 (500-820)	308 (170-550)

*Two missing values.

In all the twelve analysed preeclampsia cases, the derangement occurred before 34 weeks of gestation, and five cases were considered severe.

6. Reverse Transcription

The reverse transcription reaction was performed with the SuperScript™ III First-Strand Synthesis Supermix for qRT-PCR, using RT primers specific for miR-1, miR-181a, miR-195, miR-210 and miR-584.

The RT primers were designed, synthesized and purchased from TIBMOLBIOL, and their sequence can be found in Appendix E, along with the sequences of the qPCR primers and respective probes. These primers were made to hybridize with fragments adjacent to the miRNA sequences.

The reverse-transcription process involves a mix of RT polymerase from Moloney murine leukemia virus, RNase inhibitor, dNTPs, RNA template, specific primers and random hexamers. This mix is subjected to different temperature changes to ensure the activation, action and inactivation of the polymerase. Afterwards, incubation with *E. coli* RNase H is used to degrade residual RNA, so only the desired cDNA remains (79). Schematic 6 represents the workflow used in this cDNA synthesis.

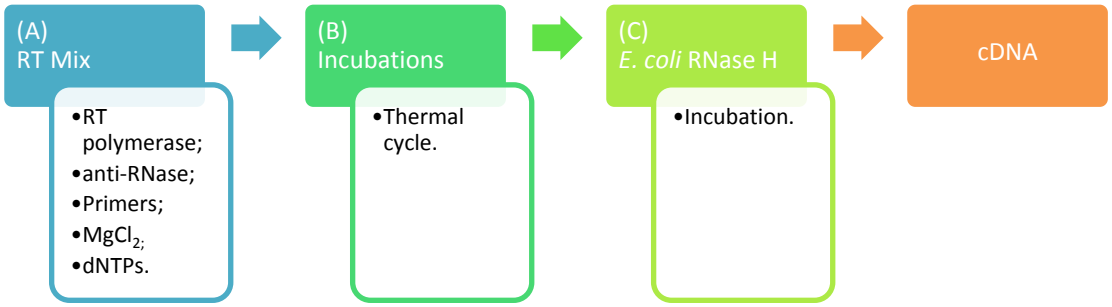

Schematic 6 – cDNA synthesis process. The RNA is mixed with the polymerase, primers, nucleotides and other components that assure the stability and success of the reaction (A). This is followed by an incubation that ensures the synthesis of the cDNA (B). Subsequently, the RNA template is degraded by RNAse H, only the newly synthesized cDNA remaining (C).

Since the goal of this project was to perform a comparative analysis between samples, the baseline RNA concentration should be equal for all samples in order for the experiments to be comparable. This prerequisite was met at the reverse transcription stage, with all samples being diluted to match the concentration of the sample with the lowest RNA yield (Appendix F).

7. Quantitative PCR

The quantitative PCR assays were performed using the LightCycler® Software 4.1 and a LightCycler® 2.0, a carousel system, where samples are placed in 20 µL capillaries (maximum of thirty capillaries per run). The Cp values were obtained using the default LightCycler® Software 4.1 settings.

This stage of the project consisted of two distinct steps where qPCR was used. Firstly, the quality of the reactions was evaluated and optimized; subsequently, the relative miRNA quantities between samples were assessed.

Pools of each miRNA were used for the optimizations and in every run. They were produced combining 2 µL of all the RT products for each miRNA, meaning there were four miRNA pools in total (one per miRNA species, with a total of 44 µL).

7.1. Reaction quality assessment and optimization of reactions

In order to test the quality of the reactions, including efficiency and primer-dimer formation, the LightCycler® FastStart DNA Master^{PLUS} SYBR Green I was used.

Determination of PCR efficiency is based on a double-strand intercalating fluorescent dye instead of a probe, and makes use of a reference sample, which has been subjected to a series of serial dilutions. A qPCR is performed on these diluted samples and the calibrator (the original undiluted sample), and their Cp values are acquired. Afterwards, the LightCycler® Software 4.1 generates a plot with each Cp value in the y-axis and the log of the respective relative experimental concentration on the x-axis. A line that best fits the plotted points is created, and the efficiency of the reaction is obtained from its slope, through the formula:

$$E = 10^{(-1/Slope)} - 1$$

This means a PCR with 100% efficiency, produces a line with a slope of -3.32 (70).

In this case, each miRNA-derived cDNA pool served as a calibrator and each underwent four serial dilutions of 1:10. They were subjected to the amplification and melting programs, specified in Appendix G, with each primer having a final concentration of 0.3 µM.

Optimization of reaction conditions was performed according to the LightCycler® TaqMan Master protocol, a method based on a mix of *Taq* polymerase, reaction buffer, $MgCl_2$, dNTPs, miRNA-specific primer pairs and probes, and template cDNA (68).

The optimizations consisted of runs with one parameter modified at a time (primer concentration (C_{primer}), annealing temperature (T_a) and annealing time), compared to a "No Optimization" programme (outlined in Appendix G). This was done in order to identify the best run conditions, through a trial and error process (80). The optimization plan is outlined in Appendix H. The resulting PCR products were further analysed with the Agilent 2100 Bioanalyzer, DNA 1000 Assay, a kit similar to the previously described, dedicated to DNA.

7.2. Assessment of relative miRNA quantity

The assessment of relative miRNA quantities was also achieved resorting to the already described LightCycler® TaqMan Master. According to the results of the optimizations, this evaluation was performed with a T_a=55^{o} C, an annealing time of 30 s and a final primer concentration of 0.3 µM. In addition, miR-181a was not analysed, also according to optimization runs.

The assessment of relative miRNA quantities was designed taking into account that there were twenty-four capillaries to be run simultaneously (twenty-two samples, negative control and standard pool) and four miRNAs to be analysed. Therefore, there were a total of twelve runs, with twenty-four capillaries each, making a total of 288 capillaries on which qPCR was run (as seen below, in Table 4).

Table 4 – Setup of qPCR experiments to assess the relative quantities of each miRNA in cases and control samples. For each miRNA, every run consisted of twenty two capillaries with samples, one with a negative control and one with the corresponding pool. This means there were a total of 24 capillaries analysed per run; every run was performed in triplicate. In total, twelve runs were performed and 288 capillaries analysed.

miRNA	Capillaries	Replicates
miRNA-1	• 22 Samples • 1 Negative Control • miRNA-1 pool sample	3
miR-195	• 22 Samples • 1 Negative Control • miRNA pool-195 sample	3
miR-210	• 22 Samples • 1 Negative Control • miRNA-210 pool sample	3
miR-584	• 22 Samples • 1 Negative Control • miRNA-584 pool sample	3
Subtotal	**96**	**12**
Total	**288 Capillaries**	

As already stated, the specific primers and probes for the miRNA under analysis in each run were designed, synthesized and purchased from TIBMOLBIOL (sequences found in Appendix E).

8. Statistical analysis

The statistical analysis was performed using IBM® SPSS® Statistics (version 20.0.0.1) and Microsoft Excel® 2010, based on the means of the triplicate results for each sample.

Initially, in order to assess the distribution of the results, their histograms and normal probability plots were elaborated.

Next, given the distribution of the results, the statistical analysis was performed using the Wilcoxon Rank Sum Test (two-tailed). When the differences between groups were considered statistically significant, the comparative miRNA expression was deduced considering the means of cases and controls. It must be noted that the analysis was performed on Cp values for each miRNA, meaning that a superior Cp mean corresponds to a lower miRNA detection and, consequently, content (and vice-versa).

The correlation between the expression of different miRNAs and between miRNA expressions and clinical data was assessed using the Spearman Rank Correlation Coefficient.

This coefficient can take any value between +1 and -1, and the closer it is to one of these values, the more likely it is the variables are positively or negatively correlated, respectively (81).

9. miRNA target prediction

The prediction of possible targets and cellular functions affected by each miRNA included several steps.

First, the targets for each of the molecules were searched for in TargetScanHuman (April 2013), a well-known database (82).

Afterwards, the existing literature on miRNAs and preeclampsia was searched, and the published miRNA target claims were crossed with the ones indicated in TargetScanHuman. Their functions were found on NCBI Gene (83).

Finally, starBase was used for a "KEGG Analysis for miRNA target genes" (BC>=2), checking for common processes for the miRNAs which expression denoted a correlation in the statistical analysis (84).

Results

1. Quality Control

The means of the concentration measurements, A_{260}/A_{280} and A_{260}/A_{230} ratios for each of the analysed twenty-two samples can be found in Table 5. The obtained triplicate values can be found in Appendix I.

Table 5 – Sample concentration. Each sample was read, at least, three times for concentration, A_{260}/A_{280} and A_{260}/A_{230} ratios; the presented values are means of the triplicate reads. The lowest total RNA concentration obtained is 38.79 ng/µL; the highest is 183.78 ng/µL. All A_{260}/A_{280} ratios are all between 1.8 and 2.0. All A_{260}/A_{230} ratios are between 0.5 and 1.98.

Samples	RNA Concentration (ng/µL)	260/280 Ratio	260/230 Ratio
C1	79.29	1.98	0.96
C2	59.02	2.04	1.44
C3	141.68	1.96	1.68
C4	128.16	1.93	1.70
C5	58.05	1.84	0.68
C6	99.01	2.00	1.24
C7	50.35	1.97	1.10
C8	54.36	1.95	1.13
C9	72.94	2.02	1.06
C10	187.91	2.06	0.75
P1	53.23	2.00	1.27
P2	41.54	1.74	1.02
P3	63.65	1.91	0.87
P4	103.09	1.94	1.73
P5	156.74	2.04	0.78
P6	38.79	1.85	1.12
P7	44.85	1.87	0.50
P8	48.80	2.03	1.98
P9	89.62	1.74	0.80
P10	87.69	2.02	0.89
P11	43.55	2.04	0.41
P12	183.78	2.08	1.59

All the A_{260}/A_{280} ratio values are between 1.8 and 2.0, and all A_{260}/A_{230} ratios are above 0.5. The lowest total RNA concentration was 38.79 ng/µL and the highest was 183.78 ng/µL.

The Agilent 2100 Bioanalyzer provided gel images and electropherograms such as the one presented in Figure 10, for eleven PE samples, using the Pico kit. The remaining results, including duplicates and results obtained with the Nano kit, can be found in Appendix J.

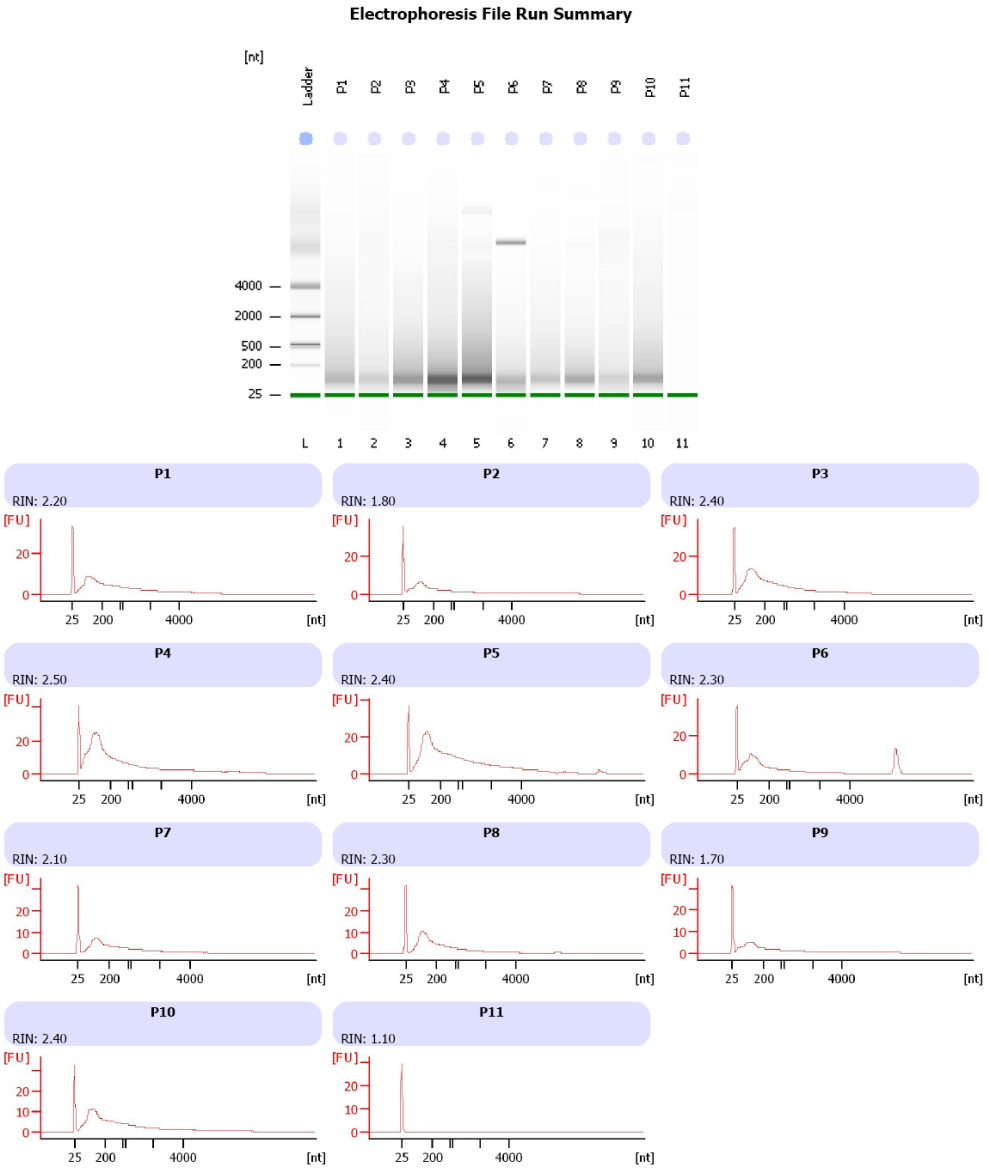

Figure 9 – Gel image, electropherograms and RIN scores obtained for P1 through to P11, with the Pico kit, on the Agilent 2100 Bioanalyzer. All samples, except for P11 display an RNA peak with about 100 nucleotides. P11 does not seem to have any RNA molecules. P6 displays a heavier band, with more than 4000 nucleotides, which does not seem reproducible.

Among the results presented in Figure 10, the highest obtained RIN score was 2.50, and the lowest was 1.00. All samples display an RNA band with about 100 nucleotides, except for P11, which does not appear to contain any RNA. In addition, in this case, P6 presents a band with more than 4000 nucleotides, which is not reproducible (see Appendix J). P12 presented a reproducible band of high molecular weight, when using both the Nano and Pico kit (check Appendix J).

2. Quantitative PCR

2.1. Reaction quality assessment and optimization of reactions

The graphs obtained using the LightCycler® FastStart DNA Master^{PLUS} SYBR Green I for evaluation of qPCR quality can be found in Appendix K.

A summary of the PCR and Bioanalyzer results obtained from the optimization reactions with the LightCycler® TaqMan Master can be found in Table 6. The detailed assessment of each of these optimization products can be found in Appendix L.

Table 6 – Summary of the results of the PCR optimization reactions. The lowest Cp value obtained was 21.98 (for miR-195, annealing time 40 s, T_a= 55^o C, C_{primer}=0.3 µM); the highest Cp value obtained was 38.81 (for miR-210, annealing time 30 s, T_a= 60^o C, C_{primer}=0.1 µM). All the specific fragments detected by the Bioanalyzer had lengths between 47 and 69 bps; other bands could be seen by eye, but were not detected by the instrument.

Sample		No Optimization (55^o C, 20 s)		T_a 60^o C	T_a 57^o C	Annealing Time 30 s		Annealing Time 40 s	
		PCR (Cp)	Bioanalyzer (bps)	PCR (Cp)	PCR (Cp)	PCR (Cp)	Bioanalyzer (bps)	PCR (Cp)	Bioanalyzer (bps)
miR-1	C_{primer}= 0.3 µM	31.13	*	37.25	34.18	32.57	*	27.26	*; *[2]
	C_{primer}= 0.1 µM	33.76	*[2]	38.62	35.23	27.47	*[4]	27.23	*[4]
miR-181a	C_{primer}= 0.3 µM	0	47	0	0	0	*	22.50	*; *[2]
	C_{primer}= 0.1 µM	0	*; *[3]	0	0	0	*[4]	0	*[4]
miR-195	C_{primer}= 0.3 µM	23.01	65,5	26.51	23.95	22.84	63*[2]	21.98	63*[2]
	C_{primer}= 0.1 µM	25.04	63*[2]	28.61	25.56	23.79	*[4]	22.93	*[4]
miR-210	C_{primer}= 0.3 µM	35.50	*	35.58	32.78	29.30	*[2];*[3]	26.09	*[2]; *[3]
	C_{primer}= 0.1 µM	33.57	*[2]	38.81	30.78	27.99	*[4]	27.42	*[4]
miR-584	C_{primer}= 0.3 µM	31.55	69*[2]	35.08	32.21	28.55	*; *[2]	25.12	*; *[2]
	C_{primer}= 0.1 µM	27.02	*; *[2]	32.45	32.59	25.44	*[4]	24.86	*[4]

* Small peak detected between 50 and 100 bps; not large enough to be detected by the Bioanalyzer, but visible by eye.

*[2] Larger peak, with more than 1500bps visible by eye.

*[3] Double peak between 100 and 150 bps; reproducible.

*[4] Sample not run in the Bioanalyzer.

The annealing temperature which gave rise to the overall lowest Cp values was T_a=55^o C (No Optimization), followed by T_a=57^o C, and finally T_a=60^o C.

The annealing time which resulted in lowest Cp values was 40 s, followed by 30 s, and 20 s (No Optimization).

Comparing Cp values, from lowest to highest, the following order of conditions is obtained: annealing time 40 s < annealing time 30 s < No Optimization (55^{o} C, 20 s) < T_a=57^{o} C < T_a=60^{o} C.

The Cp values do not show strong variation when 0.1 µM and 0.3 µM of final primer concentrations were used, with 0,3 µM displaying lower and more stable values, to some extent.

In all PCR runs, miRNA-181a was only detected once, with a Cp value of 45; in all other experiments for this miRNA, no amplification was detected.

Concerning the Bioanalyzer results, the conditions that gave rise to the most specific results were No Optimization (55^{o} C, 20 s), followed by annealing time 30 s and by annealing time 40 s. The condition that resulted in most production of large peaks above 15000 bps of length was annealing time 40 s.

2.2. Assessment of relative miRNA quantities

The average Cp values obtained from the LightCycler® TaqMan Master PCRs on the control and preeclampsia samples are outlined in Table 7. The complete results can be found in Appendix M.

Table 7 – Average of Cp results of LightCycler® TaqMan Master assay triplicates for each miRNA, in control and preeclampsia samples. The lowest obtained Cp value was 21.26 and the highest was 34.83.

	miR-1	miR-195	miR-210	miR-584
C1	33.32	24.47	34.83	30.71
C2	30.86	22.29	27.94	25.99
C3	31.28	21.93	28.25	27.59
C4	31.51	22.06	29.81	28.22
C5	31.60	22.86	27.58	26.35
C6	29.80	21.26	29.17	29.06
C7	28.38	21.92	28.64	27.98
C8	30.30	23.07	28.80	28.27
C9	32.47	21.95	28.41	26.59
C10	30.91	22.97	28.94	25.74
P1	30.42	22.18	28.73	25.86
P2	33.23	22.29	30.85	31.41
P3	32.29	23.31	30.89	30.79
P4	33.80	23.07	31.12	30.32
P5	31.69	22.56	30.21	29.12
P6	34.22	22.63	32.32	31.50
P7	32.60	23.26	31.66	30.84
P8	32.88	23.10	30.27	29.67
P9	33.78	23.41	31.27	30.69
P10	31.20	22.60	30.49	29.68
P11	30.06	21.80	29.89	29.63
P12	33.20	22.84	30.84	28.77

All samples revealed the presence of cDNA, except for samples P11 and P12, in the second miR-195 run (see Appendix M). The lowest Cp value obtained was 21.26, for miR-195, in a control sample; the highest was 34.83 for miR-210, also in a control sample.

The results obtained running each pool, during each qPCR replicate, for each miRNA, can be seen in Table 8.

It can be noticed that the Cp values obtained for the triplicates, remain similar in all cases, the difference never surpassing 1.71 cycles. A value for miR-195 was obtained running a 1:6 pool dilution, due to lack of enough material for the final run; its Cp value increased slightly, compared to the remaining miR-195 pool Cp values.

Table 8 – Cp values resulting from each triplicate, for each miRNA. The resulting figures are similar for each of the triplicates. One of the values obtained for miR-195 was obtained from running 1/6th of the concentration ran in the other runs; in this case, the obtained Cp value is higher, as expected.

	miR-1	miR-195	miR-210	miR-584
Pool	32.85	23.15	30.84	29.66
	32.20	23.21	31.09	29.69
	31.95	24.86*	29.94	28.60

*Concentration of the original pool/6

3. Statistical Analysis

The results indicate an overall higher Cp values in PE cases, compared to control samples, for all investigated miRNAs. The most prominent differences are observed in miR-210 and miR-584. The differences are less accentuated in miR-1 and almost non-existent in miR-195. The boxplot seen in Graph 1 provides an overview of these results.

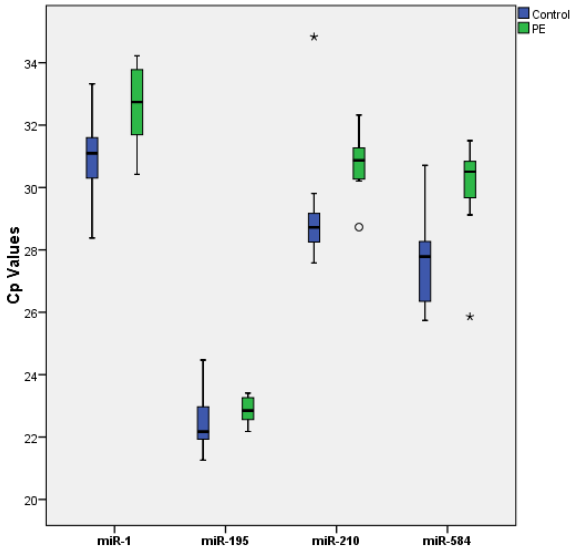

Graph 1 – Boxplot of the obtained data, for each miRNA, in controls and diseased samples. Overall, it seems the preeclamptic samples display higher Cp values, compared to the controls. For miR-210 and miR-584, both groups seem to be fairly different. This difference is not as pronounced for miR-1, and even less for miR-195.

A statistical description of the results can be found in Appendix N, as well as the histograms and normal probability plots, elaborated for evaluation of the distribution of the experimental results.

The results obtained computing the Wilcoxon Ranked-Sum test are displayed in Table 9 (extended version available in Appendix N). The obtained p-values for miR-1, miR-210 and miR-584 are 0.036, 0.003 and 0.003, respectively (all lower than 0.05); the p-value for miR-195 is 0.197 (above 0.05).

Table 9 – Statistical evaluation of the differences in miRNA expression between PE and control samples. (-) signifies the miRNA is under-expressed in PE, compared to healthy cases; when the miRNA is considered over-expressed in the diseased cases, the symbol (+) is used. (=) stands for no detection of differential miRNA expression.
The obtained p-values for miR-1, miR-210 and miR-584 are below the chosen 0.05 threshold. The p-value for miR-195 is above this value.

miRNA	p-value (Wilcoxon Rank-Sum Test)	Comparative expression (in preeclamptic samples, relatively to controls)
miR-1	0.036	-
miR-195	0.197	=
miR-210	0.003	-
miR-584	0.003	-

The results were retested after exclusion of the severe preeclampsia cases, five in total. The obtained significance probability measurements can be found in Table 10, below (extended version found in Appendix N). The obtained p-values are below 0.05 for miR-1, miR-210 and miR-584 (0.002, 0.005 and 0.002, respectively); the p-value for miR-195 is 0.083, above the threshold value.

Table 10 - Statistical evaluation of the differences in miRNA expression between mild PE and control samples. (-) signifies the miRNA is under-expressed in PE, compared to healthy cases; when the miRNA is considered over-expressed in the diseased cases, the symbol (+) is used. (=) signifies that no differential miRNA expression was detected.
The obtained probability values for miR-1, miR-210 and miR-584 remain under the chosen 0.05 threshold; likewise, p-value for miR-195 remains above this figure.

miRNA	p-value (Wilcoxon Rank-Sum Test)	Comparative expression (in preeclamptic samples, relatively to controls)
miR-1	0.002	-
miR-195	0.083	=
miR-210	0.005	-
miR-584	0.002	-

The correlations between the expression levels of the different miRNAs, in the different groups, are presented in Table 11. The associations between miR-1 and miR-195 and miR-210 and miR-584 are positive and noteworthy in both control and preeclampsia groups. No correlation can be seen between miR-1 and miR-210 in control samples, but it becomes positive to significant levels in PE. The same occurs for miR-1 and miR-584, and for miR-195 and miR-210, respectively.

Table 11 – Correlation coefficients calculated with the Spearman Rank Correlation Coefficient, between the different miRNAs, in the control and PE groups. The relationship between miR-1 and miR-210, and miR-1 and miR-584 seems random in the controls, but there is a clear apparent correlation between them in the preeclamptic samples. The same occurs with miR-195 and miR-210. The relation between miR-1 and miR-195, and miR-210 and miR-584 is positive in the controls, and it is enhanced very slightly in PE.

Correlations in controls				
	miR-1	**miR-195**	**miR-210**	**miR-584**
miR-1	1.000			
miR-195	0.455	1.000		
miR-210	0.055	0.176	1.000	
miR-584	-0.030	-0.030	0.673*	1.000

Correlations in PE				
	miR-1	**miR-195**	**miR-210**	**miR-584**
miR-1	1.000			
miR-195	0.490	1.000		
miR-210	0.783**	0.664*	1.000	
miR-584	0.594*	0.392	0.832**	1.000

**Correlation is significant at the 0.01 level (2-tailed).

*Correlation is significant at the 0.05 level (2-tailed).

The correlations between the different miRNA expressions, in the different groups, and the available clinical data are presented in Table 12. Note that these results were obtained correlating Cp values (and not miRNA quantities), with the clinical data. This signifies that, when the coefficient has a positive figure, there is a negative correlation in terms of miRNA level, and reciprocally. BMI and placental miR-1 are negatively correlated in controls, but not in PE cases. miR-195 shows a positive correlation to birth weight in healthy samples, and miR-210 and placental weight are negatively related in controls, but no such correlations can be observed in PE. Contrarily, placental miR-584 is not correlated to weight gain during pregnancy in control cases, but there is a negative correlation in preeclampsia. No association was detected between the miRNAs, in preeclampsia cases, and the development of foetal growth restriction.

Table 12 – Spearman Rank Correlation Coefficient, assessing the associations between the expressions of miRNAs, in both study groups, and their clinical data. miR-1 is negatively correlated to BMI in controls; in PE there is an inversion of this trend. miR-195 is very positively correlated to birth weight in controls, but no relation is observed in PE cases. miR-210 seems to be negatively correlated with the placental weight in controls, losing any association with it in preeclampsia cases. miR-584 does not seem to have a correlation with weight gain during pregnancy in controls, but in preeclamptic placentas, there seems to be a negative association. Correlating the different miRNAs in the preeclampsia group with development of growth restriction yielded no significant values.

Correlations in controls				
	miR-1	**miR-195**	**miR-210**	**miR-584**
Gestational Age	-0.043	-0.213	-0.134	0.079
BMI	0.345	0.006	0.055	-0.018
Weight Gain	0.449	0.068	0.031	-0.166
Placental Weight	-0.134	-0.505	0.505	0.614
Birth Weight	0.164	-0.661*	-0.152	0.091

Correlations in PE				
	miR-1	**miR-195**	**miR-210**	**miR-584**
Gestational Age	-0.014	-0.431	-0.032	0.249
BMI	-0.442	-0.261	-0.055	-0.018
Weight Gain	0.222	-0.018	0.300	0.388
Placental Weight	0.172	-0.151	0.018	0.211
Birth Weight	-0.116	-0.336	-0.151	-0.032
Growth Restriction	0.051	-0.051	0.051	0.205

*Correlation is significant at the 0.05 level (2-tailed).

4. miRNA target prediction

The top five hits indicted as targets for miR-1, miR-195 and miR-210 and miR-584, result from searching TargetScanHuman, can be found in Appendix O.

4.1. Crossing TargetScanHuman hits with existing literature

miRNA-1

The results obtained intersecting the miR-1 target genes provided by TargetScanHuman with relevant targets indicated in the bibliographic references, for miR-1, are displayed in Table 13.

Table 13 – Relevant targets for miR-1, crossing the TargetScanHuman results with targets indicated in the bibliographic references (58, 74, 83, 85). Enquobahrie *et al*, 2010 reported MEF2a and GATA4 as targets, none of which are present in TargetScanHuman nowadays. However, the algorithm indicates CACNA2D4 and CASK. Both TargetScanHuman and Zhu *et al*, 2009 present GJA1 as a possible miR-1 target. In addition, both also specify CORO1C and ARCN1 as putative targets of this miRNA.

miR-1		
Source	**Target Gene**	**Function of target**
Enquobahrie *et al*, 2010	MEF2a	Transcription factor involved in cell growth control and apoptosis, activating growth factor-induced genes. Related to calcium deficiency.
	GATA4	Transcriptional activator, mediator of embryogenesis. Related to calcium deficiency.
TargetScanHuman (April 2013)	CACNA2D4	Part of voltage-dependent calcium channels, mediating entry of calcium into cells.
	CASK	Calcium/calmodulin-dependent serine protein kinase.
Zhu *et al*, 2009	GJA1	Connexin, a major gap-junction protein.
	CORO1C	Protein involved in cell cycle progression, signal transduction, apoptosis and gene regulation.
TargetScanHuman (April 2013)	ARCN1	Protein involved in vesicle structure or trafficking.

It was observed that the genes MEF2a and GATA4, reported by Enquobahrie *et al*, 2010 as targets for this miRNA in the framework of preeclampsia, are not currently identified in TargetScanHuman (58, 85). Instead, CACNA2D4 and CASK, with related functions, are found (85).

Still concerning miRNA-1, indicated by both the algorithm and Zhu *et al*, 2009, are GJA1, CORO1C and ARCN1 (74, 85).

miRNA-195

The seemingly most relevant putative targets concerning preeclampsia, reported by TargetScanHuman and bibliographic references, for miR-195, can be found in the Table 14.

It seems like the ActRIIA transcript, a target indicated by Bai *et al*, 2012 as being of importance, is not indicated by the algorithm (85, 86).

Moreover, out of a great number of miR-195 targets pointed out by Hu *et* al, 2009, only the transcripts for ADAMTS1, VEGFA, IL15, PPAP2A and CD163 are presently shown in TargetScanHuman (60, 85). The case is similar for PISD, FGF2 and PAPPA, some of the mRNA targets indicated by Zhu et al, 2009 which are still present in the database (74, 85).

Table 14 - Relevant targets for miR-195, result from crossing the TargetScanHuman results with the targets indicated by the references (60, 74, 83, 85, 86). Bai *et al*, 2012 reports ActRIIA as a target of this miRNA. Hu *et al*, 2009 and TargetScanHuman specify ADAMTS1, VEGFA, IL15, PPAP2A and CD163. Finally, Zhu *et al*, 2009 and the algorithm indicate PISD, FGF2 and PAPPA as targets of miR-195.

miR-195		
Source	**Target Gene**	**Function of target**
Bai *et al*, 2012	ActRIIA	Receptor of Activin A, a growth and differentiation factor.
Hu *et al*, 2009	ADAMTS1	Metalloproteinase involved in inflammatory processes, fertility and organ morphology/function.
TargetScanHuman (April 2013)	VEGFA	Growth factor which induces cell migration and growth, angiogenesis and vasculogenesis.
	IL15	Interleukine involved in the activation/proliferation of T cells and NK cells.
	PPAP2A	Surface enzyme important for the uptake of lipids from the extracellular area.
	CD163	Protein receptor which provides protection against oxidative damage.
Zhu *et al*, 2009	PISD	Phosphatidylserine decarboxylase targeted to the inner mitochondrial membrane.
TargetScanHuman (April 2013)	FGF2	Fibroblast growth factor with mitogenic and angiogenic activities.
	PAPPA	Metalloproteinase involved in proliferative processes.

miR-210

The genes predicted as miR-210 targets with possible importance in the setting of PE, are listed in the Table 15, as are their likely functions.

One of the top results indicated by TargetScanHuman for this miRNA is THSD7A, which has a function possibly related to the pathologic condition (85). However, this gene does not seem to have been mentioned by any other study concerning preeclampsia and miRNAs.

Moreover, out of the two targets mentioned by Zhang *et al*, 2012, only EFNA3 is currently present in TargetScanHuman (85, 87).

It can be seen that Lou *et al*, 2012 mentions Notch1 as a miR-210 target, although it was not listed in the consulted algorithm (85, 88). The case is similar for HSD17B1, indicated by Ishibashi *et al*, 2012 (59, 85).

Both Mayor-Lynn *et al*, 2011 and Muralimanoharan *et al*, 2012 indicate HIFA1A as a target gene for this miRNA (34, 89). Even though it is not listed in TargetScanHuman, the similar HIF3A is (85).

Finally, both Kelly *et al*, 2011 and TargetScanHuman refer the GPD1L transcript; as both TargetScanHuman and Lee *et al*, 2012 mention the ISCU gene (85, 90).

Table 15 - Relevant targets for miR-210, result from crossing the TargetScanHuman results with the targets indicated in the bibliographic references (34, 59, 83, 85, 87-92). TargetScanHuman indicates THSD7A is a main target of miR-210. EFNA3 is reported by both Fasanaro *et al*, 2008 and Zhang *et al*, 2012. This latest study also reported HOXA9. Lou *et al*, 2012 indicated Notch1; Ishibashi *et al*, 2012 indicated HSD17B1; and Mayor-Lynn *et al*, 2011 and Muralimanoharan *et al*, 2012 indicated HIF1A. This target is not found in TargetScanHuman, unlike HIF3A. Moreover, Kelly *et al*, 2011 reported GPD1L and Lee *et al*, 2012 reported ISCU, as miR-210 targets.

miR-210		
Source	**Target Gene**	**Function of target**
TargetScanHuman (April 2013)	THSD7A	Protein inhibitor of endothelial cell migration and tube formation, found in endothelial cells from the placenta and umbilical cord.
Fasanaro *et al*, 2008	EFNA3	Receptor responsible for targeting trophoblasts to the uterine tissue and spiral arteries.
Zhang *et al*, 2012		
TargetScanHuman (April 2013)		
Zhang *et al*, 2012	HOXA9	Transcription factor involved in regulation of angiogenesis and cell migration, during embryonic development.
Lou *et al*, 2012	Notch1	Protein involved in the Notch signalling pathway, vital for trophoblast invasion and remodeling of the maternal blood vessels.
Ishibashi *et al*, 2012	HSD17B1	Enzyme involved in the metabolism of estrogens and androgens.
Mayor-Lynn *et al*, 2011	HIF1A	Negative regulators of hypoxia-inducible gene expression.
Muralimanoharan *et al*, 2012		
TargetScanHuman (April 2013)	HIF3A	
Kelly *et al*, 2011	GPD1L	Protein which binds an integral membrane protein, responsible for mediating sodium permeability dependent of voltage, in excitable membranes.
TargetScanHuman (April 2013)		
Lee *et al*, 2012	ISCU	Fe-S cluster scaffold protein, essential for the function of mitochondrial enzymes.
TargetScanHuman (April 2013)		

miR-584

The resulting putative targets for miRNA-584, and their respective possible functions, from crossing TargetScanHuman with preeclampsia-related references are displayed in the table below.

Table 16 - Relevant targets for miR-584, result from crossing the TargetScanHuman results with the targets indicated in the bibliographic references (58, 74, 83, 85). Zhu *et al*, 2012 reported PRRX1, ACYP2 and ARL13B as targets of miR-584. In addition, Enquobahrie et al, 2010 denoted LfR. Out of these targets, only PRRX1 is currently present in TargetScanHuman.

miR-584		
Source	**Target Gene**	**Function of target**
Zhu *et al*, 2012	PRRX1	Transcription co-activator in various mesodermal-derived tissues.
TargetScanHuman (April 2013)		
Zhu *et al*, 2012	ACYP2	Enzyme responsible for the hydrolysis of the phosphoenzyme intermediate of various membrane pumps, (such as Ca^{2+}/Mg^{2+}-ATPases).
	ARL13B	Cilia GTPase.
Enquobahrie *et al*, 2010	LfR	Regulates the functions of lactoferrin.

One of the obtained top five hits for this miRNA is the PRRX1 transcript, which was also indicated by Zhu *et al*, 2009 (74, 85).

Zhu *et al*, 2009 also mentions ACYP2 and ARL13B as targets, none of which can currently be found by TargetScanGene (74, 85).

Lastly, Enquobahrie *et al*, 2010 states that miR-584 targets LfR mRNA, but this is not presently observed in TargetScanHuman (58, 85).

4.2. Common pathways for correlated miRNAs

The target genes and pathways in common for the miRNAs that were considered correlated can be found in Appendix O. Table 17 constitutes a simplified version.

According to starBase, the most likely processes miR-1 and miR-210 participate in, simultaneously, are cell cycle and RNA splicing regulation. miR-1 and miR-584 commonly seem to take part in the spliceosome machinery, but also in infections by the genus *Shigella*. Apparently, miR-195 and miR-210 are implicated in TGF-β signalling and cell cycle, as are miR-195 and miR-584. This latter pair is also involved in protein processing and circadian rhythm regulation (84).

Table 17 - Processes in common with the miRNAs that displayed higher correlation in the preeclamptic group, according to starBase (84). miR-1 and miR-210 are involved in cell cycle and RNA splicing regulation. miR-1 and miR-584 commonly take part in the spliceosome machinery, but also in infections by the genus *Shigella*. miR-195 and miR-210 are implicated in TGF-β signalling and cell cycle, as are miR-195 and miR-584. This latter pair is also involved in protein processing and circadian rhythm regulation.

Interacting miRNAs	miR-1 + miR-210	miR-1 + miR-584	miR-195 + miR-210	miR-195 + miR-584
Common Processes	Spliceosome	Spliceosome	TGF-beta signalling pathway	TGF-beta signalling pathway
				Protein processing in endoplasmic reticulum
	Cell Cycle	Shigellosis	Pathways in cancer (including small cell lung and prostate)	Pathways in cancer (including small cell lung and prostate)
			Cell cycle	Circadian rhythm
				Cell cycle

Discussion

1. Biological Implications

1.1. Comparison with previously published reports

The results obtained in the present study are in concordance with the conclusions by Enquobahrie *et al*, 2010 and Zhu *et al*, 2009, concerning the under-expression of miR-1 in preeclamptic placentas. The same cannot be said about the remaining analysed miRNAs: there was no apparent difference in miR-195 expression in cases and controls, in the present study, which is at variance with the over-expression reported by Noack *et* al, 2011 and its under-expression described by Zhu *et al*, 2009; miR-210 was found to be over-expressed by all three referenced authors, contrasting with the under-expression observed in the present project; and finally, even though miR-584 was described as over-expressed by Zhu *et al*, 2009, our results are in agreement with Enquobahrie *et al*, 2010, who also reported on under-expression.

A representation of the comparison between these studies can be found in Table 18.

Table 18 – Overview of the results obtained in this project and in previous studies. The present study seems to corroborate the findings of Enquobahrie *et al*, 2010 and Zhu *et al*, 2009, confirming the relative under-expression of miR-1, in preeclamptic placentas. It seems there is no significant difference between the levels of miR-195 in healthy and preeclamptic samples detected in this study, compared to the differential expression detected by Noack *et al*, 2011 and Zhu *et al*, 2009. The obtained results do not support the reported over-expression of miR-210 by Enquobahrie *et al*, 2010 and Noack *et al*, 2011. miR-584 was found to be under-expressed in our study, which is in agreement with Enquobahrie et al, 2010, but in disagreement with Zhu *et al*, 2009.

miRNA	Enquobahrie *et al*, 2010 (58)	Noack *et al*, 2011 (73)	Zhu *et al*, 2009 (74)	Present Study
miR-1	-		- (severe PE)	-
miR-195		+	- (severe PE)	=
miR-210	+	+	+ (severe PE) - (mild PE)	-
miR-584	-		+ (severe PE)	-

It should be noted that the various studies have utilized experimental methods with different sensitivities. Moreover, the study populations differ somewhat between the projects, particularly with respect to race and gestational age at which the samples were taken. These factors should not be dismissed in the search of reasons for some of the differences detected among studies (58, 93).

When comparing the results obtained in this study and to those of previous reports, it is noted that only Zhu *et al*, 2009 made a distinction between severe and mild preeclampsia cases, evaluating them as separate entities (74). Noack *et al*, 2011 only conducted studies in severe cases; and Enquobahrie *et al*, 2010 classified all samples as preeclamptic, not making any further distinctions (58, 73). In the present study the majority of the samples derived from mild preeclampsia cases (only five were considered severe); and all were classified as being early PE (arising before 34 weeks of gestation).

As mentioned earlier, the hypothesis that preeclampsia may encompass several pathological entities has arisen. This seems to be supported by our results which diverge from the literature, namely concerning miR-210 and, possibly, miR-1.

The detected differential expression of miR-210 between the two groups (p-value=0.003) is significant, indicating that it is extremely unlikely due to chance. Even though these results were not in concordance with those reported by Enquobahrie *et al*, 2010, Noack *et al*, 2011 and numerous other studies, there are two studies in the literature which also reported an under-expression of this miRNA: Mayor-Lynn *et al*, 2011 and Zhu *et al*, 2009 (34, 57-59, 73, 74, 89, 92). The paper by Mayor-Lynn *et al,* 2011 does not mention which kind of preeclampsia was under analysis, but Zhu *et al*, 2009 reported the under-expression of the miRNA in mild cases, in contrast to its over-expression in severe cases (74, 89). Even though the significance probability measure rose when the severe cases were removed from the analysis (p-value=0.005), this could be due to the smaller sample size, which overshadowed the differential expression of the miRNA between groups (Zhu *et al*, 2009 reported a small significant 0.526-fold decrease in the expression of this miRNA in mild cases compared to controls). This appears to support our results, possibly indicating a divergent miR-210 expression in different preeclampsia phenotypes.

Concerning the expression of miR-1, a significant difference in its expression was detected between groups (p-value=0.036). Interestingly, when the cases of severe preeclampsia were removed from the statistical analysis, this difference became dramatically more apparent, in spite of the lower number of observations (p-value=0.002). This may be an indication that the differential expression of miR-1 tends to be more pronounced in mild cases.

These results seem to point towards a very solid differential expression of miR-1 and miR-210 in mild preeclampsia cases, compared to healthy controls. Furthermore, there seems to be a difference in expression of these miRNAs in mild and in severe cases, lending support to the hypothesis that different pathogenic processes may be involved in different preeclampsia phenotypes. All the same, some mechanisms seem to be common to the different subtypes of the syndrome, as illustrated by miR-584, which is very significantly under-expressed whether the severe cases are included in the analysis or not.

Moreover, taking into account that all the samples are considered to be from early preeclampsia and that the significances of the differential expressions are altered when severe cases are removed from the analysis, the commonly held view that early PE cases tend to be severe is challenged, suggesting further research to clarify this issue.

Concerning the detected non-differential expression of miR-195, which contrasted with other studies, it can be argued to be related to the low number of observations in the present project (60, 73, 86). This claim is based on the study by Zhu *et al*, 2009, which reported the differential expression of this miRNA between preeclamptic and healthy samples to be of 0.405-fold, a small figure, which possibly demands a higher number of analysed cases, in order to be detected.

1.2. miRNA target prediction

The presented target genes for each of the studied miRNAs constitute a small fraction of all the possibilities provided by the used algorithm, TargetScanHuman, combined with interesting remarks found in bibliographic references, which may hold biological importance in the context of preeclampsia.

The functions of the miRNA targets mentioned below strengthen the view that the analysed miRNAs may play a role in preeclampsia. All these functions seem to be easily connected to preeclampsia characteristics and symptoms, and it is plausible that alterations in coding-mRNA levels may interfere with vital functions in the placenta.

1.2.1. Crossing TargetScanHuman hits with existing literature

Cell proliferation, adhesion and differentiation

Impaired proliferation and differentiation of trophoblasts have been shown to play an important role in the preeclamptic placenta (19). Therefore, it comes as no surprise when transcripts for growth factors (such has VEGFA and FGF2), growth and differentiation-regulating molecules (for instance, ActIIA), and migration and invasion-related proteins (like PAPPA, Notch1 and THSD7A) are indicated as possible targets of placental miRNA expression regulation. Moreover, altered levels of transcripts involved in cell cycle progression and apoptosis (like CORO1C) are also anticipated to be important in this pathological condition.

Likewise, it seems that intercellular adhesion molecules, such as GJA1, involved in gap-junctions, are central moderators of proliferation and differentiation of trophoblasts, making these proteins also likely to be targeted in this context (94).

Hypoxia, oxidative stress and mitochondrial dysfunction

Preeclamptic placentas are subjected to hypoxic conditions, which are related to higher oxidative stress levels and mitochondrial dysfunction (24). Therefore, mRNAs coding products responsible for adaptation to hypoxia (such as HIF1A and HIF3A), oxidative stress protection (like CD163) and mitochondrial proteins (PISD) seem probable to be affected in preeclampsia.

Interestingly, there seems to be a very special miRNA with the potential for influencing all these three parameters at once: miR-210. This miRNA has been reported as being hypoxia-induced in a number of studies (87, 90-92). In fact, miR-210 seems to target the GPD1L transcript, stabilizing a hypoxia inducible factor, HIF1A (90).

In placentation, HIF1A has a regulatory effect over trophoblasts and it normally decreases with gestational age, but not in preeclampsia (34). On the other hand, HIF1A is a transcription factor which attaches to the hypoxia responsive element in the miR-210 promoter, augmenting its expression. This positive feedback process is enhanced in the presence of oxidative stress products, which further stabilize HIF1A, and also activates NF-kB, another transcription factor that upregulates miR-210 expression (87, 90). HIF1A is not listed in TargetScanHuman, but instead HIF3A is. Furthermore, ISCU-coding mRNA, also a miR-210 target, is a mitochondrial protein that could be involved in the pathological process, being responsible for deficient trophoblastic iron metabolism and consequent dysfunctional mitochondrial respiration (34, 92).

This process which includes miR-210 induction by hypoxia and ROS, leading to atypical mitochondrial activity is integrated and illustrated in Schematic 7.

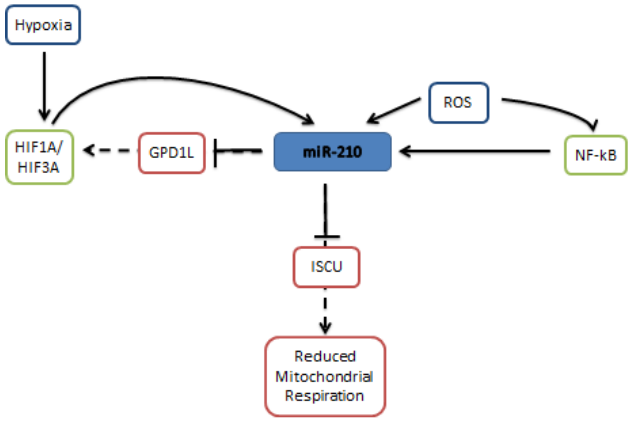

Schematic 7 – Interactions of miR-210 in preeclamptic placentas. Hypoxia induces miR-210 expression, through HIF1A/HIF3A. miR-210 is also positively influenced, directly and indirectly, by oxidative stress. Moreover, this miRNA negatively influences the expression of GPD1L, further stabilizing HIF1A. This miRNA impairs the expression of ISCU, reducing mitochondrial respiration (34, 92).

Inflammatory processes

As described, maternal systemic inflammation is characteristic of preeclampsia (9). Interestingly, proteins involved in inflammatory processes, such as ADAMTS1, are predicted as targets of placental miRNAs.

Other inflammatory molecules, responsible for the actions of immune cells such as cytokines and interleukines (namely, IL15), may also be regulated by miRNAs which levels are altered in preeclampsia, contributing to the abnormal systemic immune reaction characteristic of the syndrome. Likewise, molecules with immune functions, such as lactoferrin (responsible for platelet aggregation), are affected by the altered expression of their receptors, conditioning their functions.

Calcium signalling

Since calcium signalling seems to play an important part in the preeclamptic placenta, where its intracellular levels and metabolism are disrupted, targets such as MEF2a and GATA4, both associated with an impairment of calcium signalling in cardiovascular diseases, seem to be plausible targets in the context of preeclampsia (83, 95). Ca^{2+} and its successful transportation through the placenta seem to be especially important for transcription, cell cycle, cell adhesion, proliferation and differentiation regulation, also being vital for foetal skeletal development, in later stages of the pregnancy (96).

1.2.2. Common pathways for correlated miRNAs

Concerning the pathways common to the pairs of miRNAs identified as being correlated, roles shared by most of them seem to emerge. The most flagrant examples are processes related to splicing and cell cycle regulation, which appear plausible, given that abnormal gene expression and cell proliferation may lead to abnormal development of the placenta, and contribute to the pathophysiology of preeclampsia.

Two pairs of correlated miRNAs (miR-195 and miR-210, and miR-195 and miR-584) seem to be connected to TGF-beta signalling. TGF-β1 and TGF-β3 levels are amplified in preeclamptic placentas; in addition, other members of the TGF- β superfamily (Activin A and Nodal) regulate growth and differentiation of trophoblasts (86). Therefore, this pathway warrants further study, as a possible link between miRNA deregulation and preeclampsia. It also brings into attention that miR-584 targets TGFB2 transcripts (according to TargetScanHuman), which has not been mentioned in the consulted bibliographic references (85).

Furthermore, miR-195 and miR-584 appear to affect protein processing in the endoplasmic reticulum. This may be of interest since placental ERs are dilated in preeclampsia, with the possibility that important proteins of this organelle are perturbed by miRNA alterations, thereby contributing to ER stress. High levels of ER stress are known to lead to oxidative stress and the production of pro-inflammatory cytokines in preeclampsia, constituting a possible mechanism through which these correlated miRNAs may act (97, 98).

Lastly, this same pair of miRNAs (miR-195 and miR-584) seems to be implicated in circadian rhythm regulation. This can also been related to the syndrome, which has been linked to nocturnal steep drops in blood pressure or even an inversion of the circadian blood pressure rhythm (99).

Nonetheless, these suggested associations between different miRNAs must be regarded with discretion. The efficiencies of the different PCRs should be tested further, improved and matched, so these correlations can be successfully assessed and proven not to be influenced by contaminants or faulty PCR optimization (70).

Even though the discussed functions seem important in the framework of preeclampsia, the uncovered miRNA targets may not always fit the simple mechanistic model of preeclampsia pathogenesis. However, it must be noted that differential expressions of a miRNA may be a cause or a consequence of the condition, constituting either an origin for the pathological processes or a compensation mechanism to counter alterations already induced. In addition, it must be kept in mind that miRNAs have also been implicated in gene activation through unknown mechanisms (49, 51). Therefore, the targets could either be positively or negatively regulated by the miRNAs. Likewise, there is the possibility of the presence of ceRNAs in the placental trophoblasts, which may inhibit the actions of the deregulated miRNAs (49). In order to confirm the actions and effects of the studied miRNAs in preeclamptic trophoblasts, further downstream assessments, such as proteomics approaches, RNAi experiments or microarrays should be carried out (82).

1.3. Correlation between miRNAs and clinical data

It was noted that three miRNAs (miR-1, miR-210 and miR-584) were associated with BMI, placental weight and weight gain, respectively.

Out of these associations, it is interesting to observe that lower amounts of miR-584 are related to a higher weight gain during pregnancy in preeclampsia. This miRNA has been reported to be involved in nutrient metabolism, with this correlation possibly holding a biological meaning that may warrant further exploration in the future (100).

However, the reported under-expression of miR-1 is correlated to a lower BMI in preeclampsia, which seems difficult to reconcile with the fact that high BMI is a known risk factor for PE (9). The same could be said for miR-210, with its quantities being negatively correlated to placental weight in controls, but not in PE (preeclamptic placentas are generally smaller and lighter than their healthy counterparts) (33). However, it must be remembered that the performed analysis involved only four molecules out of the thousands that could be involved in the pathogenesis. It is possible that other molecules are more directly responsible for the association of preeclampsia to high BMI and low placental weight.

2. Technical Considerations

2.1. Sample and RNA choice

The present study used samples which display characteristics as similar as possible, given the available material at the St. Olavs University Hospital biobank, and taking into consideration it was implemented in a Master Thesis framework. Therefore, the analysis of more samples or more miRNAs was not considered to be practical. Moreover, choosing authors that agreed on certain miRNAs and disagreed on others seemed to yield a manageable study design with the potential to settle conflicting claims.

The age of the used FFPE blocks (some up to nine years old, at the time of RNA extraction) could be questioned, since it is considered miRNA degradation may become pronounced in samples stored for many years. Thus, a major decrease in miRNA accessibility in FFPE tissue has been reported to occur after ten years of storage, especially with the use of non-buffered formalin, which was not the case (101).

miRNA notation constituted an issue in the process of choosing miRNAs and in the primer design, due to its great evolution in the last years as a result of the better understanding of these molecules. Unfortunately, this is translated into miRNAs being named according to one system, in certain papers, but being found with a different terminology in current databases. Even though this question was resolved taking into account the update notes, on the miRBase blog, it is appropriate to emphasize the importance of a consistent nomenclature system, in order to ensure reliable research (102).

At the present, looking back, it seems the preeclampsia samples could have been chosen taking into account a stratification of the disease, since there is more than one phenotype associated to preeclampsia (14, 15). However, this was not brought to focus by the previous studies, explaining why it was not implemented at the time of the project design.

2.2. RNA extraction and purification

It should be noted that, even though three cylinders were removed from areas marked as having a high villous density, in each FFPE block, the blocks/areas were not matched for villous density and what was considered the highest villous density in one sample might have been considered low in the next. Moreover, while the villous areas were observed on microscopical slides, the tissue was removed from blocks, in another visual plane. Consequently, it is possible that some areas which were seen under the microscope did not match the tissue which was extracted from the FFPE block.

The three cylinders extracted from the placental blocks were mixed and treated as one, meaning that this study has no biological triplicates. Unfortunately, the analysis of biological triplicates would have demanded more resources and extra time for completion of the study, which would not have been feasible in this case. It is, however, an important step that should be undertaken whenever possible.

It should be noticed that the protocol used in this step was optimized for prostate tissue. In order for the best total RNA concentration values to have been obtained in this case, the protocol could have been optimized for placental tissue. In a next effort, this optimization should be attempted, with less time, financial and material constrictions.

2.3. Quality Control

In order to reduce inaccuracies related to the NanoDrop photometer measurements, the concentration of each sample was read, at least, three times, making sure the differences were not greater than 0.5 ng/µL, between a minimum of two readings. Notwithstanding, the NanoDrop can be considered quite an inaccurate device, often overestimating measurements.

This challenge arises from the fact that it reads UV absorbance and frequently does not distinguish between DNA, RNA, free nucleotides and other contaminants (103). The suspicion rises even further, looking at the obtained A_{260}/A_{230} ratios, which are as low as 0.5 in some cases, and could contribute to an increased deviation of the measured concentration value (104). If the NanoDrop readings were not accurate, then it may have had an impact on the rest of the study, leading to questionable results. In a next attempt to conduct a study of this kind, it could be interesting to compare the values obtained with the NanoDrop with the ones obtained with the Qubit, often considered to be more selective, sensitive and accurate for quantification of nucleic acids (103).

Concerning the Bioanalyzer readings, it can be noticed that the obtained RIN scores are very low, on a one to ten scale. However, this is not thought to imply reduced miRNA integrity, being only indicative of mRNA degradation, characteristic of FFPE tissues. mRNA degradation is also indicated by the 100 nucleotide fragments detected in the electrophoretic assays.

Moreover, it can be noticed that, in both the Pico and the Nano kit results, there is no trace of compounds of higher molecular weight in the samples (except for P12). This is indicative of a pure total RNA solution, with no DNA contamination. P12 seems to contain molecules of higher molecular weight. However, qPCR is such a specific procedure, that this contamination was considered not to be relevant.

According to the Pico kit measurements, there is no RNA present in sample P11, a finding which is contradicted by the Nano kit results (see Appendix J). This could be indicative of an experimental mistake, since the samples were diluted for the Pico kit. It is possible that the RNA of the P11 sample was never diluted and the results displayed in the Pico kit electropherograms are merely measurements of water. This hypothesis is further supported by the amplification of cDNA of this sample, during the qPCR.

In future studies, it would be recommended to use the Agilent Small RNA kit, which is optimised for detection of a minimum of 100 pg of miRNA, in samples of total RNA isolate, since the Pico and Nano kits were not originally intended for miRNA detection and quality assessment (78, 105).

2.4. Reverse Transcription

As denoted, the reverse transcription process is decisive for the success of qPCR experiments. Unfortunately, the success of the RT process was not confirmed, with the NanoDrop and Bioanalyzer being unable to provide accurate cDNA readings (106). Nonetheless, a “no-RT” control sample could have been run, in order to assess the presence of contaminations in the cDNA (107, 108).

For additional studies, in order to obtain the best possible results, the RT protocol could be optimized, since the mentioned incubation temperatures and times are recommended as a starting point, which can be changed to better fit the template to be reversely transcribed (79). In addition, the reverse transcription could be performed in triplicate for each sample, in order to make the results more robust (108). Regrettably, this was not possible, within the frame of a Master Thesis.

2.5. qPCR

2.5.1. Reaction quality assessment

It is generally established that testing for primer-dimer formation and PCR efficacy is a key step for optimal validation of qPCR results, since PCR efficiency is usually correlated with its sensitivity and robustness. Furthermore, the formation of primer-dimers gives rise to the detection of false-positive results, affecting and compromising the obtained results (108).

Even though the results achieved with the LightCycler® FastStart DNA Master^{PLUS} SYBR Green I seem far from optimal, with efficiencies as low as 1,3 and melting curves displaying unspecific amplifications (see Appendix K), it was considered this assay should be disregarded and that optimizations should be done using the LightCycler® TaqMan Master. The reasons behind this decision are numerous: firstly, the used primers were commercially designed and purchased, passing many quality control steps (109). Moreover, personal inexperience with the method may have contributed to these results, with technical help being needed if they should have been taken any further. Additionally, the RT reaction included random hexamers, yielding other cDNA products, which may have been detected with this non-specific detection technique (70). The usage of the LightCycler® TaqMan Master, a probe-based method, for the assessment of relative miRNA quantities, ensures the detected nucleic acid polymers are not only reverse transcribed and hybridize with the specific primers, but they also contain a sequence complementary to the specific probe, making the procedure more stringent and less likely to detect unspecific products (68). The final reason behind this choice involves the experimental design itself: this project focuses on making an evaluation between groups, not assessing the magnitude of the difference between them or quantifying their absolute amounts. In this case, efficiency does not constitute a critical parameter, nor does primer-dimer formation, as long as the unspecific products are not detected and there is no exhaustion of the qPCR mix components (which does not seem to occur, since amplification occurs until the very last cycle, for all samples and all miRNAs).

Even though time and material constrictions did not allow a more extensive examination of reactions and optimizations with this assay, in a future effort, the protocol should be controlled and optimized.

2.5.2. Optimization of reactions

Optimization of conditions is also an important step for PCR reactions, since poor amplification is not desirable. The parameters decided to be optimized (T_a, annealing time and C_{primer}) were in accordance with the literature, expert opinions and available time and material (110, 111).

According to the amplification results, changing the T_a did not improve the reaction quality, with Cps rising with higher temperatures, probably due to double-helix destabilization in such small amplicons (112). Therefore, a T_a=55^o C was chosen as most fitting. Lower T_a's were not tried, since they are known to yield a greater synthesis of unspecific products (112).

Even though it may seem like choosing a longer annealing time yielded lower Cp values, looking at the Bioanalyzer results, it seems like the higher the annealing time, the more unspecific products are amplified (112). Consequently, choosing an annealing time of 30 s seemed to yield a better balance between low Cp values and lesser unspecific syntheses.

In addition, PCR products were not analysed by electrophoretic processes for T_a=60° C, T_a=57° C and for C_{primer}=0.1 µM with annealing times of 30 s and 40 s, since these results did not seem to hold substantial added value.

In a next attempt perform these experiments, parameters such as *Taq* pol, Mg^{2+}, dNTPs and probe concentration should be optimized (70). More variations of the T_a should also be tested.

2.5.3. Assessment of relative miRNA quantities

For the qPCR assessment of the miRNA quantities in the samples, it can be noted there were no positive controls. However, there are no known miRNAs that have a constant expression in both healthy and preeclamptic placental villi, nor is there a certain tissue type that is known to contain a constant high level of these studied miRNAs (107). Nonetheless, the miRNA pools, present in all runs for each miRNA, constituted a standard to evaluate if the samples underwent similar conditions in every run. The triplicates appear to have been run very similarly, and any noticeable change in Cp values between them should be attributed to human error in pipetting. The miR-195 pool, which was diluted for the last run, generated a Cp slightly higher than the other replicates, behaving as expected.

miR-181a was not analysed, since the results obtained with the TaqMan Master optimizations yielded no amplification. Since amplification occurred during the SYBR Green I experiments, it is probable there was a problem with the miR-181a TaqMan probe, resulting in no detection of the miRNA in TaqMan assays.

Another noteworthy matter is the fact that the used qPCR primers were made to hybridize adjacently to the miRNA sequences. This signifies that the detected molecules were not categorically miRNAs, but rather precursor molecules (pri-miRNAs and pre-miRNAs). This could constitute an issue if these precursors were degraded before they could be processed into miRNA (58, 73, 74). Nonetheless, it would not have been possible to place two primers and a TaqMan probe within a twenty to twenty-four bases long molecule (109).

2.6. Statistical analysis

It could be argued that the Wilcoxon Rank-Sum test is not the most adequate in this case, since the experimental results could be considered approximately normal (113, 114). However, all the obtained normal probability plots can be claimed to display an s-shaped distribution of the results nearby the theoretical gaussian line, indicating non-normally distributed results (81).

Therefore, the Wilcoxon Rank-Sum test was used, since it is superior to T-tests, when distributions are non-normal. Moreover, both the T-test and Wilcoxon's have a very similar power in normally distributed populations, but when the Wilcoxon test is more powerful than the t-test, it is so by a great magnitude (115). Accordingly, it seems reasonable that, in case of uncertainty of the distribution of the data, the Wilcoxon Rank-Sum test is used.

In order to consistently resort to non-parametric measures, the Spearman Rank Correlation Coefficient was used to measure the statistical dependence between miRNAs, and between miRNAs and clinical data parameters.

2.7. miRNA target prediction

For the assessment of possible miRNA targets, TargetScanHuman, one of the most popular miRNA target prediction algorithms, was used (82).

Unfortunately, different algorithms predict, at times, very different targets, due to the lack of certainty concerning miRNA targeting mechanisms. Consequently, the predicted mRNA targets are not assured to be accurate.

Nonetheless, it has been shown that TargetScan has a better performance than other algorithms, when comparing *in vivo* results and *in silico* predictions, but also when correlated with protein expressions (82).

Concerning the, sometimes, weak concordance found between the predicted targets and the ones mentioned in the literature, it may be related to updates that have been made to the databases and algorithms since those papers were published.

Finally, it is worth mentioning that the same problem found in the RNA choice and primer design was found also in this step: different databases and algorithms use different miRNA notations, which may generate misinterpretations.

3. Future Perspectives

The main suggestion for future research that arises from this study concerns a better characterization and stratification of preeclampsia. There are many pointers to indicate that different pathophysiologies underlie different phenotypes of this syndrome, which should be further explored (116). New findings in this front would open doors to understanding the differing and common mechanisms in the subtypes of the condition. Moreover, a direct impact of the lack of knowledge about preeclampsia mechanisms and pathophysiology is the absence of a consensus concerning the parameters for diagnosis of different types of the condition, which seem to be somewhat subjective (117). For instance, in the latest years, studies have been defining early preeclampsia as arising before thresholds that vary between twenty-eight and thirty-seven weeks of gestation. Others have described severe preeclampsia according to various blood pressure values, and early preeclampsia has frequently been assumed to be severe (15, 117).

Therefore, it would be of great value for researchers if a definition was internationally accepted and used, preferably taking into account not only phenotypical characteristics, but also molecular markers. This could open doors for more personalized approaches when managing the syndrome, possibly leading to better outcomes.

Concerning miRNAs, more knowledge about their mechanisms would be of great importance, in order to have a better understanding of their roles and shed light on how they affect disease. In addition, the targeting of a mRNA by multiple miRNAs has recently been hypothesized to be determinant to gene expression, constituting a new research possibility which may be unveiled as crucial in the future (118). In addition, while known complications associated to target-prediction algorithms are not solved, any putative miRNA targets should be validated experimentally (118). These experiments could include a range of assays, from RNAi assays to proteome analysis and microarrays (82).

It seems imperative for future studies to convey explicitly when the diagnosis was established and the severity of the condition, in order to assess which miRNAs are differentially expressed in the different phenotypes. This would be crucial to shed light on the mechanistic differences and similarities between them. Equally, the specific location from where the tissue under analysis derives should be clearly mentioned, since it has been shown that different areas of the placenta, and even different types of chorionic villi, have different miRNA profiles (119, 120). In addition, an effort should be made to include larger numbers of cases, since they would allow small differences to be detected. All these parameters constitute possible reasons for the many contrasting results found in the literature. These conflicting reports due to such technical constraints are an obstacle to reaching reasonable conclusions and obtaining further knowledge about preeclampsia.

Recently, miRNA *in* situ hybridization has been used in the context of preeclampsia. This technique may unveil vital morphological and functional information on how miRNAs are distributed in the placenta and how they may act in pathological states. It has already been applied in some studies, yielding remarkable results concerning miRNA distribution throughout the different placental structures (121).

Likewise, miRNA detection in maternal serum may hold a very promising future. Indeed, these molecules are generally detected in higher levels in maternal circulating blood in preeclampsia cases, compared to healthy pregnancies (122). Moreover, the study of shed placental debris, such as exosomes, is a very interesting line of research which has recently started to be explored concerning miRNAs and preeclampsia. Interestingly, among other substances, these nanovesicles carry trophoblastic miRNAs throughout the maternal body, seemingly contributing to trigger inflammatory reactions (123, 124). Analysis of serum miRNA may, in the future, constitute a good, pre-symptomatic and non-invasive diagnostic tool. If certain miRNA profiles are identified as biomarkers for preeclampsia, there is hope for a better understanding and management of this pathological condition.

Conclusion

The obtained results indicate that certain miRNAs are differentially expressed in preeclamptic placentas, compared to healthy controls. Revisiting divergent studies concerning placental miRNAs in preeclampsia, our findings partly confirm previous reports, and partly may contribute to resolve these discrepancies. Even more importantly, the results, combined with bibliographical references, lend support to the notion that mild and severe preeclampsia may be different entities, suggesting that while some pathways and mechanisms are common to preeclampsia as a whole, others are more specific of each subtype. If this hypothesis is confirmed, it may constitute a partial explanation for the great divergence commonly found in studies concerning miRNAs and preeclampsia.

Opening doors and raising new questions, this study incites new projects to improve the characterization of different phenotypes of preeclampsia, to better describe placental miRNA profiles, and to produce more findings about miRNA mechanisms and targets. New questions will undoubtedly arise, as will new lines of study, and each step will gradually contribute to the generation of new knowledge, providing new insights to the origins, and the possibility to shape the outcomes, of preeclampsia.

Glossary

Abrupto placentae – when the placental lining detaches from the uterus, before birth; also known as placental abruption (130).

Activin A – protein complex with effects on cell differentiation and embryonic development (131).

ActRIIA – activin receptor coding gene (83).

ACYP2 – enzyme responsible for the hydrolysis of the phosphoenzyme intermediate of different membrane pumps (83).

ADAMTS1 – gene for a metalloproteinase involved in inflammatory processes, fertility and organ morphology/function (83).

AlphaVbeta3 Integrin – protein that modulates cell adhesion, regulating angiogenesis and cell migration (131).

Angiopoietin – a proteic growth factor involved in the regulation of angiogenesis (131).

Antiphospholipid antibody syndrome – disorder associated to anticardiolipin antibodies, blood clots, miscarriage and unsuccessful pregnancy outcomes (130).

Apoptosis – programmed death of specific cells, at particular time points (132).

Arterial disease – condition characterized by reduced blood perfusion, resulting from atherosclerosis (131).

ARCN1 –coding gene of an intracellular protein involved in vesicle structure or trafficking.

Argonaute proteins (AGO) – family of proteins involved in gene silencing, part of the RISC (43).

ARL13B – gene for a small GTPase localized in the cilia (83).

Aspiration pneumonia – inflammation of airways and lungs (133).

Blastocyst – structure in foetal development preceded by the morula stage (134).

Body mass index – a measure of "body build", based on the individual's height and weight (130).

Breech presentation – when the foetus presents the feet towards the birth canal, creating a difficulty for delivery (135).

B-cells – lymphocytes that produce antibody-producing plasma cells (132).

5' Cap – structure present in mature mRNAs, characterized by a modified A or G bound to the rest of the chain by an unusual 5'-5' triphosphate link; it contributes to the stability and translation of mRNA (132).

Calmodulin – protein activator dependent on Ca^{2+} binding (131).

CACNA2D4 –coding gene of part of the voltage-dependent calcium channels, mediating entry of calcium into cells (83).

CASK –coding gene of a calcium/calmodulin-dependent serine protein kinase (83).

CD163 –coding gene for a receptor which provides protection against oxidative damage, having a role in cell iron recycling (83).

Chorionic villi – structures responsible for providing a greater area of contact with maternal blood in order to increase oxygen and nutrient exchange between the foetus and the mother (134).

Chromatin – complex of DNA and associated proteins, histones (132).

Chronic hypertension – persistent high blood pressure (130).

Chronic renal disease – condition resulting from damaged kidneys which filter blood waste products deficiently, leading to their accumulation in the body (136).

Competing endogenous RNAs (ceRNAs) – RNA molecules that sequester miRNA complexes, keeping them from binding to other RNA targets (49).

CORO1C – gene coding a protein involved in cell cycle progression, signal transduction, apoptosis and gene regulation (83).

Cytokine – class of molecules that bind to specific receptors of antigen-presenting cells and influence growth, differentiation and antibody production (132).

Cytotrophoblast – inner layer of mononucleated cells differentiated from trophoblasts (134).

Decidua – specialized modification of the endometrium to accommodate pregnancy (134).

Diabetes mellitus – metabolic disease in which the liver produces excessive glucose that is underutilized by the organism; type I is characterized by its low blood insulin levels, while type II of the disease is characterized by unresponsiveness to the present hormone (132).

Dicer – member of the RNase III family, specific for double-stranded RNA; it plays a role in the processing that leads to the formation of mature miRNAs (43).

Drosha – member of the RNase III family, involved in the processing of pri-miRNAs into pre-miRNAs (43).

Eclampsia – pregnancy disorder characterized by convulsions during which the patients lose consciousness and do not perform respiratory efforts (6, 130).

EFNA3 – gene coding ephrin 3A, responsible for targeting trophoblasts to the uterine tissue and spiral arteries (83).

eIF4F complex – protein complex which includes eukaryotic initiation factors -4A, -4E and -4G; it plays a role in the initiation of mRNA translation (131).

Endometrium – innermost membrane of the uterus, developed to accommodate embryo implantation and placentation (134).

Endoplasmic reticulum – cellular organelle defined by a membrane connected to the nuclear membranes; its functions include drug detoxification and protein post-translational modifications (132).

Epigastric – that which is in the upper central area of the abdomen (130).

Exonucleolytic degradation – results from removal of nucleotides from either end of the nucleotidic strand, by an exonuclease (132).

FFPE tissue – standardized method for preservation of specimens, creating large archives; compatible with anatomy and morphology studies, but also molecular analyses (62).

FGF2 – gene coding a fibroblast growth factor with mitogenic and angiogenic activities (83).

GATA4 – gene for a transcriptional activator, mediator of embryogenesis (83).

GJA1 – connexin coding gene, a major gap-junction protein (83).

GPD1L –coding gene of a protein which binds an integral membrane protein, encoded by SCN5A, responsible for mediating sodium permeability dependent of voltage, in excitable membranes (83).

Glycodelin A – protein produced in the reproductive tract, isolated from amniotic fluid, with immunosuppressive functions (137).

HELLP syndrome – a possible outcome of severe preeclampsia characterized by haemolysis, high liver enzymes and decreased platelet count (130).

HIF1A – gene coding for a subunit of a negative regulator of hypoxia-inducible gene expression (83).

HIF3A – gene coding for a subunit of a transcription factor which inhibits expression of hypoxia-inducible genes (83).

HLA-G – non-classical class I human histocompatibility surface antigen, expressed on cells derived from the foetus (131).

HOXA9 – gene for a transcription factor involved in regulation of angiogenesis and cell migration, during embryonic development (83).

Hyperhomocysteinemia – disease associated to raised levels of plasma homocysteine and associated metabolites; it can be acquired or familial; it is a risk factor for cardiovascular diseases and pregnancy complications (131).

Hypoplasia – partial development or under development of a tissue or an organ (131).

Hypoxia – reduced presence of oxygen (131).

Interferon-γ (IFN-γ) – a cytokine mainly produced by NK cells, which stimulates the immune system (132).

Interleukine-1β (IL-1β) – an interleukin-1 subtype; synthesized as a membrane pro-protein (131).

Interleukine-6 (IL-6) – interleukine that functions as a growth factor, responsible for stimulating growth and differentiation of B-lymphocytes (131).

Interleukine-8 (IL-8) – molecules involved in inflammatory responses, inducing chemotaxis of inflammatory cells (131).

Interleukine-16 (IL-16) – molecules that stimulate migration of lymphocytes and monocytes (131).

ISCU – gene coding a Fe-S cluster scaffold protein, essential for the function of mitochondrial enzymes (83).

Keratin – class of scleroproteins; main component of the epidermis, responsible for the protective and supportive characteristics of hair and nails (131).

Lacunae – intercommunicating channels that permeate the syncytiotrophoblastic structure (134).

LfR – coding gene of the intestinal lactoferrin receptor, which regulates the functions of lactoferrin (83).

Macrophage – cells of the immune system with phagocytic properties (131).

Major histocompatibility antigen – antigen detected by the MHC surface proteins (131).

MEF2a – gene for transcription factor involved in cell growth control and apoptosis, activating growth factor-induced genes (83).

Metalloproteinases – proteins that affect cell migration, acting intercellularly (131).

MHC – immune response genes responsible for controlling the response to antigens (131).

MHC class I protein – molecule that presents peptides from foreign cytoplasmic proteins to $CD8^+$ cytotoxic T-cells (132).

MicroRNA – class of small non-coding RNAs that are implicated in gene expression regulation (132).

Microvilli – structures on the syncytiotrophoblastic surface that enhance direct contact with maternal blood (134).

mRNA – template for protein synthesis (132).

miRNA* - less stable strand produced from the cleavage of pre-miRNA by Dicer; traditionally thought to be degraded and non-functional (49).

miRNA-3p – miRNA molecule produced from the 3' arm of a pre-miRNA molecule (53).

miRNA-5p – miRNA molecule produced from the 5' arm of a pre-miRNA molecule (53).

miRtron pathway - network that leads to the production of miRNAs from introns, resorting to the splicing machinery (54).

Mitochondrion – cellular organelle responsible for providing energy (ATP) to the cell. It is also involved in apoptosis (132).

Molar pregnancy – gestation associated to trophoblastic hypoplasia, characterised by swollen chorionic villi and high levels of chorionic gonadotropin (131).

Natural killer cells – group of lymphocytes with non-antigen-specific cytotoxic properties (131).

Necrosis – unregulated death of cells with irreparable damages (131).

NF-kB – Tumour necrosis factor receptor activated by reactive oxygen species (83).

Nodal – protein of the TGF superfamily: expressed asymmetrically in the body, after gastrulation, which mediates the genesis of left-right asymmetry in developmental stages (131).

Notch signalling – signalling pathway centred on Notch receptors, composed of an extracellular and a cytoplasmic domain; the latter is released upon ligand binding, and serves as a transcription factor (131).

Nulliparity – first gestation (130).

Oliguria – diminished production of urine (<20 mL per hour, for two successive hours) (130).

Oxidative stress – higher levels of oxidative molecules compared to antioxidants; it may lead to cellular damage, namely of DNA bases (131).

Paxillin – protein involved in focal cell adhesion (131).

PCR – molecular biology experimental method for exponential DNA amplification (132).

PISD – gene coding for the phosphatidylserine decarboxylase targeted to the inner mitochondrial membrane (131).

Placental growth factor – proangiogenic factor produced by decidual natural killer cells (134).

Placental infarction – consequence of villous necrosis due to local blockage of uteroplacental blood circulation (138).

Poly(A) – polyadenilation which is added to the 3'end of most mRNAs; it confers enhanced stability and improves translation efficiency (132).

Poly(A)-binding protein (PABP) – protein that binds to the 3' poly(A) tail of mRNAs (45).

Polymerase – Enzyme that polymerises daughter strands from a nucleic acid template sequence (131).

PAPPA – gene for a metalloproteinase involved in proliferative processes (83).

PPAP2A – gene for a surface enzyme important for the uptake of lipids (83).

pre-miRNAs – structures resulting from the processing of pri-miRNAs by Drosha; characterized by an imperfect double-stranded RNA hairpin (43).

pri-miRNAs – long RNA molecules that are the first intermediate in the formation of miRNAs; their processing produces pre-miRNAs (49).

Proteinuria – presence of protein in urine (130).

PRRX1 – gene for a transcription co-activator in various mesodermal-derived tissues (83).

Pulmonary oedema – condition characterized by an excessive accumulation of extravascular fluid in the lung, which prevents gas exchange (131).

Reverse transcriptase – enzyme that synthesizes DNA from an RNA template, performing a reverse transcription (131).

Rheumatic diseases – conditions of the connective tissue, characterized by inflammation, deterioration and/or metabolic instability (131).

RISC – large complex of proteins, involved in gene silencing; once coupled with miRNA molecules, it becomes miRISC (49).

Serine-protease – enzyme that cleaves peptide bonds due to a reactive serine residue (132).

Spiral arteries – arterial vessels which regulate the blood flow to the placenta (139).

Syncytial knots – structures formed on the terminal villi, where degenerated syncytiotrophoblast nuclei are accumulated (31).

Syncytiotrophoblast – outer multinucleated syncytium, originated from the differentiation of trophoblasts (134).

Syncytiotrophoblast microparticles – membrane vesicles created by flaking of cell membrane blebs (131).

THSD7A – gene coding for an inhibitor of endothelial cell migration and tube formation, found in endothelial cells from the placenta and umbilical cord (83)

Transforming growth factor-β1 (TGF-β1) – subtype of TGF-beta; connected to embryonic development, cell differentiation, secretion of hormones and immune system activities (131).

Transforming growth factor-β3 (TGF-β3) – TGF-beta subtype that in involved in epithelial-mesenchymal interactions in the embryonic development (131).

Tumour necrosis factor-α (TNF-α) – glycoprotein with necrotic activity against tumour cells; produced by activated mononuclear leukocytes (131).

Th2 phenotype – phenotype characterized mostly by humoral immune responses, with proliferation of B-cells, and induced production of neutralizing antibodies (131).

Thrombocytopenia – low quantity of platelets in the blood (130).

Thrombophilia – disorder associated with a greater chance for the individual to form blood clots (130).

Trophoblast – cellular layer that encloses the blastocyst; vital for correct implantation in the uterus (134).

T-cells – cytotoxic lymphocytes responsible for killing cells invaded by pathogens (132).

Untranslated region (UTR) – portion of the mRNA sequence that does not code for any peptide product (131).

Vascular endothelial growth factors – signalling molecules that enable the development of blood vessels (132).

VEGFA – vascular endothelial growth factor, inducer of cell migration, angiogenesis, vasculogenesis and growth (83).

XPO5 – protein mediator of molecule transport from the nucleus to the cytoplasm (49).

References

1. Gunel T, Zeybek YG, Akcakaya P, Kalelioglu I, Benian A, Ermis H, et al. Serum microRNA expression in pregnancies with preeclampsia. Genetics and molecular research. 2011;10(4). PubMed PMID: 22095477. Epub 2011/11/19. Eng.

2. Ghulmiyyah L, Sibai B. Maternal mortality from preeclampsia/eclampsia. Seminars in perinatology. 2012;36(1):56-9. PubMed PMID: 22280867. Epub 2012/01/28. eng.

3. Anderson UD, Olsson MG, Kristensen KH, Akerstrom B, Hansson SR. Review: Biochemical markers to predict preeclampsia. Placenta. 2012;33 Suppl:S42-7. PubMed PMID: 22197626. Epub 2011/12/27. eng.

4. Dahlstrom BL, Engh ME, Bukholm G, Oian P. Changes in the prevalence of pre-eclampsia in Akershus County and the rest of Norway during the past 35 years. Acta obstetricia et gynecologica Scandinavica. 2006;85(8):916-21. PubMed PMID: 16862468. Epub 2006/07/25. eng.

5. Redman CW, Sargent IL. Latest advances in understanding preeclampsia. Science. 2005;308(5728):1592-4. PubMed PMID: 15947178. Epub 2005/06/11. eng.

6. Leeman L, Fontaine P. Hypertensive disorders of pregnancy. American family physician. 2008;78(1):93-100. PubMed PMID: 18649616. Epub 2008/07/25. eng.

7. Salvador-Moysén J, Martínez-López Y, Ramírez-Aranda JM, Aguilar-Durán M, Terrones-González A. Genesis of Preeclampsia: An Epidemiological Approach. Improvement Science Research Network: Obstetrics and Gynecology. 2012;2012. PubMed PMID: 22462008. eng.

8. Roberts JM, Lain KY. Recent Insights into the pathogenesis of pre-eclampsia. Placenta. 2002;23(5):359-72. PubMed PMID: 12061851. Epub 2002/06/14. eng.

9. Sibai B, Dekker G, Kupferminc M. Pre-eclampsia. The Lancet. 2005;365(9461):785-99.

10. Maternal Health and Safe Motherhood Programme DoFH, World Health Organization. Detecting pre-eclampsia: a practical guide. Geneva: World Health Organization; 2005 2005. 52 p.

11. World Health Organization. WHO recommendations for prevention and treatment of pre-eclampsia and eclampsia. Geneva: World Health Organization; 2011.

12. Quinn KH, Lacoursiere DY, Cui L, Bui J, Parast MM. The unique pathophysiology of early-onset severe preeclampsia: role of decidual T regulatory cells. Journal of reproductive immunology. 2011;91(1-2):76-82. PubMed PMID: 21782252. Epub 2011/07/26. eng.

13. Hernandez-Diaz S, Toh S, Cnattingius S. Risk of pre-eclampsia in first and subsequent pregnancies: prospective cohort study. British Medical Journal. 2009;338:b2255. PubMed PMID: 19541696. Pubmed Central PMCID: 3269902.

14. Phillips JK, Janowiak M, Badger GJ, Bernstein IM. Evidence for Distinct Preterm and Term Phenotypes of Preeclampsia. The journal of maternal-fetal & neonatal medicine : the

official journal of the European Association of Perinatal Medicine, the Federation of Asia and Oceania Perinatal Societies, the International Society of Perinatal Obstet. 2010;23(7):622-6. PubMed PMID: 20482241. eng.

15. Vatten LJ, Skjærven R. Is pre-eclampsia more than one disease? BJOG: An International Journal of Obstetrics & Gynaecology. 2004;111(4):298-302.

16. Fisher SJ. The placental problem: linking abnormal cytotrophoblast differentiation to the maternal symptoms of preeclampsia. Reproductive biology and endocrinology : RB&E. 2004;2:53. PubMed PMID: 15236649. Pubmed Central PMCID: 493282. Epub 2004/07/09. eng.

17. Jensen F, Wallukat G, Herse F, Budner O, El-Mousleh T, Costa SD, et al. CD19+CD5+ cells as indicators of preeclampsia. Hypertension. 2012;59(4):861-8. PubMed PMID: 22353610. Epub 2012/02/23. eng.

18. Wang Y, Zhao S. Placental Blood Circulation. Vascular Biology of the Placenta. Integrated Systems Physiology: from Molecules to Function to Disease. San Rafael (CA)2010.

19. Huppertz B. Placental origins of preeclampsia: challenging the current hypothesis. Hypertension. 2008;51(4):970-5. PubMed PMID: 18259009. Epub 2008/02/09. eng.

20. da Graça LMB, J.J.S. Morfologia da placenta e dos anexos fetais. In: Lidel, editor. Medicina materno-fetal. Lisboa: Lidel; 2010. p. 14-31.

21. Gilbert SF. Early Mammalian Development. In: Sunderland, editor. Developmental biology. 6th ed. MA: Sinauer Associates; 2000.

22. Schöni-Affolter F, Dubuis-Grieder C, Strauch E. embryology.ch: Universities of Fribourg, Lausanne and Bern 2005 [updated 2008; cited 2012 July]. Available from: http://www.embryology.ch/indexen.html.

23. Calhaz-Jorge C. Ovulação, fecundação e implantação. In: Lidel, editor. Medicina Materno-Fetal. Lisboa: Lidel; 2010. p. 3-13.

24. Kim YN, Kim HK, Warda M, Kim N, Park WS, Prince Adel B, et al. Toward a better understanding of preeclampsia: Comparative proteomic analysis of preeclamptic placentas. Proteomics Clinical applications. 2007;1(12):1625-36. PubMed PMID: 21136660. Epub 2007/12/01. eng.

25. da Graça LM. Fisiologia da unidade feto-placentária. In: Lidel, editor. Medicina materno-fetal. Lisboa: Lidel; 2010. p. 32-8.

26. Dormer A, Beck G. Evolutionary analysis of human vascular endothelial growth factor, angiopoietin, and tyrosine endothelial kinase involved in angiogenesis and immunity. In silico biology. 2005;5(3):323-39. PubMed PMID: 15984940. Epub 2005/06/30. eng.

27. Laresgoiti-Servitje E, Gomez-Lopez N, Olson DM. An immunological insight into the origins of pre-eclampsia. Hum Reprod Update. 2010;16(5):510-24. PubMed PMID: 20388637. Epub 2010/04/15. eng.

28. Hunt JS, Petroff MG, Burnett TG. Uterine leukocytes: key players in pregnancy. Seminars in cell & developmental biology. 2000;11(2):127-37. PubMed PMID: 10873709. Epub 2000/06/30. eng.

29. Wang Y, Zhao S. Oxygen Tension and Placental Vascular Development. Vascular Biology of the Placenta. Integrated Systems Physiology: from Molecules to Function to Disease. San Rafael (CA)2010.

30. Wang Y, Zhao S. Structure of the Placenta. Vascular Biology of the Placenta: Morgan & Claypool; 2010.

31. Heazell AEP, Moll SJ, Jones CJP, Baker PN, Crocker IP. Formation of Syncytial Knots is Increased by Hyperoxia, Hypoxia and Reactive Oxygen Species. Placenta. 2007;28, Supplement(0):S33-S40.

32. Nikkels PGJ. Placenta pathology associated with maturation abnormalities and late intra uterine foetal death. Placenta. 2006:10:293-9.

33. Akhlaq M, Nagi AH, Yousaf AW. Placental morphology in pre-eclampsia and eclampsia and the likely role of NK cells. Indian journal of pathology & microbiology. 2012;55(1):17-21. PubMed PMID: 22499294. Epub 2012/04/14. eng.

34. Muralimanoharan S, Maloyan A, Mele J, Guo C, Myatt LG, Myatt L. MIR-210 modulates mitochondrial respiration in placenta with preeclampsia. Placenta. 2012;33(10):816-23. PubMed PMID: 22840297. Pubmed Central PMCID: PMC3439551. Epub 2012/07/31. eng.

35. Ray J, Vasishta K, Kaur S, Majumdar S, Sawhney H. Calcium metabolism in pre-eclampsia. International journal of gynaecology and obstetrics: the official organ of the International Federation of Gynaecology and Obstetrics. 1999;66(3):245-50. PubMed PMID: 10580671. Epub 1999/12/02. eng.

36. Wang Y, Zhao S. Cell Types of the Placenta. Vascular Biology of the Placenta. Integrated Systems Physiology: from Molecules to Function to Disease. San Rafael (CA)2010.

37. Roberts JM, Hubel CA. The two stage model of preeclampsia: variations on the theme. Placenta. 2009;30 Suppl A:S32-7. PubMed PMID: 19070896. Pubmed Central PMCID: 2680383. Epub 2008/12/17. eng.

38. Pennington KA, Schlitt JM, Jackson DL, Schulz LC, Schust DJ. Preeclampsia: multiple approaches for a multifactorial disease. Disease models & mechanisms. 2012;5(1):9-18. PubMed PMID: 22228789. Pubmed Central PMCID: 3255538. Epub 2012/01/10. eng.

39. Ness RB, Roberts JM. Heterogeneous causes constituting the single syndrome of preeclampsia: a hypothesis and its implications. American journal of obstetrics and gynecology. 1996;175(5):1365-70. PubMed PMID: 8942516. Epub 1996/11/01. eng.

40. Bell MJ. A historical overview of preeclampsia-eclampsia. Journal of obstetric, gynecologic, and neonatal nursing : JOGNN / NAACOG. 2010;39(5):510-8. PubMed PMID: 20919997. Pubmed Central PMCID: 2951301. Epub 2010/10/06. eng.

41. Gilad S, Meiri E, Yogev Y, Benjamin S, Lebanony D, Yerushalmi N, et al. Serum microRNAs are promising novel biomarkers. Public Library of Science One. 2008;3(9):e3148. PubMed PMID: 18773077. Pubmed Central PMCID: 2519789. Epub 2008/09/06. eng.

42. Kroh EM, Parkin RK, Mitchell PS, Tewari M. Analysis of circulating microRNA biomarkers in plasma and serum using quantitative reverse transcription-PCR (qRT-PCR). Methods. 2010;50(4):298-301. PubMed PMID: 20146939. Epub 2010/02/12. eng.

43. Filipowicz W, Bhattacharyya SN, Sonenberg N. Mechanisms of post-transcriptional regulation by microRNAs: are the answers in sight? Nature reviews Genetics. 2008;9(2):102-14. PubMed PMID: 18197166. Epub 2008/01/17. eng.

44. Lee Y, Kim M, Han J, Yeom K-H, Lee S, Baek SH, et al. MicroRNA genes are transcribed by RNA polymerase II. European Molecular Biology Organization. 2004;23(20):4051-60.

45. Lewin B. Genes 9. 9 ed. USA: Jones & Bartlett Learning; 2008.

46. Bartel DP. MicroRNAs: target recognition and regulatory functions. Cell. 2009;136(2):215-33. PubMed PMID: 19167326. Epub 2009/01/27. eng.

47. Pritchard CC, Cheng HH, Tewari M. MicroRNA profiling: approaches and considerations. Nature reviews Genetics. 2012;13(5):358-69. PubMed PMID: 22510765. Epub 2012/04/19. eng.

48. Krol J, Loedige I, Filipowicz W. The widespread regulation of microRNA biogenesis, function and decay. Nature reviews Genetics. 2010;11(9):597-610.

49. Pasquinelli AE. MicroRNAs and their targets: recognition, regulation and an emerging reciprocal relationship. Nature reviews Genetics. 2012;13(4):271-82. PubMed PMID: 22411466. Epub 2012/03/14. eng.

50. Huntzinger E, Izaurralde E. Gene silencing by microRNAs: contributions of translational repression and mRNA decay. Nature reviews Genetics. 2011;12(2):99-110.

51. Place RF, Li L-C, Pookot D, Noonan EJ, Dahiya R. MicroRNA-373 induces expression of genes with complementary promoter sequences. Proceedings of the National Academy of Sciences. 2008;105(5):1608-13.

52. Steer CJ, Subramanian S. Circulating microRNAs as biomarkers: A new frontier in diagnostics. Liver Transplantation. 2012;18(3):265-9.

53. Griffiths-Jones S, Grocock RJ, van Dongen S, Bateman A, Enright AJ. miRBase: microRNA sequences, targets and gene nomenclature. Nucleic Acids Research. 2006;34(suppl 1):D140-D4.

54. Iorio MV, Croce CM. MicroRNA dysregulation in cancer: diagnostics, monitoring and therapeutics. A comprehensive review. European Molecular Biology Organization: Molecular Medicine. 2012;4(3):143-59.

55. Orom UA, Nielsen FC, Lund AH. MicroRNA-10a binds the 5'UTR of ribosomal protein mRNAs and enhances their translation. Molecular cell. 2008;30(4):460-71. PubMed PMID: 18498749. Epub 2008/05/24. eng.

56. Meola N, Gennarino V, Banfi S. microRNAs and genetic diseases. PathoGenetics. 2009;2(1):7. PubMed PMID: doi:10.1186/1755-8417-2-7.

57. Pineles BL, Romero R, Montenegro D, Tarca AL, Han YM, Kim YM, et al. Distinct subsets of microRNAs are expressed differentially in the human placentas of patients with preeclampsia. American journal of obstetrics and gynecology. 2007;196(3):261 e1-6. PubMed PMID: 17346547. Epub 2007/03/10. eng.

58. Enquobahrie DA, Abetew DF, Sorensen TK, Willoughby D, Chidambaram K, Williams MA. Placental microRNA expression in pregnancies complicated by preeclampsia. American journal of obstetrics and gynecology. 2011;204(2):178 e12-21. PubMed PMID: 21093846. Pubmed Central PMCID: 3040986. Epub 2010/11/26. eng.

59. Ishibashi O, Ohkuchi A, Ali MM, Kurashina R, Luo SS, Ishikawa T, et al. Hydroxysteroid (17-beta) dehydrogenase 1 is dysregulated by miR-210 and miR-518c that are aberrantly expressed in preeclamptic placentas: a novel marker for predicting preeclampsia. Hypertension. 2012;59(2):265-73. PubMed PMID: 22203747.

60. Hu Y, Li P, Hao S, Liu L, Zhao J, Hou Y. Differential expression of microRNAs in the placentae of Chinese patients with severe pre-eclampsia. Clinical chemistry and laboratory medicine : CCLM / FESCC. 2009;47(8):923-9. PubMed PMID: 19642860. Epub 2009/08/01. eng.

61. Zhang Y, Diao Z, Su L, Sun H, Li R, Cui H, et al. MicroRNA-155 contributes to preeclampsia by down-regulating CYR61. American journal of obstetrics and gynecology. 2010;202(5):466 e1-7. PubMed PMID: 20452491. Epub 2010/05/11. eng.

62. Doleshal M, Magotra AA, Choudhury B, Cannon BD, Labourier E, Szafranska AE. Evaluation and validation of total RNA extraction methods for microRNA expression analyses in formalin-fixed, paraffin-embedded tissues. The Journal of molecular diagnostics : JMD. 2008;10(3):203-11. PubMed PMID: 18403610. Pubmed Central PMCID: PMC2329784. Epub 2008/04/12. eng.

63. Powledge TM. The polymerase chain reaction. Advances in physiology education. 2004;28(1-4):44-50. PubMed PMID: 15149959. Epub 2004/05/20. eng.

64. Arya M, Shergill IS, Williamson M, Gommersall L, Arya N, Patel HR. Basic principles of real-time quantitative PCR. Expert review of molecular diagnostics. 2005;5(2):209-19. PubMed PMID: 15833050. Epub 2005/04/19. eng.

65. Pray LA. The Biotechnology Revolution: PCR and the Use of Reverse Transcriptase to Clone Expressed Genes: Nature Education 1 (1); 2008 [January 2013]. Available from: http://www.nature.com/scitable/topicpage/the-biotechnology-revolution-pcr-and-the-use-553.

66. Okello JB, Rodriguez L, Poinar D, Bos K, Okwi AL, Bimenya GS, et al. Quantitative assessment of the sensitivity of various commercial reverse transcriptases based on armored HIV RNA. Public Library of Science One. 2010;5(11):e13931. PubMed PMID: 21085668. Pubmed Central PMCID: PMC2978101. Epub 2010/11/19. eng.

67. Chen C, Ridzon DA, Broomer AJ, Zhou Z, Lee DH, Nguyen JT, et al. Real-time quantification of microRNAs by stem-loop RT-PCR. Nucleic Acids Res. 2005;33(20):e179. PubMed PMID: 16314309. Pubmed Central PMCID: 1292995.

68. Roche Diagnostics. LightCyler TaqMan Master: Roche; 2013 [cited 2013 April]. Available from: https://www.roche-applied-science.com/servlet/RCProductDisplay?storeId=10202&catalogId=10202&langId=-1&countryId=us&forCountryId=us&productId=3.5.5.1.3.10.

69. Sigma Life Science. qPCR Technical Guide: Sigma-Aldrich; 2008 [cited 2013 April]. Available from:

http://www.sigmaaldrich.com/etc/medialib/docs/Sigma/General_Information/qpcr_technical_guide.Par.0001.File.tmp/qpcr_technical_guide.pdf.

70. Invitrogen. Real-Time PCR: from theory to practice: life Technologies; 2008 [cited 2013 April]. Available from: http://corelabs.cgrb.oregonstate.edu/sites/default/files/Real%20Time%20PCR.From%20Theory%20to%20Practice.pdf.

71. Meistertzheim A-L, Calves I, Artigaud S, Friedman CS, Paillard C, Laroche J, et al. High Resolution Melting Analysis for fast and cheap polymorphism screening of marine populations. Protocol Exchange. 2012.

72. Eide IP. Fetal growth restriction and pre-eclampsia: some characteristics of fetomaternal interactions in decidua basalis. Trondheim: Norwegian University of Science and Technology; 2008.

73. Noack F, Ribbat-Idel J, Thorns C, Chiriac A, Axt-Fliedner R, Diedrich K, et al. miRNA expression profiling in formalin-fixed and paraffin-embedded placental tissue samples from pregnancies with severe preeclampsia. Journal of perinatal medicine. 2011;39(3):267-71. PubMed PMID: 21309633. Epub 2011/02/12. eng.

74. Zhu XM, Han T, Sargent IL, Yin GW, Yao YQ. Differential expression profile of microRNAs in human placentas from preeclamptic pregnancies vs normal pregnancies. American journal of obstetrics and gynecology. 2009;200(6):661 e1-7. PubMed PMID: 19285651. Epub 2009/03/17. eng.

75. Dybos SA. Verdien av miRNA som biomarkør for kreft i prostata: Optimalisering av metode for RNA-isolering av formalinfiksert parafininnstøpt vev, samt undersøkelse av miRNA-uttrykk i ulik grad av prostatakreft. Trondheim: NTNU; 2012.

76. Life Technologies. Protocol - RecoverAll™ Total Nucleic Acid Islation Kit Carlsbad, USA: life Technologies; 2011 [cited 2012 November]. Available from: http://tools.invitrogen.com/content/sfs/manuals/1975MC.pdf.

77. Thermo Scientific. NanoDrop Products - How it works 2009 [cited 2013 April]. Available from: http://www.nanodrop.com/HowItWorks.aspx.

78. Agilent Technologies. RNA kits and reagents - details & specifications: Agilent Technologies; 2012 [cited 2013 April]. Available from: http://www.genomics.agilent.com/CollectionSubpage.aspx?PageType=Product&SubPageType=ProductData&PageID=1648.

79. Invitrogen. Protocol: SuperScript® III First-Strand Synthesis SuperMix 2010 [updated May 2010; cited 2012 December]. Available from: http://tools.invitrogen.com/content/sfs/manuals/superscript_firststrandsupermix_man.pdf.

80. Abilock FHSMC. Optimizing the Polymerase Chain Reaction: Life Technologies,

Applied Biosciences,; 2001 [cited 2013 April]. Available from: http://babec.org/files/2011_PCR/Optimization_Student_Guide_Fall_2011.pdf.

81. Ye RWRMSMK. Probability & Statistics For Engineers and Scientists. Ninth (International Edition) ed. Lynch D, editor. USA: Pearson Education; 2012. 791 p.

82. Witkos TM, Koscianska E, Krzyzosiak WJ. Practical Aspects of microRNA Target Prediction. Current molecular medicine. 2011;11(2):93-109. PubMed PMID: 21342132. Pubmed Central PMCID: PMC3182075. Epub 2011/02/24. eng.

83. NCBI. NCBI Gene: National Center for Biotechnology Information, U.S. National Library of Medicine 2013 [cited 2013 May]. Available from: http://www.ncbi.nlm.nih.gov/gene.

84. Yang J. starBase sRNA target Base: Nucleic Acids Res; 2011 [cited 2013 April]. D202-D209:[Available from: http://starbase.sysu.edu.cn/clipSeq.php.

85. Bioinformatics and Research Computing (Whitehead Institute for Biomedical Research). TargetScanHuman Release 6.2 - Prediction of miRNA targets Whitehead Institute for Biomedical Research; 2012 [cited 2013 April]. Available from: http://www.targetscan.org/.

86. Bai Y, Yang W, Yang HX, Liao Q, Ye G, Fu G, et al. Downregulated miR-195 detected in preeclamptic placenta affects trophoblast cell invasion via modulating ActRIIA expression. Public Library of Science One. 2012;7(6):e38875. PubMed PMID: 22723898. Pubmed Central PMCID: PMC3378540. Epub 2012/06/23. eng.

87. Zhang Y, Fei M, Xue G, Zhou Q, Jia Y, Li L, et al. Elevated levels of hypoxia-inducible microRNA-210 in pre-eclampsia: new insights into molecular mechanisms for the disease. Journal of cellular and molecular medicine. 2012;16(2):249-59. PubMed PMID: 21388517. Epub 2011/03/11. eng.

88. Lou YL, Guo F, Liu F, Gao FL, Zhang PQ, Niu X, et al. miR-210 activates notch signaling pathway in angiogenesis induced by cerebral ischemia. Molecular and cellular biochemistry. 2012;370(1-2):45-51. PubMed PMID: 22833359. Epub 2012/07/27. eng.

89. Mayor-Lynn K, Toloubeydokhti T, Cruz AC, Chegini N. Expression profile of microRNAs and mRNAs in human placentas from pregnancies complicated by preeclampsia and preterm labor. Reproductive Sciences. 2011;18(1):46-56. PubMed PMID: 21079238. Epub 2010/11/17. eng.

90. Kelly TJ, Souza AL, Clish CB, Puigserver P. A hypoxia-induced positive feedback loop promotes hypoxia-inducible factor 1alpha stability through miR-210 suppression of glycerol-3-phosphate dehydrogenase 1-like. Molecular and cellular biology. 2011;31(13):2696-706. PubMed PMID: 21555452. Pubmed Central PMCID: PMC3133367. Epub 2011/05/11. eng.

91. Fasanaro P, D'Alessandra Y, Di Stefano V, Melchionna R, Romani S, Pompilio G, et al. MicroRNA-210 modulates endothelial cell response to hypoxia and inhibits the receptor tyrosine kinase ligand Ephrin-A3. The Journal of biological chemistry. 2008;283(23):15878-83. PubMed PMID: 18417479. Pubmed Central PMCID: PMC3259646. Epub 2008/04/18. eng.

92. Lee DC, Romero R, Kim JS, Tarca AL, Montenegro D, Pineles BL, et al. miR-210 targets iron-sulfur cluster scaffold homologue in human trophoblast cell lines: siderosis of interstitial trophoblasts as a novel pathology of preterm preeclampsia and small-for-gestational-age pregnancies. The American journal of pathology. 2011;179(2):590-602. PubMed PMID: 21801864. Pubmed Central PMCID: PMC3160082. Epub 2011/08/02. eng.

93. Fu G, Brkic J, Hayder H, Peng C. MicroRNAs in Human Placental Development and Pregnancy Complications. International journal of molecular sciences. 2013;14(3):5519-44. PubMed PMID: 23528856. Epub 2013/03/27. eng.

94. Nishimura T, Dunk C, Lu Y, Feng X, Gellhaus A, Winterhager E, et al. Gap junctions are required for trophoblast proliferation in early human placental development. Placenta. 2004;25(7):595-607. PubMed PMID: 15193866. Epub 2004/06/15. eng.

95. Thway TM, Shlykov SG, Day MC, Sanborn BM, Gilstrap LC, 3rd, Xia Y, et al. Antibodies from preeclamptic patients stimulate increased intracellular Ca2+ mobilization through angiotensin receptor activation. Circulation. 2004;110(12):1612-9. PubMed PMID: 15381659. Epub 2004/09/24. eng.

96. Baczyk D, Kingdom JCP, Uhlén P. Calcium signaling in placenta. Cell Calcium. 2011;49(5):350-6.

97. Burton GJ, Yung HW. Endoplasmic reticulum stress in the pathogenesis of early-onset pre-eclampsia. Pregnancy Hypertens. 2011;1(1-2):72-8. PubMed PMID: 22242213. Pubmed Central PMCID: PMC3252240. Epub 2012/01/14. Eng.

98. Burton GJ, Yung HW, Cindrova-Davies T, Charnock-Jones DS. Placental endoplasmic reticulum stress and oxidative stress in the pathophysiology of unexplained intrauterine growth restriction and early onset preeclampsia. Placenta. 2009;30 Suppl A:S43-8. PubMed PMID: 19081132. Pubmed Central PMCID: PMC2684656. Epub 2008/12/17. eng.

99. Larry CD, Yeo S. The circadian rhythm of blood pressure during pregnancy. Journal of obstetric, gynecologic, and neonatal nursing : JOGNN / NAACOG. 2000;29(5):500-8. PubMed PMID: 11012129. Epub 2000/09/30. eng.

100. Liao Y, Lonnerdal B. miR-584 mediates post-transcriptional expression of lactoferrin receptor in Caco-2 cells and in mouse small intestine during the perinatal period. The international journal of biochemistry & cell biology. 2010;42(8):1363-9. PubMed PMID: 19665576. Epub 2009/08/12. eng.

101. Siebolts U, Varnholt H, Drebber U, Dienes HP, Wickenhauser C, Odenthal M. Tissues from routine pathology archives are suitable for microRNA analyses by quantitative PCR. Journal of Clinical Pathology. 2009;62(1):84-8. PubMed PMID: 18755714. eng.

102. sam. miRBase blog: miRBase news and views [Internet]2011. [cited 2012]. Available from: http://www.mirbase.org/blog/2011/04/whats-in-a-name/.

103. Invitrogen. Comparison of fluorescence-based quantitation with UV absorbance measurements: Qubit™ Quantitation Platform vs. spectrophotometer: Invitrogen; 2010 [cited 2013 April]. Available from: http://www.invitrogen.com/site/us/en/home/brands/Product-Brand/Qubit/Qubit-Fluorometer-vs-Nanodrop-ND-1000-Spectrophotometer.html.

104. Thermo Scientific. NanoDrop Spectrophotometers: Assessment of Nucleic Acid Purity [cited 2013 April]. 2]. Available from: http://www.nanodrop.com/Library/T042-NanoDrop-Spectrophotometers-Nucleic-Acid-Purity-Ratios.pdf.

105. Agilent Technologies. Agilent Technologies Introduces Small RNA Kit for Bioanalyzer, Allowing miRNA to be Routinely Quantified in Total RNA Agilent Technologies; 2007 [cited 2013 April]. Available from: http://www.agilent.com/about/newsroom/presrel/2007/16apr-ca07023.html.

106. JMG - PI of Posters. cDNA Quantification BioTechniques Molecular BIology Techniques Forums2009 [cited 2013 May]. Available from: http://forums.biotechniques.com/viewtopic.php?f=16&t=23897.

107. EXIQON - Seek Find Verify. Pitfalls and recommendations for microRNA expression analysis using qPCR 2012 [cited 2013 May]. v2.1:[Available from: http://www.exiqon.com/ls/Documents/Scientific/miRNA-qPCR-guidelines.pdf.

108. Bustin SA, Benes V, Garson JA, Hellemans J, Huggett J, Kubista M, et al. The MIQE guidelines: minimum information for publication of quantitative real-time PCR experiments. Clinical chemistry. 2009;55(4):611-22. PubMed PMID: 19246619. Epub 2009/02/28. eng.

109. Leider M. Design. In: Sousa A, editor. E-mail2013.

110. Roux KH. Optimization and troubleshooting in PCR. Cold Spring Harbor protocols. 2009;2009(4):pdb ip66. PubMed PMID: 20147122. Epub 2010/02/12. eng.

111. Jegou T. LC2.0. In: Sousa A, editor. E-mail2013.

112. Henegariu O. PCR and multiplex PCR guide USA: Yale University; [cited 2013 April]. Available from: http://medicine.yale.edu/labs/henegariu/www/tavi/Guide.html.

113. Guilford JP, Fruchter B. Fundamental statistics in psychology and education. education Fsipa, editor: McGraw-Hill; 1978.

114. Boneau CA. The effects of violations of assumptions underlying the t test. Psychological bulletin. 1960;57:49-64. PubMed PMID: 13802482. Epub 1960/01/01. eng.

115. Blair RC, Higgins JJ. A Comparison of the Power of Wilcoxon's Rank-Sum Statistic to That of Student's t Statistic under Various Nonnormal Distributions. Journal of Educational Statistics. 1980;5(4):309-35.

116. Raymond D, Peterson E. A critical review of early-onset and late-onset preeclampsia. Obstetrical & gynecological survey. 2011;66(8):497-506. PubMed PMID: 22018452. Epub 2011/10/25. eng.

117. Tranquilli AL, Brown MA, Zeeman GG, Dekker G, Sibai BM. The definition of severe and early-onset preeclampsia. Statements from the International Society for the Study of Hypertension in Pregnancy (ISSHP). Pregnancy Hypertension: An International Journal of Women's Cardiovascular Health. 2013;3(1):44-7.

118. Peter ME. Targeting of mRNAs by multiple miRNAs: the next step. Oncogene. 2010;29(15):2161-4.

119. Ji L, Brkic J, Liu M, Fu G, Peng C, Wang YL. Placental trophoblast cell differentiation: Physiological regulation and pathological relevance to preeclampsia. Molecular aspects of medicine. 2012. PubMed PMID: 23276825. Epub 2013/01/02. Eng.

120. Wang D, Song W, Na Q. The emerging roles of placenta-specific microRNAs in regulating trophoblast proliferation during the first trimester. The Australian & New Zealand journal of obstetrics & gynaecology. 2012;52(6):565-70. PubMed PMID: 23046105. Epub 2012/10/11. eng.

121. Wang W, Feng L, Zhang H, Hachy S, Satohisa S, Laurent LC, et al. Preeclampsia up-regulates angiogenesis-associated microRNA (i.e., miR-17, -20a, and -20b) that target ephrin-B2 and EPHB4 in human placenta. The Journal of clinical endocrinology and metabolism. 2012;97(6):E1051-9. PubMed PMID: 22438230. Pubmed Central PMCID: PMC3387422. Epub 2012/03/23. eng.

122. Wu L, Zhou H, Lin H, Qi J, Zhu C, Gao Z, et al. Circulating microRNAs are elevated in plasma from severe preeclamptic pregnancies. Reproduction. 2012;143(3):389-97. PubMed PMID: 22187671. Epub 2011/12/22. eng.

123. Redman CW, Tannetta DS, Dragovic RA, Gardiner C, Southcombe JH, Collett GP, et al. Review: Does size matter? Placental debris and the pathophysiology of pre-eclampsia. Placenta. 2012;33 Suppl:S48-54. PubMed PMID: 22217911. Epub 2012/01/06. eng.

124. Germain SJ, Sacks GP, Sooranna SR, Sargent IL, Redman CW. Systemic inflammatory priming in normal pregnancy and preeclampsia: the role of circulating syncytiotrophoblast microparticles. Journal of immunology. 2007;178(9):5949-56. PubMed PMID: 17442979. Epub 2007/04/20. eng.

125. Guo L, Yang Q, Lu J, Li H, Ge Q, Gu W, et al. A comprehensive survey of miRNA repertoire and 3' addition events in the placentas of patients with pre-eclampsia from high-throughput sequencing. Public Library of Science One. 2011;6(6):e21072. PubMed PMID: 21731650. Pubmed Central PMCID: PMC3120834. Epub 2011/07/07. eng.

126. Guo L, Tsai SQ, Hardison NE, James AH, Motsinger-Reif AA, Thames B, et al. Differentially expressed microRNAs and affected biological pathways revealed by modulated modularity clustering (MMC) analysis of human preeclamptic and IUGR placentas. Placenta. 2013(0).

127. Liu L, Wang Y, Fan H, Zhao X, Liu D, Hu Y, et al. MicroRNA-181a regulates local immune balance by inhibiting proliferation and immunosuppressive properties of mesenchymal stem cells. Stem Cells. 2012;30(8):1756-70. PubMed PMID: 22714950. Epub 2012/06/21. eng.

128. Lazar L, Nagy B, Molvarec A, Szarka A, Rigo J, Jr. Role of hsa-miR-325 in the etiopathology of preeclampsia. Molecular medicine reports. 2012;6(3):597-600. PubMed PMID: 22710575. Epub 2012/06/20. eng.

129. Fu G, Ye G, Nadeem L, Ji L, Manchanda T, Wang Y, et al. MicroRNA-376c Impairs Transforming Growth Factor-beta and Nodal Signaling to Promote Trophoblast Cell Proliferation and Invasion. Hypertension. 2013. PubMed PMID: 23424236. Epub 2013/02/21. Eng.

130. National Collaborating Centre for Women's and Children's Health. Hypertension in Pregnancy: The Management of Hypertensive Disorders in Pregnancy. 2012. In: NICE Clinical Guidelines [Internet]. UK, London: RCOG Press. Available from: http://www.ncbi.nlm.nih.gov/books/NBK62634/.

131. National Center for Biotechnology Information. MeSH Database Bethesda MD: U.S. National Library of Medicine; 2013 [cited 2013 January]. Available from: http://www.ncbi.nlm.nih.gov/mesh.

132. Berg JM, Tymoczko JL, Stryer L. Biochemistry. 6th ed. USA: W. H. Freeman; 2006.

133. MedlinePlus. Aspiration Pneumonia Bethesda, MD: National Library of Medicine; 2011 [cited 2013 January]. Available from: http://www.nlm.nih.gov/medlineplus/ency/article/000121.htm.

134. Cunningham F, Leveno K, Bloom S, Hauth J, Rouse D, Spong C. Williams Obstetrics: 23rd Edition: McGraw-Hill Education; 2009.

135. MedlinePlus. Delivery presentations Bethesda, MD: National Library of Medicine 2012 [cited 2013 January]. Available from: http://www.nlm.nih.gov/medlineplus/ency/article/002060.htm.

136. MedlinePlus. Chronic Kidney Disease Bethesda, MD: National Library of Medicine 2012 [cited 2013 January]. Available from: http://www.nlm.nih.gov/medlineplus/chronickidneydisease.html.

137. Scholz C, Heublein S, Lenhard M, Friese K, Engelstaedter V, Mayr D, et al. Glycodelin A is a prognostic marker to predict poor outcome in advanced stage ovarian cancer patients. BioMed Central research notes. 2012;5(1):551. PubMed PMID: 23036050. Epub 2012/10/06. Eng.

138. PathologyOutlines. Placental gross/microscopic abnormalities, non-neoplastic infarct: PathologyOutlines.com, Inc; 2011 [updated November 2011; cited 2013 February]. Available from: http://www.pathologyoutlines.com/topic/placentaplainfarct.html.

139. Hirano H, Imai Y, Ito H. Spiral artery of placenta: development and pathology-immunohistochemical, microscopical, and electron-microscopic study. The Kobe journal of medical sciences. 2002;48(1-2):13-23. PubMed PMID: 11912350. Epub 2002/03/26. eng.

Appendices

Appendix A - Differential expression of miRNAs in preeclamptic placentas, according to in different studies, as of May 2013.

miRNAs	Expression in PE	Authors
let-7b	+	Noack *et al*, 2011(73)
miR-1	-	Enquobahrie *et al*, 2010 (58)
	-	Zhu *et al*, 2009 (74)
miR-7f	+	Hu *et al*, 2009 (60)
miR-10b	-	Zhu *et al*, 2009 (74)
	+	Ishibashi *et al*, 2012* (59)
miR-15b	-	Mayor-Lynn *et al*, 2011
miR-16	+	Noack *et al*, 2011 (73)
	+	Hu *et al*, 2009 (60)
miR-18a	-	Zhu *et al*, 2009 (74)
	+	Ishibashi *et al*, 2012* (59)
miR-18b	-	Zhu *et al*, 2009 (74)
miR-19a	-	Zhu *et al*, 2009 (74)
	+	Ishibashi *et al*, 2012* (59)
	+	Ishibashi *et al*, 2012* (59)
miR-20b	+	Hu *et al*, 2009 (60)
miR-22*	+	Ishibashi *et al*, 2012* (59)
miR-26b	+	Hu *et al*, 2009 (60)
miR-27a	+	Hu *et al*, 2009 (60)
miR- 29a	+	Guo *et al*, 2011* (125)
miR-29b	+	Hu *et al*, 2009 (60)
miR-30e	+	Hu *et al*, 2009 (60)
miR-30a-3p	+	Zhu *et al*, 2009 (74)
miR-32	-	Zhu *et al*, 2009 (74)
miR-34C-5p	-	Enquobahrie *et al*, 2010 (58)
	=	Muralimanoharan *et al*, 2012 (34)
miR-101	-	Zhu *et al*, 2009 (74)
miR-104	+	Noack *et al*, 2011 (73)
miR-105	-	Zhu *et al*, 2009 (74)
miR-126	+	Hu *et al*, 2009 (60)
miR-126*	+	Ishibashi *et al*, 2012* (59)
	-	Zhu *et al*, 2009 (74)
miR-128a	+	Noack *et al*, 2011 (73)
miR-129	=	Muralimanoharan *et al*, 2012 (34)
miR-130a	+	Guo *et al*, 2011* (125)
miR-133b	+	Noack *et al*, 2011 (73)
miR-139-5p	-	Enquobahrie *et al*, 2010 (58)
miR-141	+	Hu *et al*, 2009 (60)

miR-142-3p	+	Ishibashi *et al*, 2012* (59)
miR-144	-	Zhu *et al*, 2009 (74)
miR-144*	+	Ishibashi *et al*, 2012* (59)
miR-146b-5p	+	Ishibashi *et al*, 2012* (59)
miR-149	-	Guo *et al*, 2013* (126)
miR-150	-	Zhu *et al*, 2009 (74)
miR-152	+	Zhu *et al*, 2009 (74)
miR-154*	+	Noack *et al*, 2011 (73)
	-	Zhu *et al*, 2009 (74)
miR-155	+	Zhang *et al*, 2010 (61)
miR-181a	-	Mayor-Lynn *et al*, 2011
	+	Noack *et al*, 2011 (73)
	+	Zhu *et al*, 2009 (74)
	+	Hu *et al*, 2009 (60)
	+	Liu *et al*, 2012 (127)
miR-182	+	Pineles *et al*, 2007* (57)
miR-182*	+	Noack *et al*, 2011 (73)
	+	Pineles *et al*, 2007* (57)
miR-185	+	Ishibashi *et al*, 2012* (59)
miR-193b	+	Ishibashi *et al*, 2012* (59)
miR-194	-	Guo *et al*, 2013* (126)
miR-195	+	Noack *et al*, 2011 (73)
	-	Zhu *et al*, 2009 (74)
	+	Hu *et al*, 2009 (60)
	-	Bai *et al*, 2012* (86)
miR-204	-	Zhu *et al*, 2009 (74)
miR-210	-	Mayor-Lynn *et al*, 2011
	+	Enquobahrie *et al*, 2010 (58)
	+	Noack *et al*, 2011 (73)
	+	Pineles *et al*, 2007* (57)
	+ (severe PE); - (mild PE)	Zhu *et al*, 2009 (74)
	+	Lee *et al*, 2012* (92)
	+	Ishibashi *et al*, 2012* (59)
	+	Muralimanoharan *et al*, 2012 (34)
miR-214	-	Hu *et al*, 2009 (60)
miR-218	-	Zhu *et al*, 2009 (74)
miR-222	+	Noack *et al*, 2011 (73)
	+	Hu *et al*, 2009 (60)
miR-223	-	Zhu *et al*, 2009 (74)
miR-296	+	Zhu *et al*, 2009 (74)
miR-302c*	+	Noack *et al*, 2011 (73)
miR-325	-	Lázár *et al*, 2012* (128)
miR-328	-	Enquobahrie *et al*, 2010 (58)
	=	Muralimanoharan *et al*, 2012 (34)
miR-335	+	Hu *et al*, 2009 (60)
miR-362	+	Zhu *et al*, 2009 (74)
miR-363	-	Zhu *et al*, 2009 (74)

miR-374	-	Zhu *et al*, 2009 (74)
miR-376c	-	Fu *et al*, 2013* (129)
miR-377	-	Zhu *et al*, 2009 (74)
	-	Mayor-Lynn *et al*, 2011 (89)
miR-411	-	Zhu *et al*, 2009 (74)
miR-423-5p	-	Hu *et al,* 2009 (60)
miR-450	-	Zhu *et al*, 2009 (74)
miR-450a	+	Hu *et al*, 2009 (60)
miR-451	+	Hu *et al*, 2009 (60)
	+	Guo *et al*, 2011* (125)
	+	Ishibashi *et al*, 2012* (59)
miR-483-5p	-	Mayor-Lynn *et al*, 2011 (89)
miR-486-3p	+	Hu *et al*, 2009 (60)
miR-491-5p	-	Hu *et al*, 2009 (60)
miR-496	+	Mayor-Lynn *et al*, 2011 (89)
miR-500	-	Enquobahrie *et al*, 2010 (58)
miR-508-5p	-	Hu *et al*, 2009 (60)
miR-517*	+	Zhu *et al*, 2009 (74)
miR-517a	+	Guo *et al*, 2011* (125)
miR-517c	+	Guo *et al*, 2011* (125)
	+	Ishibashi *et al*, 2012* (59)
miR-518b	+	Zhu *et al*, 2009 (74)
miR-518c	+	Ishibashi *et al*, 2012* (59)
miR-518f*	+	Ishibashi *et al*, 2012* (59)
miR-519a	+	Guo *et al*, 2011* (125)
miR-519d	+	Guo *et al*, 2011* (125)
miR-520g	+	Hu *et al*, 2009 (60)
miR-519b-3p	+	Hu *et al*, 2009 (60)
miR-519e*	+	Zhu *et al*, 2009 (74)
	+	Ishibashi *et al*, 2012* (59)
miR-520a-3p	+	Ishibashi *et al*, 2012* (59)
miR-520g	+	Guo *et al*, 2011* (125)
miR-525-5p	+	Ishibashi *et al*, 2012* (59)
miR-526b*	+	Ishibashi *et al*, 2012* (59)
miR-532-3p	-	Hu *et al*, 2009 (60)
miR-542-3p	-	Zhu *et al*, 2009 (74)
miR-565	+	Hu *et al*, 2009 (60)
miR-584	-	Enquobahrie *et al*, 2010 (58)
	+	Zhu *et al*, 2009 (74)
miR-590	-	Zhu *et al*, 2009 (74)
miR-590-5p	+	Ishibashi *et al*, 2012* (59)
miR-612	-	Hu *et al*, 2009 (60)
miR-625	-	Zhu *et al*, 2009 (74)
miR-638	+	Zhu *et al*, 2009 (74)
miR-658	-	Hu *et al*, 2009 (60)
miR-1247	-	Enquobahrie *et al*, 2010 (58)

*No indication of what type of placental tissue was analysed. All other studies were performed on chorionic villi.

Appendix B - RecoverAll™ Total Nucleic Acid Isolation Kit (Cat. No. AM1975): Modified Protocol.

A. Before beginning

1) Precautions

a. Read the protocol "Routines in the molecular lab" written specifically for this lab.
b. Read MSD sheets for the hazardous chemicals.
c. Make sure the surfaces and equipment you are using are RNase free.
d. Wear protective equipment according to the routines of this lab.

2) Prepare Wash solutions before initial use

a. Add 42 mL of ACS grade 100% ethanol to the bottle labeled **Wash 1** Concentrate. Mix well.
b. Add 48 mL of ACS grade 100% ethanol to the bottle labeled **Wash 2/3** Concentrate. Mix well.
c. Cap the wash solution bottles tightly to prevent evaporation.
d. Mark the labels with date and initials to indicate that the ethanol has been added.

The final solutions will be referred to as ***Wash 1*** and ***Wash 2/3*** in the procedure.

B. Deparaffinization

1) Set the Thermomixer at 50°C

2) Add 1 mL xylene, mix, and incubate for 3 min at 50°C

a. Add 1 mL 100% xylene to the sample.
b. Vortex briefly to mix.
c. Centrifuge briefly to bring any tissue that is stuck to the sides of the tube down into the xylene.
d. Incubate the sample for 3 min at 50°C to melt the paraffin.

3) Centrifuge for 2 min at maximum speed and discard the xylene

a. Centrifuge the sample for 2 min at 14.000rpm to pellet the tissue.
b. (Optional) If the sample does not form a tight pellet, re-centrifuge for an additional 2 min.
c. Remove the xylene (gently) without disturbing the pellet. Discard the xylene in the xylene- waste. The pellet can be clear and difficult to see. If the pellet is loose, you may need to leave some xylene in the tube to avoid removing any tissue pieces.

4) Wash the pellet twice with 1 mL 100% ethanol

The ethanol washes remove xylene from the sample and accelerate drying of the tissue.

a. Add 1 mL of 100% ethanol to the sample and vortex to mix. The tissue should turn opaque.
b. Centrifuge the sample for 2 min at 14.000rpm.
c. Gently remove and discard the ethanol without disturbing the pellet. The ethanol contains traces of xylene and must be discarded in the xylene- waste.
d. Repeat steps a-c above to wash a second time.

e. Briefly centrifuge again to collect any remaining drops of ethanol in the bottom of the tube. Remove as much residual ethanol as possible without disturbing the pellet.

5) Air dry the pellet

a. Air dry for 15-45 min to remove residual ethanol. Larger samples may need longer than 45 min.

C. Protease Digestion

1) Add Digestion Buffer and Protease

a. Add digestion buffer to each sample (according to the table).

Sample size	Digestion Buffer per sample
≤40 µm	100 µL
40-80 µm	200 µL

b. Add 4 µL Protease to each sample.

c. Swirl the tube gently (do not vortex!) to mix and to immerse the tissue. If the tissue sticks to the sides of the tube, briefly centrifuge to bring the tissue down into the solution.

2) Incubate at 50°C

a. Incubate the sample in heat block for 3 hours at 50°C (Optional extra 15min at 80°C).

The sample may not clarify after 3 hours. Avoid removing undigested tissue pieces when applying to the Filter Cartridge in step D3.

STOPPING POINT: Samples can be stored at -20°C and then thawed on ice before proceeding. (Spin down to make sure the cylinders are inside the solution.)

D. Nucleic Acid Isolation

1) Prepare Isolation Additive/ethanol mixture

a. Combine the indicated amounts of isolation additive and ethanol, according to the volume of digestion buffer used in your sample. For multiple samples, prepare a master mix for all samples, plus an extra ~5%.

	Volume of digestion buffer	
	100 µL	**200 µL**
Isolation additive	120 µL	240 µL
100% ethanol	275 µL	550 µL
Total	395 µL	790 µL

2) Add isolation additive/ ethanol and mix

b. Add the appropriate volume of Isolation Additive/ethanol mixture to each sample.

c. Mix by pipetting up and down. Some samples may appear white and cloudy after mixing.

3) Pass the mixture through a Filter Cartridge

d. For each sample, place a Filter Cartridge in one of the Collection Tubes supplied.

e. Pipet up to 700µL of the sample/ethanol mixture onto the Filter Cartridge and close the lid. To prevent clogging of the filter, avoid pipetting large pieces of undigested tissue onto the Filter Cartridge.

f. Centrifuge at 10.000 rpm for 30 sec to pass the mixture through the filter. The nucleic acids are now in the filter.

Note: Do not centrifuge Filter Cartridges at relative centrifugal forces greater than 10.000 rpm; higher forces may damage the filters.

g. Discard the flow-through, and re-insert the Filter Cartridge in the same Collection Tube.

h. If necessary, repeat steps a-d until all the sample mixture has passed through the filter.

4) Wash with 700 µL of Wash 1

i. Add 700 µL of Wash 1 to the Filter Cartridge.

j. Centrifuge for 30 sec at 10.000 rpm to pass the mixture through the filter.

k. Discard the flow-through, and re-insert the Filter Cartridge in the same Collection Tube.

5) Wash with 500 µL of Wash 2/3, and then centrifuge to remove residual fluid

l. Add 500 µL of Wash 2/3 to the Filter Cartridge.

m. Centrifuge for 30 sec at 10.000 rpm to pass the mixture through the filter.

n. Discard the flow-through, and re-insert the Filter Cartridge in the same Collection Tube. Spin the assembly for an additional 30 sec to remove residual fluid from the filter.

E. Nuclease Digestion and Final Nucleic Acid Purification

1) Add 60 µL DNase mix and incubate for 30 min at room temp

a. Combine the following solutions to make DNase mix (a master mix can be used if there is more than one sample).

Amount (per reaction)	Component
6 µL	10X DNase Buffer
4 µL	DNase
50 µL	Nuclease-free Water

b. Add 60 µL of the DNase mix to the *center* of each Filter Cartridge.

c. Cap the tube and incubate for 30 min at room temp (22-25°C).

2) Wash with 700 µL of Wash 1

a. Add 700 µL of Wash 1 to the Filter Cartridge.

b. Incubate for 30-60 sec at room temperature.

c. Centrifuge for 30 sec at 10.000 rpm.

d. Discard the flow-through, and re-insert the Filter Cartridge in the same Collection Tube.

3) Wash twice with 500 µL of Wash 2/3, then centrifuge to remove residual fluid

a. Add 500 µL of Wash 2/3 to the Filter Cartridge.
b. Centrifuge for 30 sec at 10.000 rpm.
c. Discard the flow-through, and re-insert the Filter Cartridge in the Collection Tube.
d. Repeat steps a-c to wash a second time with 500 µL of Wash 2/3.
e. Centrifuge the assembly for 1 min at 10.000 rpm to remove residual fluid from the filter.

4) Elute with 60 µL Elution Solution at room temp

a. Transfer the Filter Cartridge to a fresh Collection Tube.
b. Apply 60 µL of Elution Solution to the *center of the filter*, and close the cap.
   Note: the Elution Solution contains salts that, if concentrated, may affect downstream applications. (If you intend to vacuum dry the sample, elute in nuclease-free water).
c. Allow the sample to sit at room temperature for 1 min.
d. Centrifuge for 1 min at 14.000 rpm for the solution to pass through the filter. The eluate contains the RNA.
e. Store the nucleic acid at -20°C or colder.
f. (Optional) To store your sample for an extended period of time, or if a very small amount of nucleic acid was recovered, transfer the eluate to a non-stick tube to prevent loss of nucleic acid.

Appendix C – Total RNA Dilutions for using the 6000 RNA Pico Kit.

Sample	Theoretical						Practical (Pippetable=Theoretical x 10)		
	Before Dilution			After Dilution					
	Vf (Solution)	Ci (Sample)	x=Average(Wanted)/Average(Average(Real)	Cf (sample)	Within Range 0,5-4	Vi (Sample) = theoretical	Vf (Solution)	Vi (sample) = pippetable	V(buffer)
C1	4,00	79,29	0,02	1,39	Yes	0,07	40,00	0,70	39,30
C2		59,02		1,03	Yes				
C3		141,68		2,48	Yes				
C4		128,16		2,24	Yes				
C5		58,05		1,02	Yes				
C6		99,01		1,73	Yes				
C7		50,35		0,88	Yes				
C8		54,36		0,95	Yes				
C9		72,94		1,28	Yes				
C10		187,91		3,29	Yes				
P1		53,23		0,93	Yes				
P2		41,54		0,73	Yes				
P3		63,65		1,11	Yes				
P4		103,09		1,80	Yes				
P5		156,74		2,74	Yes				
P6		38,79		0,68	Yes				
P7		44,85		0,78	Yes				
P8		48,80		0,85	Yes				
P9		89,62		1,57	Yes				
P10		87,69		1,53	Yes				
P11		43,55		0,76	Yes				
P12		183,78		3,22	Yes				

Ci		
	Average (Wanted)	1,50
	Average (Real)	85,73

Appendix D – Sample clinical information

Sample	Detection of condition (w.d)	Gestational age at birth (d)	Maternal age at birth (a)	Race	Historg of PE in the famila	Other Children	Earlier abortions	Earlier PE	BMI	In first control during this pregnancy			In last control during this pregnancy			Smokes	Placental Weight (g)	Birthweight (g)
										Proteinuria (g/L)	Blood Pressure	Weight (kg)	Proteinuria (g/L)	Blood Pressure	Weight (kg)			
C1	-	264	36	Scandinavian	No	2	0	No	29,39	No	110/70	81	No	125/75	96	No	645	3260
C2	-	273	22	Scandinavian	No	0	0	No	31,98	No	122/70	86	No	127/81	101	No	600	3470
C3	-	271	37	Scandinavian	No	1	0	No	19,00	No	104/61	53	No	108/70	72	No	560	3720
C4	-	285	28	Scandinavian	No	0	0	No	34,77	No	130/80	89	No	145/85	101	No	820	4490
C5	-	272	32	Scandinavian	No	1	0	No	31,96	No	120/80	87	No	110/75	95	No	520	3610
C6	-	271	26	Scandinavian	No	1	0	No	24,91	No	131/70	72	No	120/70	80	No	770	3650
C7	-	274	29	Scandinavian	No	1	0	No	24,56	No	100/60	59	No	92/60	67	No	750	3510
C8	-	275	30	Scandinavian	No	1	1	No	18,47	No	115/70	54	No	112/80	59	No	530	3280
C9	-	281	27	Scandinavian	No	1	0	No	24,57	No	95/65	71	No	105/60	81	No	600	4200
C10	-	263	22	Scandinavian	No	0	0	No	20,90	No	110/60	59	No	128/72	70	No	500	2800
P1	29,5	215	28	Scandinavian	No	0	0	No	26,03	No	120/70	77	5,37	162/93	85	No	250	1213
P2	33	247	30	Scandinavian	No	1	1	Yes	24,42	No	98/66	80	Yes (+)	122/86	92	No	430	1840
P3	33	235	28	Scandinavian	No	0	0	No	25,83	No	102/65	80	Yes (+)	146/94	107	No	450	2414
P4	31,1	221	27	Scandinavian	No	1	0	Yes	27,61	No	130/80	77	4,7	150/100	87	No	420	2030
P5	26,3	205	32	Scandinavian	No	1	0	Yes	34,16	No	150/80	93	Yes (+)	198/115	102	No	260	1136
P6	31,1	223	22	Scandinavian	Yes (father's)	0	0	No	23,31	No	110/60	65	Yes (+)	151/96	78	No	360	1286
P7	25	186	26	Scandinavian	No	0	0	No	35,69	No	162/88	96	Yes (+)	162/95	105	No	170	685
P8	27	193	28	Scandinavian	No	1	1	No	20,08	No	150/96	54	Yes (+)	150/95	62	No	280	768
P9	29,3	210	39	Scandinavian	No	0	0	No	19,75	No	115/65	64	4,8	140/90	73	No	260	1100
P10	31	216	26	Scandinavian	?	0	0	No	?	No	140/87	?	6,1	162/97	?	No	250	1393
P11	33	251	20	Scandinavian	No	0	0	No	?	No	115/75	54	5,89	160/102	71,6	No	550	2610
P12	30	215	28	Scandinavian	?	0	0	No	21,11	No	116/72	61	Yes (+)	130/95	72	No	335	1840

Appendix E – Sequences of primers and probes

Target	miR-1	miR-181a	miR-195	miR-210	miR-584
Forward Primer	CAAgCggTACCTggAATg	CgACCCTACggAACATTCA	CTTCACCgTTTAgCAgCAC	CATAgCCgTAACTgTgCgT	CCACCgCTACCTTATggTT
Reverse Primer	gCCTCTCAAgCTgACgAAT	gCgACTCATgCTgACgAA	gCCTCTCAAgCTgACgAAT	gCCTCTCAAgCTgACgAAT	gCCTCTCAAgCTgACgAAT
Reverse Transcription Primer	gCCTCTCAAgCTgACgAATTATgAgAggCCCTCCATACATAC	GCGACTCATGCTGACGAATTTTGAGTCGCACTCACC	gCCTCTCAAgCTgACgAATTATgAgAggCTgCCAATAT	gCCTCTCAAgCTgACgAATTATgAgAggCTCAgCCgCt	gCCTCTCAAgCTgACgAATTATgAgAggCTCTCAGTC
TaqMan Probe	FAM-TgAgAggCCCTCCATACATACTTCTTT-BBQ	FAM-TgAgTCgCACTCACCgACAgC-BBQ	FAM-AtgAgAggCTgCCAATATTTCTgTg-BBQ	FAM-AgAggCTCAgCCgCTgTCA-BBQ	FAM-TgAgAggCTCTCAgTCCCAggC-BBQ
Melting Temperatures (Forward Primer; Reverse Primer; TM Probe) (° C)	54,2; 54,4; 61,6	55,3; 55,1; 63,5	54,3; 54,4; 59,1	54,7; 54,4; 59,7	54,8; 54,4; 63,6
Amplicon Size (bps)	30	26	23	24	25

Appendix F – RT Dilutions

	Sample	Cf Lowest Concentration (ng/µL)	Vf Extracted Sample Volume (µL)	Vi Volume of RNA to add (µL)	Volume of water/buffer to add (µL)
CTR	C1	38,79	7	3,4	3,6
	C2			4,6	2,4
	C3			1,9	5,1
	C4			2,1	4,9
	C5			4,7	2,3
	C6			2,7	4,3
	C7			5,4	1,6
	C8			5	2
	C9			3,7	3,3
	C10			1,4	5,6
PE	P1			5,1	1,9
	P2			6,5	0,5
	P3			4,3	2,7
	P4			2,6	4,4
	P5			1,7	5,3
	P6			7	0
	P7			6,1	0,9
	P8			5,6	1,4
	P9			3	4
	P10			3,1	3,9
	P11			6,2	0,8
	P12			1,5	5,5

Appendix G – PCR Programmes

- For LightCycler® FastStart DNA Master^{PLUS} SYBR Green I (final primer concentration 0.3 µM):

Programs

Program Name	Heating		
Cycles	1	Analysis Mode	None

Target (°C)	Hold (hh:mm:ss)	Slope (°C/s)	Sec Target (°C)	Step size (°C)	Step Delay (cycles)	Acquisition Mode
95	00:10:00	20	0	0	0	None

Program Name	PCR		
Cycles	45	Analysis Mode	None

Target (°C)	Hold (hh:mm:ss)	Slope (°C/s)	Sec Target (°C)	Step size (°C)	Step Delay (cycles)	Acquisition Mode
95	00:00:10	20	0	0	0	None
55	00:00:10	20	0	0	0	None
72	00:00:01	20	0	0	0	Single

Program Name	Melting		
Cycles	1	Analysis Mode	Melting Curves

Target (°C)	Hold (hh:mm:ss)	Slope (°C/s)	Sec Target (°C)	Step size (°C)	Step Delay (cycles)	Acquisition Mode
95	00:00:00	20	0	0	0	None
65	00:01:00	20	0	0	0	None
95	00:00:00	0.1	0	0	0	Continuous

Program Name	Cooling		
Cycles	1	Analysis Mode	None

Target (°C)	Hold (hh:mm:ss)	Slope (°C/s)	Sec Target (°C)	Step size (°C)	Step Delay (cycles)	Acquisition Mode
40	00:00:30	20	0	0	0	None

- For LightCycler® TaqMan Master ("No optimization", final TaqMan probe concentration 0.1 µM and final primer concentration 0.3 µM):

Programs

Program Name	Pre-incubation		
Cycles	1	Analysis Mode	None

Target (°C)	Hold (hh:mm:ss)	Slope (°C/s)	Sec Target (°C)	Step size (°C)	Step Delay (cycles)	Acquisition Mode
95	00:10:00	20	0	0	0	None

Program Name	Amplification		
Cycles	50	Analysis Mode	None

Target (°C)	Hold (hh:mm:ss)	Slope (°C/s)	Sec Target (°C)	Step size (°C)	Step Delay (cycles)	Acquisition Mode
95	00:00:10	20	0	0	0	None
55	00:00:20	20	0	0	0	None
72	00:00:01	20	0	0	0	Single

Program Name	Cooling		
Cycles	1	Analysis Mode	None

Target (°C)	Hold (hh:mm:ss)	Slope (°C/s)	Sec Target (°C)	Step size (°C)	Step Delay (cycles)	Acquisition Mode
40	00:00:30	20	0	0	0	None

Appendix H – Setup of the optimization runs

Run	No. Cappilary	miRNA	Primer C	T_a	Annealing Time	No. Cycles
1	1	NTC	0,3	55	20	50
	2	1				
	3	Rep 1				
	4	181				
	5	Rep. 181				
	6	195				
	7	Rep 195				
	8	210				
	9	Rep 210				
	10	584				
	11	Rep 584				
	12	1	0,1			
	13	Rep 1				
	14	181				
	15	Rep 181				
	16	195				
	17	Rep 195				
	18	210				
	19	Rep 210				
	20	584				
	21	Rep 584				
2	1	NTC	0,3	60	20	
	2	1				
	3	Rep 1				
	4	181				
	5	Rep 181				
	6	195				
	7	Rep 195				
	8	210				
	9	Rep 210				
	10	584				
	11	Rep 584				
	12	1	0,1			
	13	Rep 1				
	14	181				
	15	Rep 181				
	16	195				
	17	Rep 195				
	18	210				

	19	Rep 210				
	20	584				
	21	Rep 584				
3	1	NTC	0,3	58	20	
	2	1				
	3	Rep 1				
	4	181				
	5	Rep 181				
	6	195				
	7	Rep 195				
	8	210				
	9	Rep 210				
	10	584				
	11	Rep 584				
	12	1	0,1			
	13	Rep 1				
	14	181				
	15	Rep 181				
	16	195				
	17	Rep 195				
	18	210				
	19	Rep 210				
	20	584				
	21	Rep 584				
4	1	NTC	0,3	55	30	
	2	1				
	3	Rep 1				
	4	181				
	5	Rep 181				
	6	195				
	7	Rep 195				
	8	210				
	9	Rep 210				
	10	584				
	11	Rep 584				
	12	1	0,1			
	13	Rep 1				
	14	181				
	15	Rep 181				
	16	195				
	17	Rep 195				
	18	210				
	19	Rep 210				

	20	584				
	21	Rep 584				
5	1	NTC	0,3	55	40	
	2	1				
	3	Rep 1				
	4	181				
	5	Rep 181				
	6	195				
	7	Rep 195				
	8	210				
	9	Rep 210				
	10	584				
	11	Rep 584				
	12	1	0,1			
	13	Rep 1				
	14	181				
	15	Rep 181				
	16	195				
	17	Rep 195				
	18	210				
	19	Rep 210				
	20	584				
	21	Rep 584				

Appendix I – Quality Control NanoDrop results

Controls	RNA Concentration (ng/µL)	A_{260}/A_{280} Ratio	A_{260}/A_{230} Ratio
C1	77,38	1,98	0,96
	79,52	1,98	0,96
	79,05	1,98	0,95
C2	59,04	2,02	1,41
	58,99	2,05	1,46
	59,47	2,07	1,43
C3	141,11	1,98	1,69
	142,25	1,93	1,67
	141,09	2,00	1,67
C4	129,37	1,88	1,70
	130,00	1,91	1,69
	128,42	1,93	1,70
	127,89	1,92	1,70
C5	58,15	1,80	0,67
	57,94	1,88	0,68
	59,28	1,98	0,67
C6	99,07	2,01	1,20
	98,95	1,98	1,27
	100,13	1,97	1,27
C7	50,13	1,99	1,08
	50,56	1,94	1,12
	50,92	1,96	1,12
C8	54,31	1,95	1,11
	54,40	1,94	1,14
	55,52	1,82	1,14
C9	69,63	2,02	1,07
	72,91	2,00	1,06
	72,96	2,04	1,05
C10	184,15	2,08	0,73
	192,12	2,05	0,76
	188,05	2,06	0,75
	187,76	2,05	0,75
P1	53,29	2,00	1,30
	53,17	2,00	1,24
	55,10	1,99	1,32
P2	39,97	1,77	1,02
	41,59	1,73	1,02
	41,48	1,75	1,02
P3	63,45	1,92	0,86
	63,85	1,89	0,87

	62,74	1,91	0,87
P4	100,50	1,97	1,72
	104,01	1,94	1,70
	101,77	1,94	1,72
	103,15	1,94	1,75
	103,02	1,94	1,71
P5	157,00	2,04	0,77
	156,48	2,03	0,79
	158,81	2,07	0,79
	157,77	2,02	0,77
	159,89	2,06	0,77
P6	38,75	1,86	1,12
	38,83	1,84	1,11
	40,77	1,78	1,15
	40,13	1,80	1,16
P7	47,09	1,70	0,51
	44,99	1,85	0,50
	44,71	1,89	0,50
P8	47,99	1,98	1,93
	48,47	2,03	1,97
	49,12	2,02	1,98
P9	85,99	1,79	0,79
	86,88	1,73	0,80
	87,45	1,80	0,79
	89,90	1,73	0,80
	89,34	1,75	0,79
P10	87,94	1,98	0,89
	87,43	2,06	0,88
	89,66	1,97	0,89
	86,78	1,99	0,88
P11	42,59	2,10	0,39
	43,30	2,03	0,40
	43,80	2,04	0,41
P12	184,07	2,08	1,57
	183,48	2,08	1,60
	185,26	2,08	1,57

Appendix J – Quality Control Bioanalyzer results

- RNA 6000 Nano kit:

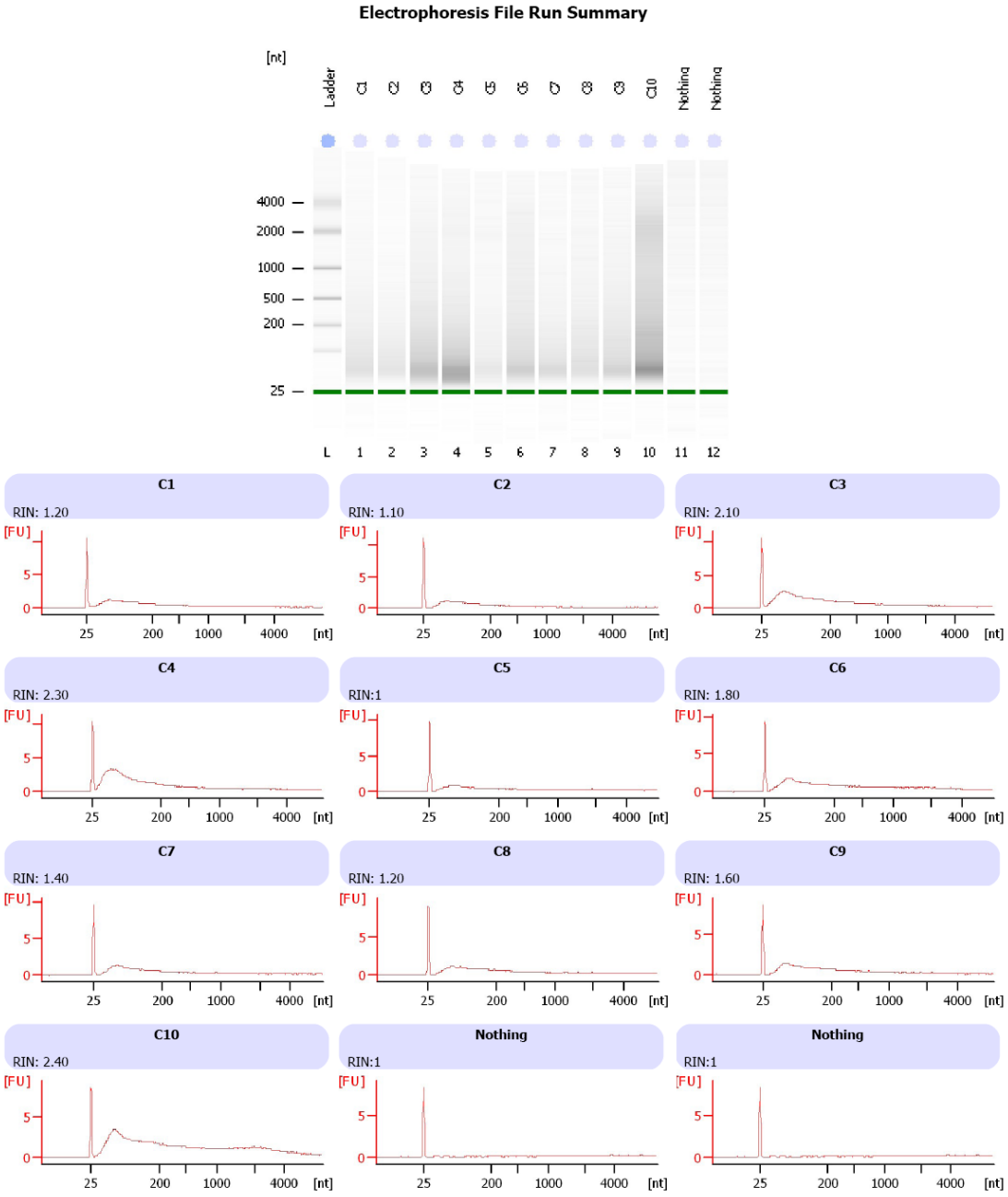

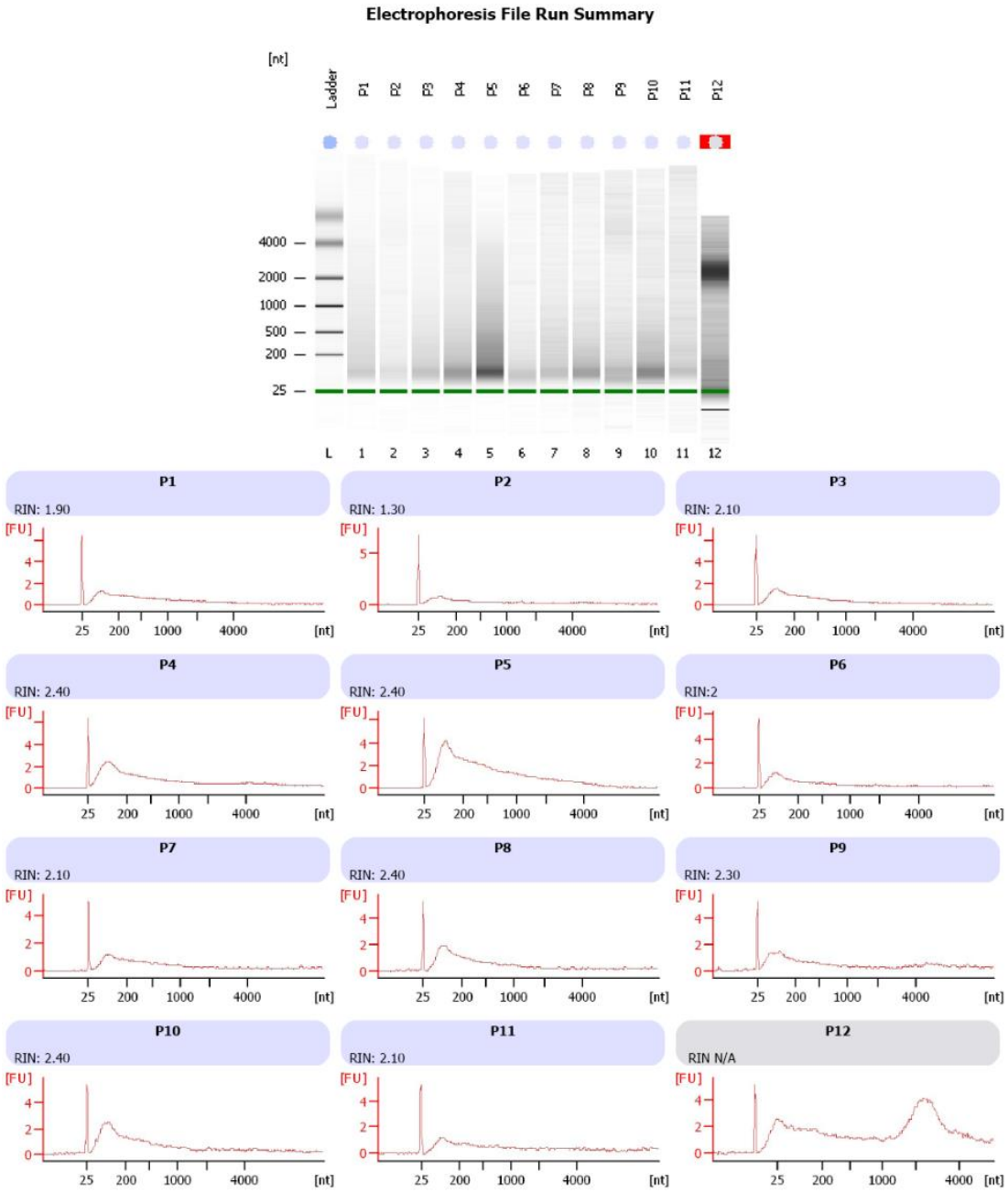
Electrophoresis File Run Summary
[nt]
Ladder
P1
P2
P3
P4
P5
P6
P7
P8
P9
P10
P11
P12
4000
2000
1000
500
200
25
L 1 2 3 4 5 6 7 8 9 10 11 12
P1
RIN: 1.90
P2
RIN: 1.30
P3
RIN: 2.10
P4
RIN: 2.40
P5
RIN: 2.40
P6
RIN:2
P7
RIN: 2.10
P8
RIN: 2.40
P9
RIN: 2.30
P10
RIN: 2.40
P11
RIN: 2.10
P12
RIN N/A
[FU]
[nt]
25 200 1000 4000

- <u>RNA 6000 Pico kit:</u>

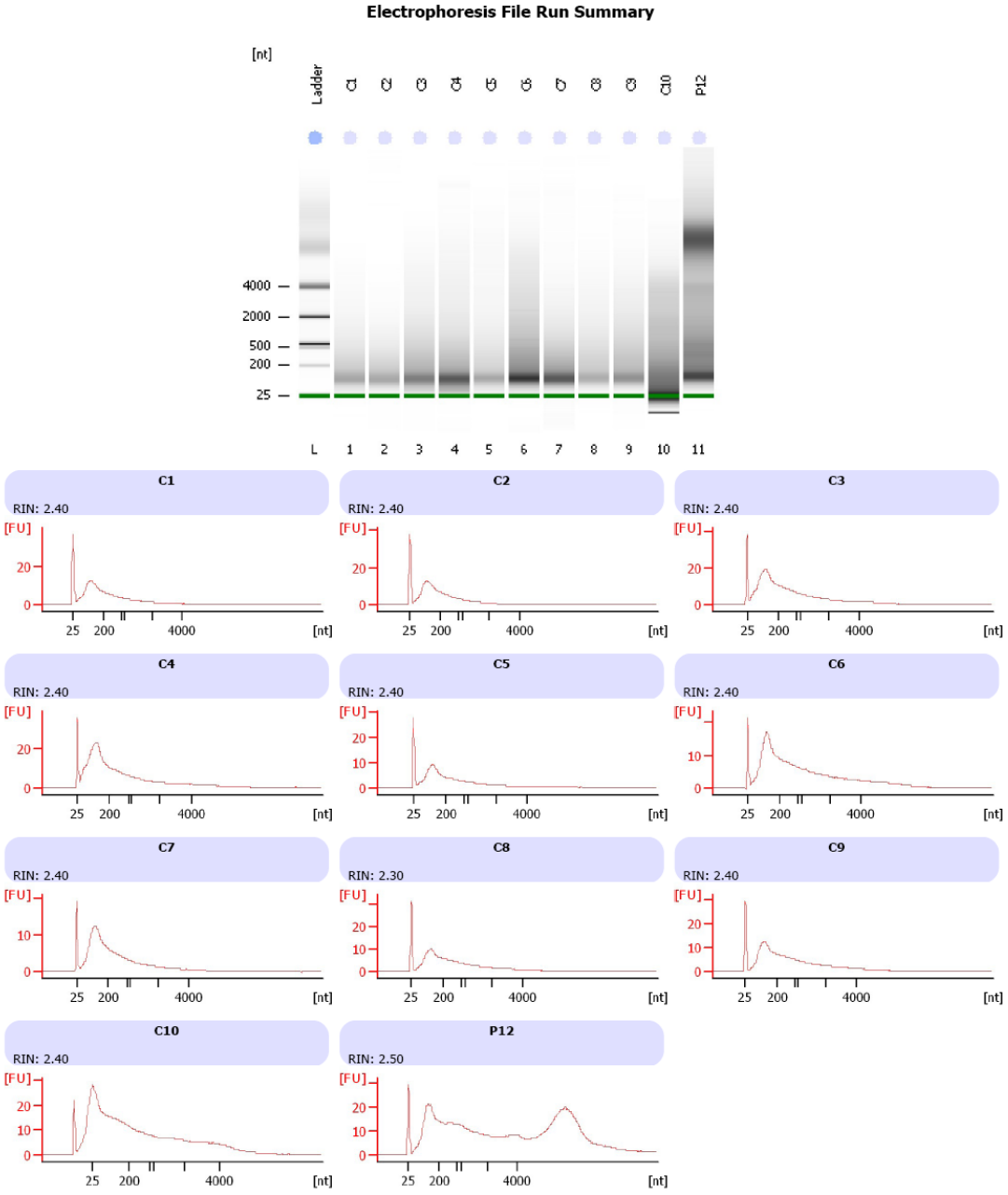

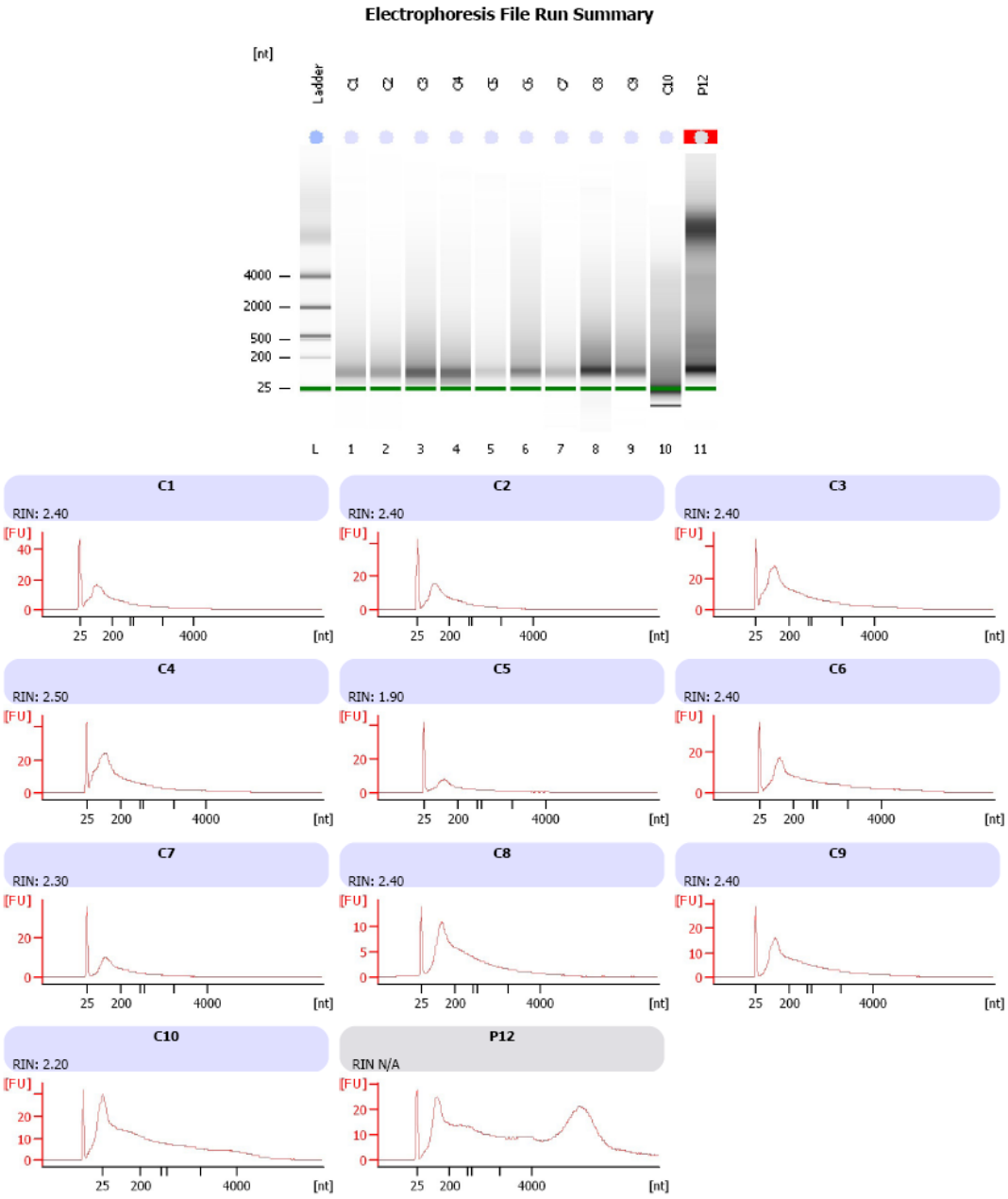
Electrophoresis File Run Summary
[nt]
Ladder
C1
C2
C3
C4
C5
C6
C7
C8
C9
C10
P12
4000
2000
500
200
25
L 1 2 3 4 5 6 7 8 9 10 11
C1
RIN: 2.40
C2
RIN: 2.40
C3
RIN: 2.40
C4
RIN: 2.50
C5
RIN: 1.90
C6
RIN: 2.40
C7
RIN: 2.30
C8
RIN: 2.40
C9
RIN: 2.40
C10
RIN: 2.20
P12
RIN N/A
[FU]
[nt]
25 200 4000

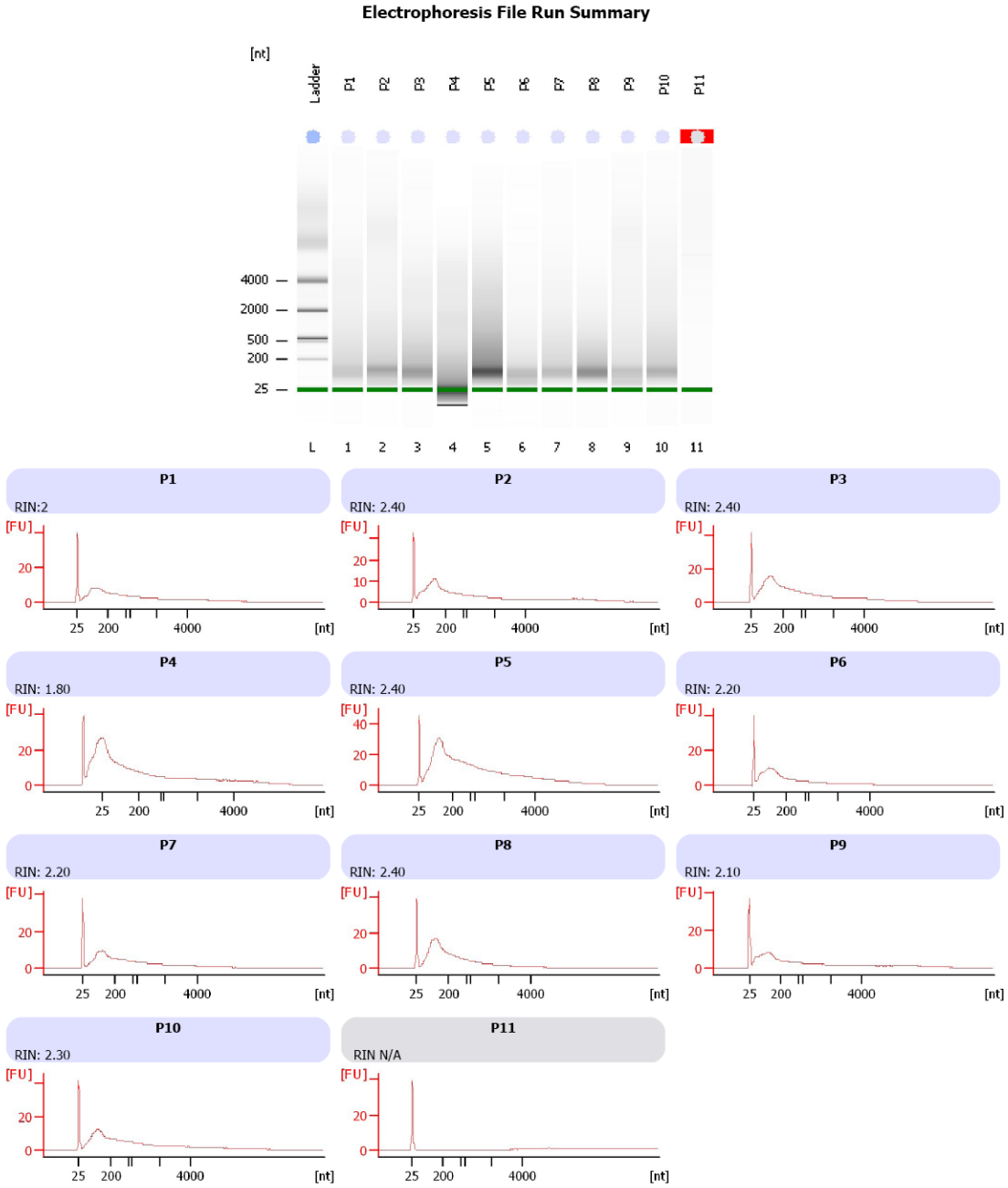
Electrophoresis File Run Summary
[nt]
Ladder
P1
P2
P3
P4
P5
P6
P7
P8
P9
P10
P11
4000
2000
500
200
25
L 1 2 3 4 5 6 7 8 9 10 11
P1
RIN:2
P2
RIN: 2.40
P3
RIN: 2.40
P4
RIN: 1.80
P5
RIN: 2.40
P6
RIN: 2.20
P7
RIN: 2.20
P8
RIN: 2.40
P9
RIN: 2.10
P10
RIN: 2.30
P11
RIN N/A
[FU]
[nt]
25 200 4000

Appendix K – Results of the evaluation of qPCR reaction quality using LightCycler® FastStart DNA MasterPLUS SYBR Green I

- Experiment with SYBR Green for miR-1 (Efficiency 1,310; Error 0,0319):

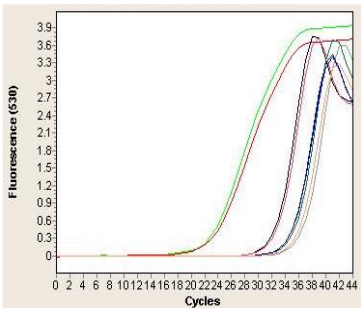

Amplification Curves

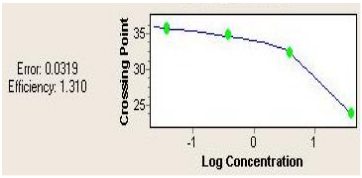

Standard Curve

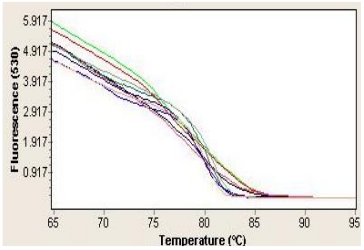

Melting Curves

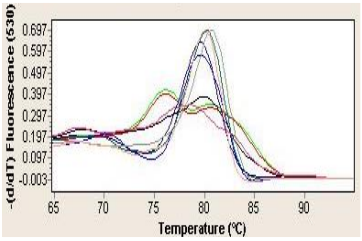

Melting Peaks

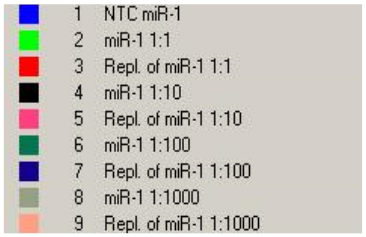

Key

- <u>Experiment with SYBR Green for miR-181a (Efficiency 1,326; Error 2,218):</u>

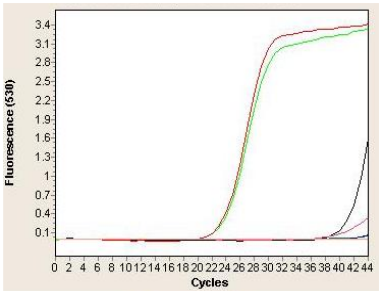

Amplification Curves

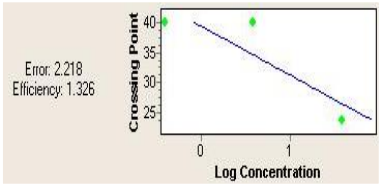

Standard Curve

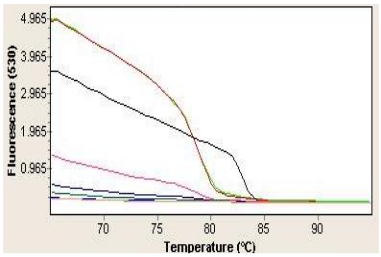

Melting Curves

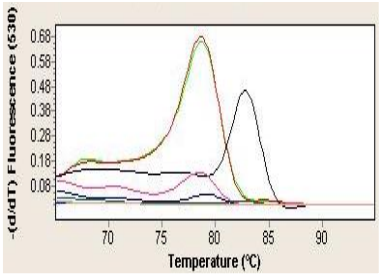

Melting Peaks

1 NTC miR-181a
2 miR181a 1:1
3 Repl. of miR181a 1:1
4 miR181a 1:10
5 Repl. of miR181a 1:10
6 miR181a 1:100
7 Repl. of miR181a 1:100
8 miR181a 1:1000
9 Repl. of miR181a 1:1000

Key

- <u>Experiment with SYBR Green for miR-195 (Efficiency 1,605; Error 0,0828):</u>

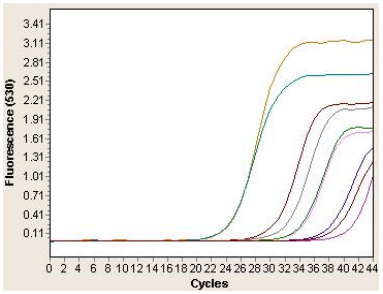

Amplification Curves

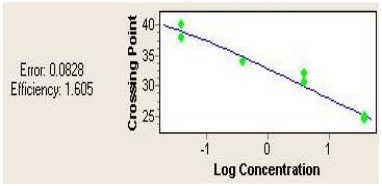

Standard Curve

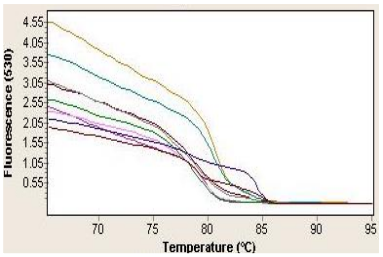

Melting Curves

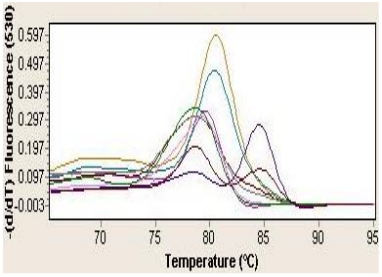

Melting Peaks

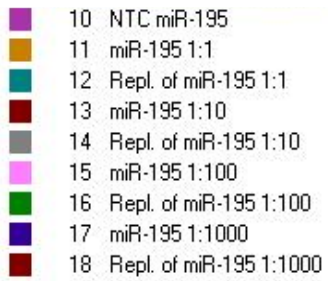

Key

- <u>Experiment with SYBR Green for miR-210 (Efficiency 1,860; Error 0,152):</u>

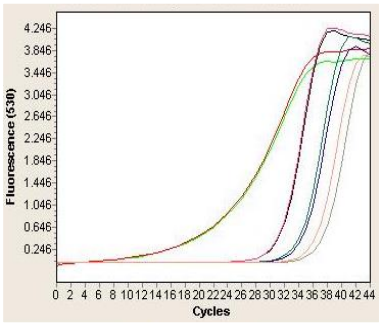

Amplification Curves

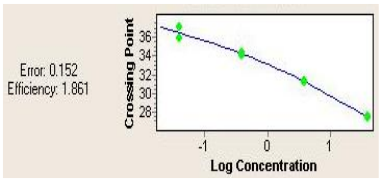

Standard Curve

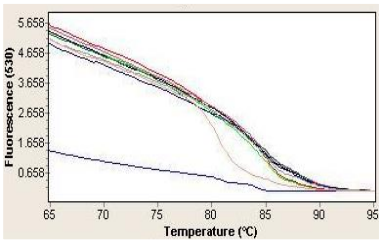

Melting Curves

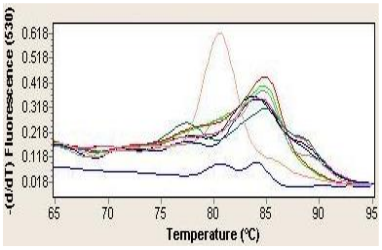

Melting Peaks

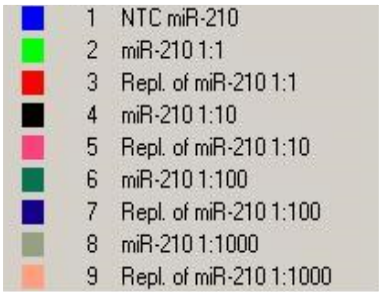

Key

- <u>Experiment with SYBR Green for miR-584 (Efficiency 1,313; Error 0,149):</u>

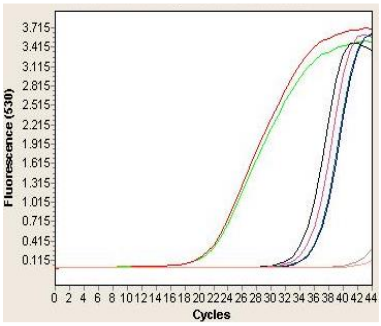

Amplification Curves

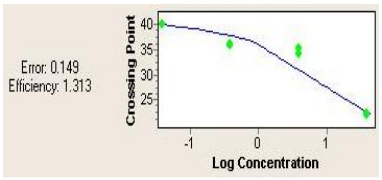

Standard Curve

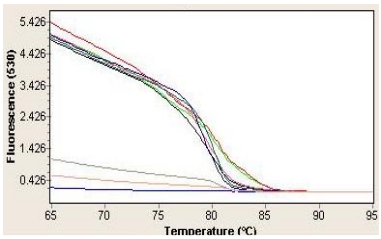

Melting Curves

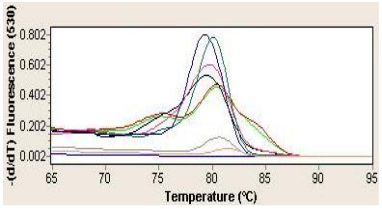

Melting Peaks

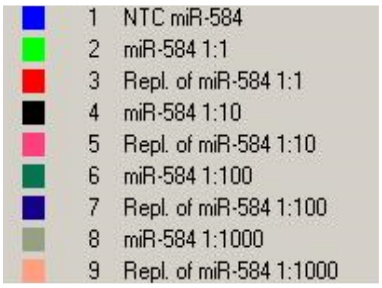

Key

Appendix L – Results of the assessment of the qPCR optimization products, using LightCycler® TaqMan Master

- PCR results:

Sample	No Optimization (55° C, 20 s)	T_a 60° C	T_a 57° C	Annealing Time 30 s	Annealing Time 40 s
NTC	0	0	0	0	0
miR-1 (C_{primer}= 0.3 µM)	29.19	37.68	34.21	34.78	27.36
Rep miR-1 (C_{primer}= 0.3 µM)	33.06	36.81	34.14	30.36	27.15
miR-181 (C_{primer}= 0.3 µM)	0	0	0	0	0
Rep miR-181 (C_{primer}= 0.3 µM)	0	0	0	0	45.00
miR-195 (C_{primer}= 0.3 µM)	22.95	26.25	24.28	22.83	22.03
Rep miR-195 (C_{primer}= 0.3 µM)	23.06	26,77	23.61	22.85	21.92
miR-210 (C_{primer}= 0.3 µM)	35.42	35.85	32.86	29.46	26.46
Rep miR-210 (C_{primer}= 0.3 µM)	35.57	35.30	32.70	29.14	25.72
miR-584 (C_{primer}= 0.3 µM)	31.65	34.85	32.01	28.40	24.60
Rep miR-584 (C_{primer}= 0.3 µM)	31.44	35.30	32.40	28.70	25.64
miR-1 (C_{primer}= 0.1 µM)	33.00	38.89	35.50	28.15	27.44
Rep miR-1 (C_{primer}= 0.1 µM)	34.52	38.34	34.95	26.79	27.01
miR-181 (C_{primer}= 0.1 µM)	0	0	0	0	0
Rep miR-181 (C_{primer}= 0.1 µM)	0	0	0	0	0
miR-195 (C_{primer}= 0.1 µM)	25.03	28.55	25.60	23.73	23.03
Rep miR-195 (C_{primer}= 0.1 µM)	25.05	28.67	25.51	23.85	22.83
miR-210 (C_{primer}= 0.1 µM)	34.55	38.63	32.32	27.76	27.10
Rep miR-210 (C_{primer}= 0.1 µM)	32.59	38.99	29.24	28.22	27.74
miR-584 (C_{primer}= 0.1 µM)	27.03	26.21	31.82	25.92	24.81
Rep miR-584 (C_{primer}= 0.1 µM)	27.00	38.69	33.36	24.95	24.90

- <u>Bioanalyzer - No optimization (C_{primer}= 0,3 µM):</u>

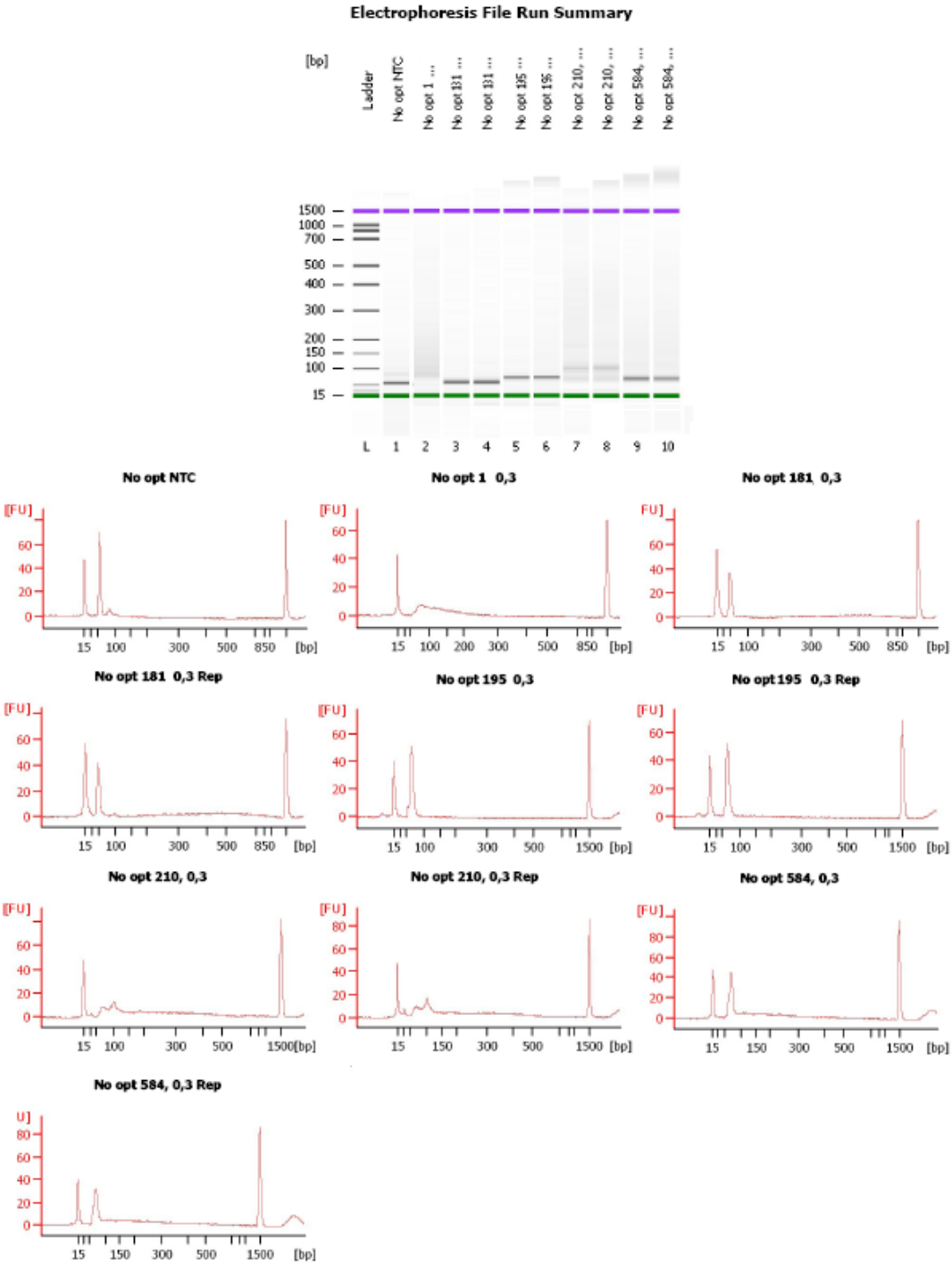

- <u>Bioanalyzer - No optimization (C_{primer}=0,1 µM):</u>

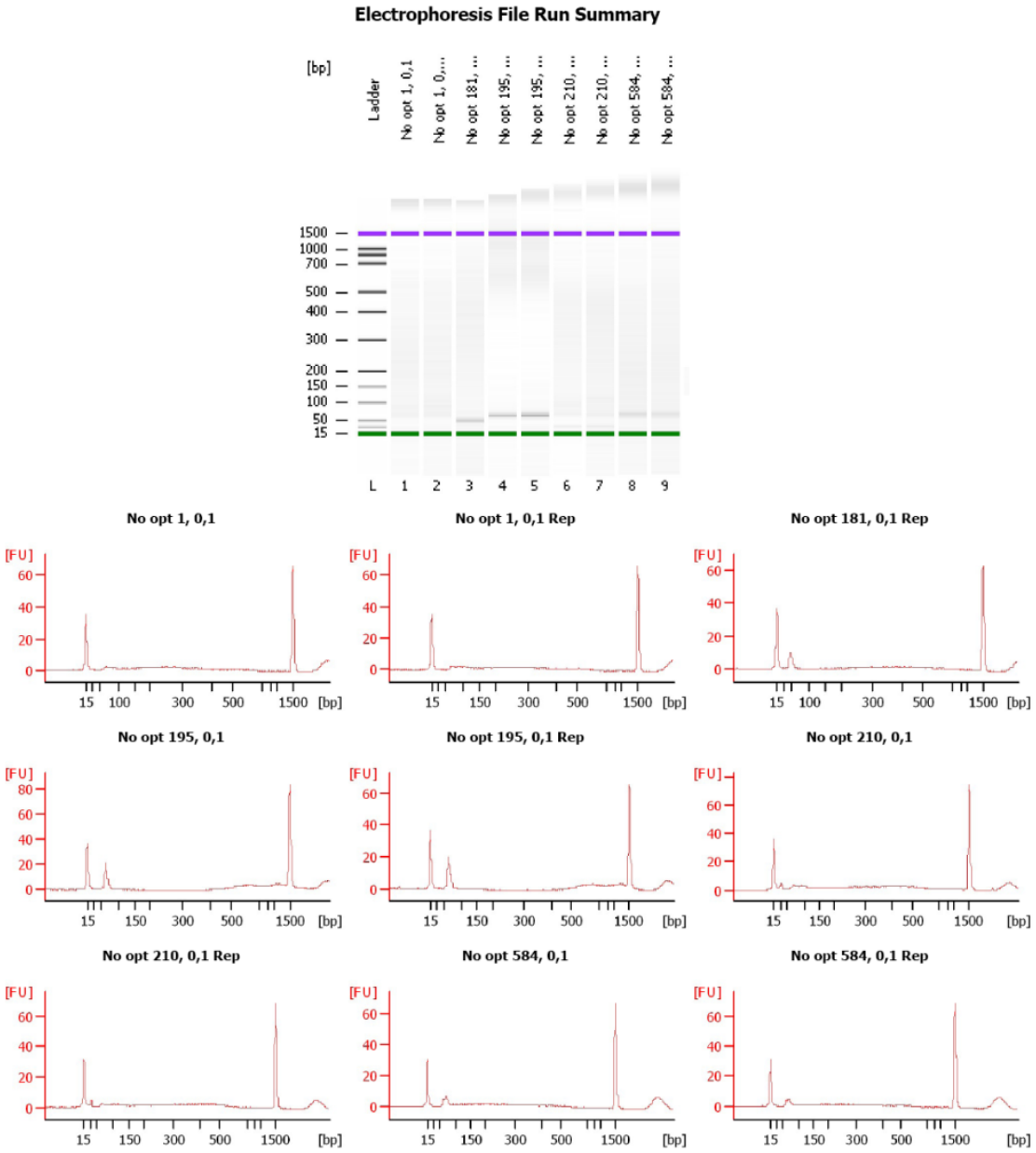

- <u>Bioanalyzer - Annealing Time 30 s (C_{primer}= 0,3 µM):</u>

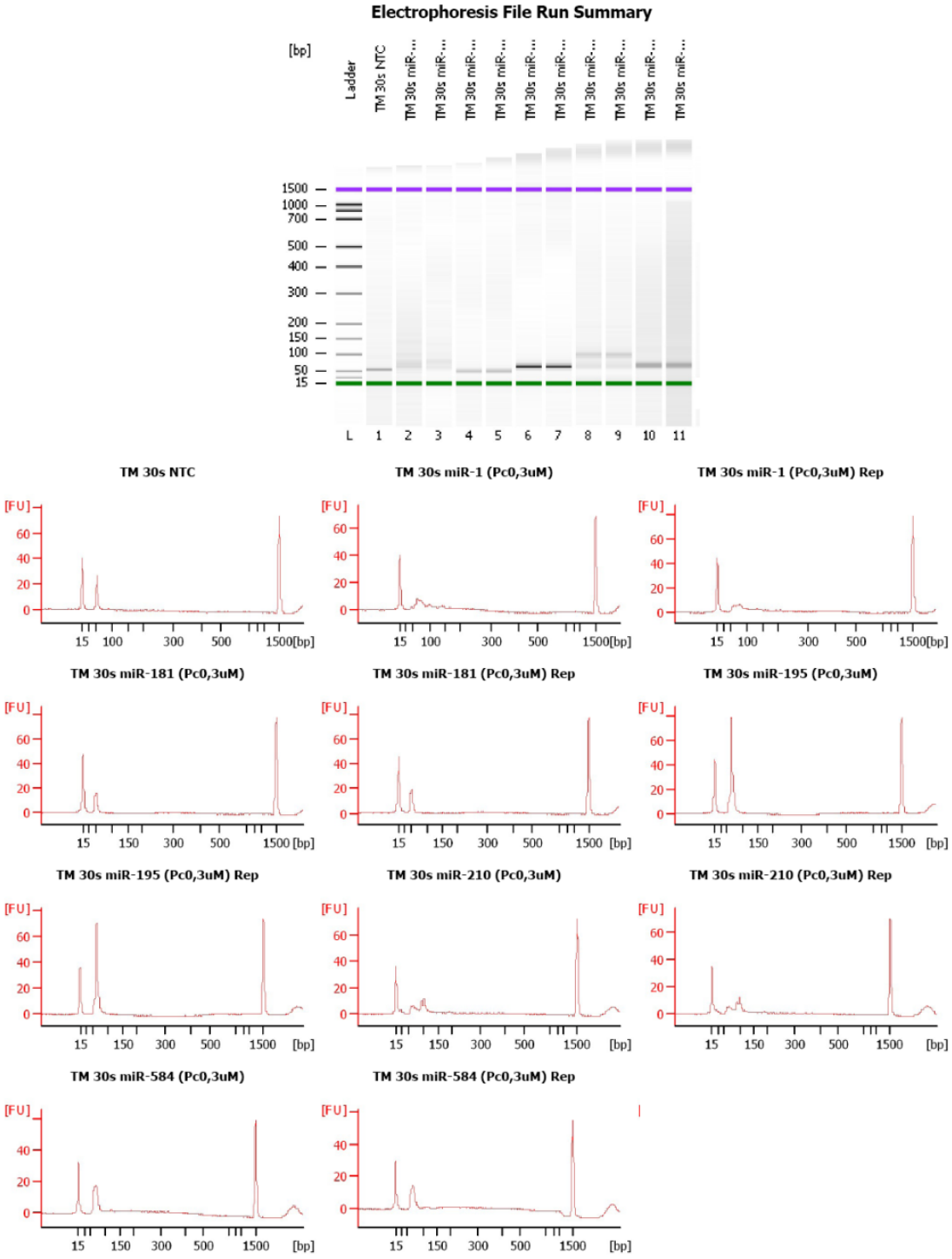

- <u>Bioanalyzer - Annealing Time 40 s (C_{primer}=0,3 µM):</u>

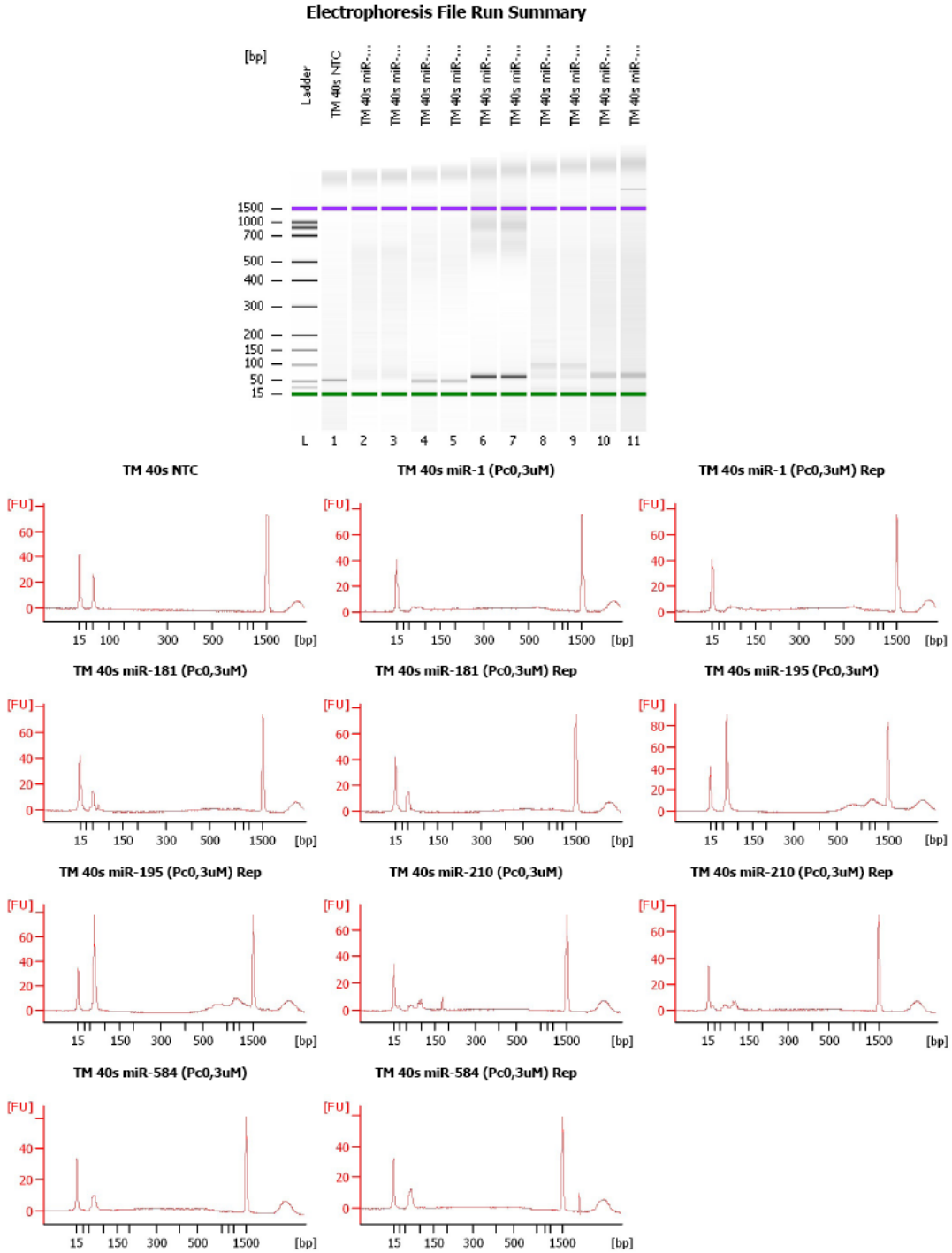

Appendix M - qPCR results

	miR-1	miR-195	miR-210	miR-584
Pool	32,85	23,15	30,84	29,66
	32,2	23,21	31,09	29,69
	31,95	C/6=24,86	29,94	28,6
C1	35	24,6	35	30,67
	35	24,68	35	30,76
	29,97	24,12	34,49	30,7
C2	30,88	22,25	28,05	26,52
	30,79	22,19	28,11	26,47
	30,92	22,44	27,65	24,97
C3	30,62	22,05	28,33	28,3
	30,99	21,83	28,48	27,89
	32,24	21,91	27,95	26,59
C4	30,71	22	29,86	28,9
	31,85	22	30,06	28,44
	31,97	22,17	29,5	27,31
C5	29,85	22,83	27,61	26,45
	30,74	22,78	27,82	26,08
	34,21	22,97	27,32	26,53
C6	28,93	21,1	29,24	29,6
	29,2	21,17	29,49	29,13
	31,28	21,5	28,79	28,45
C7	27,01	21,79	28,75	28,66
	28,42	21,8	28,55	27,65
	29,7	22,16	28,62	27,63
C8	30,5	23,04	28,48	28,74
	30,04	23,02	28,33	28,24
	30,35	23,15	29,58	27,83
C9	30,9	21,91	28,67	26,83
	33,03	21,99	27,53	25,22
	33,49	21,94	29,04	27,72
C10	30,3	22,96	29,56	26,4
	30,36	23,04	29	26,14
	32,06	22,92	28,27	24,68
P1	29,87	22,1	29,29	26,66
	30,05	22,26	28,5	25,93
	31,35	22,17	28,39	24,99
P2	34,27	22,21	30,86	31,32
	34,5	22,46	31,06	31,68
	30,91	22,2	30,62	31,22
P3	31,73	23,29	30,96	31,45

	31,95	23,35	31,1	31,38
	33,18	23,28	30,61	29,54
P4	31,97	23,06	30,95	30,43
	34,44	23,12	31,34	30,76
	35	23,03	31,07	29,77
P5	30,91	22,48	30,37	29,08
	31,93	22,64	30,4	29,84
	32,22	22,57	29,87	28,45
P6	34,65	22,63	32,22	31,31
	34,6	22,65	32,56	32,10
	33,41	22,61	32,17	31,09
P7	32,76	23,22	31,72	30,75
	32,56	23,3	31,95	30,96
	32,49	23,26	31,31	30,81
P8	32,39	22,95	30,41	29,62
	33,44	23,06	30,61	30,51
	32,8	23,28	29,78	28,87
P9	33,43	24,22	31,65	31,59
	35	23,25	31,72	31,92
	32,9	22,75	30,44	28,56
P10	31,89	22,8	30,68	30,15
	31,2	22,56	30,68	30,43
	30,52	22,45	30,12	28,45
P11	27,93	20,73	30,08	30,38
	30,77		29,97	30,58
	31,47	20,79	29,62	27,92
P12	31,02	22,83	30,9	29,25
	33,58		30,95	28,56
	35	22,84	30,66	28,51

Appendix N – Statistical Analysis

- Descriptive statistics of the results:

			Statistic	Std. Error
miR-1				
Control	Mean		31,0430	,43519
	95% Confidence Interval for Mean	Lower Bound	30,0585	
		Upper Bound	32,0275	
	5% Trimmed Mean		31,0644	
	Median		31,0950	
	Variance		1,894	
	Std. Deviation		1,37620	
	Minimum		28,38	
	Maximum		33,32	
	Range		4,94	
	Interquartile Range		1,64	
	Skewness		-,332	,687
	Kurtosis		,781	1,334
PE	Mean		32,4475	,39023
	95% Confidence Interval for Mean	Lower Bound	31,5886	
		Upper Bound	33,3064	
	5% Trimmed Mean		32,4817	
	Median		32,7400	
	Variance		1,827	
	Std. Deviation		1,35181	
	Minimum		30,06	
	Maximum		34,22	
	Range		4,16	
	Interquartile Range		2,32	
	Skewness		-,571	,637
	Kurtosis		-,766	1,232
miR-195				
Control	Mean		22,4780	,28462
	95% Confidence Interval for Mean	Lower Bound	21,8342	
		Upper Bound	23,1218	
	5% Trimmed Mean		22,4350	
	Median		22,1750	
	Variance		,810	
	Std. Deviation		,90003	

	Minimum		21,26	
	Maximum		24,47	
	Range		3,21	
	Interquartile Range		1,07	
	Skewness		1,127	,687
	Kurtosis		1,796	1,334
PE	Mean		22,7542	,14444
	95% Confidence Interval for Mean	Lower Bound	22,4362	
		Upper Bound	23,0721	
	5% Trimmed Mean		22,7707	
	Median		22,7350	
	Variance		,250	
	Std. Deviation		,50037	
	Minimum		21,80	
	Maximum		23,41	
	Range		1,61	
	Interquartile Range		,86	
	Skewness		-,448	,637
	Kurtosis		-,624	1,232
miR-210				
Control	Mean		29,2370	,65265
	95% Confidence Interval for Mean	Lower Bound	27,7606	
		Upper Bound	30,7134	
	5% Trimmed Mean		29,0183	
	Median		28,7200	
	Variance		4,260	
	Std. Deviation		2,06387	
	Minimum		27,58	
	Maximum		34,83	
	Range		7,25	
	Interquartile Range		1,16	
	Skewness		2,632	,687
	Kurtosis		7,577	1,334
PE	Mean		30,7117	,26300
	95% Confidence Interval for Mean	Lower Bound	30,1328	
		Upper Bound	31,2905	
	5% Trimmed Mean		30,7324	
	Median		30,8450	
	Variance		,830	
	Std. Deviation		,91104	
	Minimum		28,73	

	Maximum		32,32	
	Range		3,59	
	Interquartile Range		1,01	
	Skewness		-,475	,637
	Kurtosis		1,367	1,232
miR-584				
Control	Mean		27,6500	,48752
	95% Confidence Interval for Mean	Lower Bound	26,5472	
		Upper Bound	28,7528	
	5% Trimmed Mean		27,5861	
	Median		27,7850	
	Variance		2,377	
	Std. Deviation		1,54167	
	Minimum		25,74	
	Maximum		30,71	
	Range		4,97	
	Interquartile Range		2,21	
	Skewness		,644	,687
	Kurtosis		,178	1,334
PE	Mean		29,8567	,44103
	95% Confidence Interval for Mean	Lower Bound	28,8860	
		Upper Bound	30,8274	
	5% Trimmed Mean		29,9874	
	Median		30,0000	
	Variance		2,334	
	Std. Deviation		1,52777	
	Minimum		25,86	
	Maximum		31,50	
	Range		5,64	
	Interquartile Range		1,58	
	Skewness		-1,680	,637
	Kurtosis		3,839	1,232

- <u>Histogram and Normal Probability Plots for miR-1:</u>

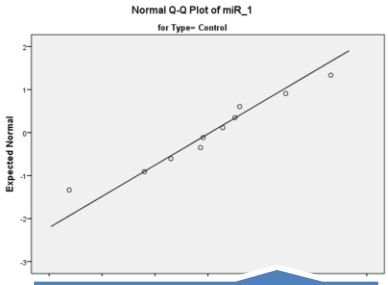

Normal Probability Plot for control samples

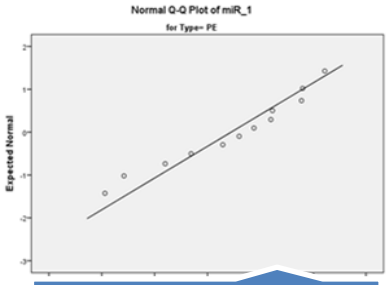

Normal Probability Plot for PE samples

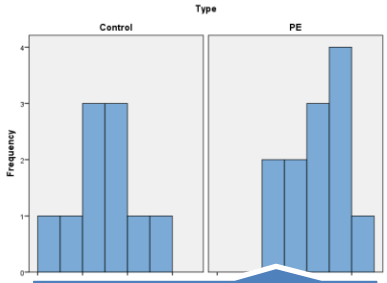

Histograms for controls (left) and PE samples (right)

- <u>Histogram and Normal Probability Plots for miR-195:</u>

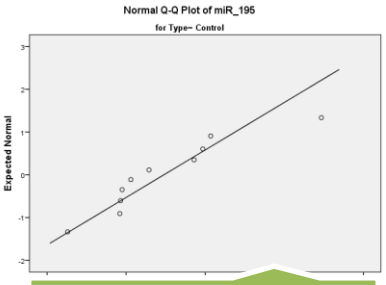

Normal Probability Plot for control samples

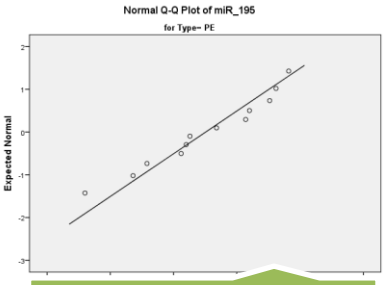

Normal Probability Plot for PE samples

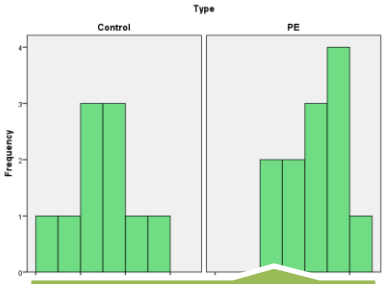

Histograms for controls (left) and PE samples (right)

- <u>Histogram and Normal Probability Plot for miR-210:</u>

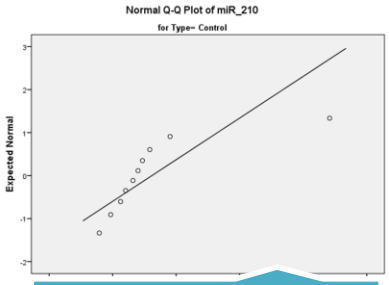

Normal Probability Plot for control samples

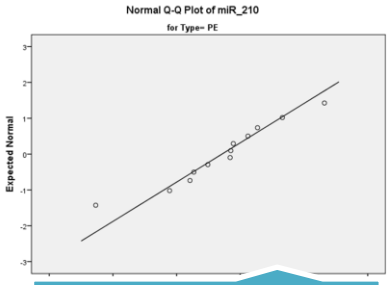

Normal Probability Plot for PE samples

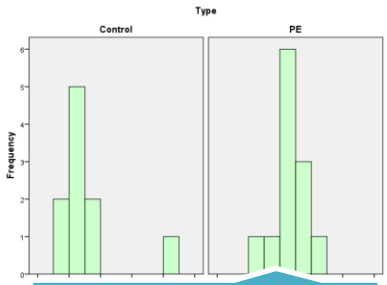

Histograms for controls (left) and PE samples (right)

- <u>Histogram and Normal Probability Plot for miR-584:</u>

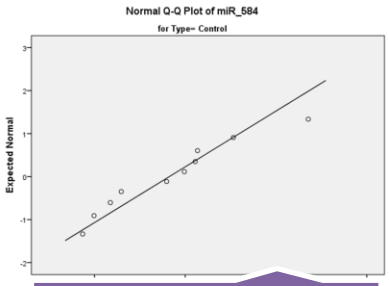

Normal Probability Plot for control samples

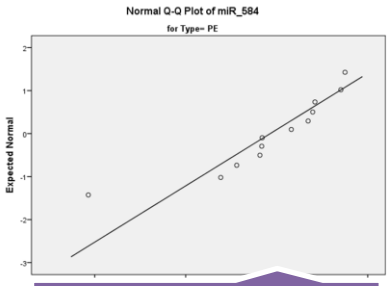

Normal Probability Plot for PE samples

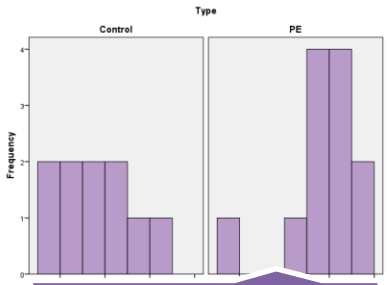

Histograms for controls (left) and PE samples (right)

- Wilcoxon Rank-Sum Test (all samples included):

miR-1			
Ranks			
	N	**Mean Rank**	**Sum of Ranks**
Control	10	8,30	83,00
PE	12	14,17	170,00
Total	22		
Test Statistics			
Wilcoxon W		83,000	
Z		-2,110	
Exact Sig. (2-tailed)		0,036	

miR-195			
Ranks			
	N	**Mean Rank**	**Sum of Ranks**
Control	10	9,50	95,00
PE	12	13,17	158,00
Total	22		
Test Statistics			
Wilcoxon W		95,000	
Z		-1,320	
Exact Sig. (2-tailed)		0,197	

miR-210			
Ranks			
	N	**Mean Rank**	**Sum of Ranks**
Control	10	7,10	71,00
PE	12	15,17	182,00
Total	22		
Test Statistics			
Wilcoxon W		71,000	
Z		-2,901	
Exact Sig. (2-tailed)		0,003	

miR-584			
Ranks			
	N	**Mean Rank**	**Sum of Ranks**
Control	10	7,20	72,00
PE	12	15,08	181,00
Total	22		
Test Statistics			
Wilcoxon W		72,000	
Z		-2,835	
Exact Sig. (2-tailed)		0,003	

- Wilcoxon Rank-Sum Test (severe samples excluded):

miR-1			
Ranks			
	N	**Mean Rank**	**Sum of Ranks**
Control	10	6,00	60,00
PE	7	13,29	93,00
Total	17		
Test Statistics			
Wilcoxon W		60,000	
Z		-2,928	
Exact Sig. (2-tailed)		0,002	

miR-195			
Ranks			
	N	**Mean Rank**	**Sum of Ranks**
Control	10	7,20	72,00
PE	7	11,57	81,00
Total	17		
Test Statistics			
Wilcoxon W		72,000	
Z		-1,759	
Exact Sig. (2-tailed)		0,083	

miR-210			
Ranks			
	N	**Mean Rank**	**Sum of Ranks**
Control	10	6,20	62,00
PE	7	13,00	91,00
Total	17		
Test Statistics			
Wilcoxon W		62,000	
Z		-2,733	
Exact Sig. (2-tailed)		0,005	

miR-584			
Ranks			
	N	**Mean Rank**	**Sum of Ranks**
Control	10	6,00	60,00
PE	7	13,29	93,00
Total	17		
Test Statistics			
Wilcoxon W		60,000	
Z		-2,928	
Exact Sig. (2-tailed)		0,002	

Appendix O – miRNA Target Prediction

- miRNA targets (TargetScanHuman):

miRNA	Targets	
miR-1	**SLC44A1**	Solute carrier family 44, member 1
	GJA1	Gap junction protein, alpha 1, 43kDa
	PHAX	Phosphorylated adaptor for RNA export
	PTPLAD1	Protein tyrosine phosphatase-like A domain containing 1
	UST	Uronyl-2-sulfotransferase
miR-195	**FGF2**	Fibroblast growth factor 2 (basic)
	SLC11A2	Solute carrier family 11 (proton-coupled divalent metal ion transporters), member 2
	PLAG1	Pleiomorphic adenoma gene 1
	ZBTB34	Zinc finger and BTB domain containing 34
	MGAT4A	Mannosyl (alpha-1,3-)-glycoprotein beta-1,4-N-acetylglucosaminyltransferase, isozyme A
miR-210	**THSD7A**	Thrombospondin, type I, domain containing 7A
	ISCU	Iron-sulfur cluster scaffold homolog (*E. coli*)
	ZNF462	Zinc finger protein 462
	NR1D2	Nuclear receptor subfamily 1, group D, member 2
	DIMT1L	DIM1 dimethyladenosine transferase 1-like (*S. cerevisiae*)
miR-584	**CCDC152**	Coiled-coil domain containing 152
	GANAB	Glucosidase, alpha; neutral AB
	NCOR1	Nuclear receptor corepressor 1
	NUFIP2	Nuclear fragile X mental retardation protein interacting protein 2
	PRRX1	Paired related homeobox 1

- Targets for the correlated miRNAs (starBASE):

Process	Targets
miR-1 + miR-210	
Cell cycle	BUB3,CDK6,CREBBP,CCND2,RAD21,CCND1,E2F3,SMC1A,WEE1
Spliceosome	SMNDC1,DDX5,HNRNPK,NAA38,SFRS9,ZMAT2,HNRNPU
miR-1 + miR-584	
Spliceosome	DDX5,SFRS5,HNRNPK,SFRS9,TCERG1,ZMAT2,HNRNPU
Shigellosis	ARPC5,CRK,ATG5,PFN1,ARPC1A
miR-195 + miR-210	
Cell cycle	BUB3,CDC27,YWHAH,CREBBP,CCND2,CCNE1,CCND1,RBX1,CCNE2,E2F3,SMC1A,WEE1,CDC25A
Pathways in cancer	FGFR1,BIRC5,CCNE1,GRB2,TPM3,BCL2,RARB,MAPK9,WNT3A,CREBBP,CHUK,CDC42,CCND1,RBX1,VEGFA,ITGA2,AXIN2,FGF2,CCNE2,CRKL,E2F3,AKT3
Prostate cancer	FGFR1,CREBBP,CHUK,CCNE1,CCND1,GRB2,BCL2,CCNE2,E2F3,AKT3
Small cell lung cancer	CHUK,CCNE1,CCND1,BCL2,ITGA2,CCNE2,E2F3,AKT3,RARB
TGF-beta signalling pathway	ACVR2B,CREBBP,SMAD7,RBX1,ACVR1,SMAD5,SMURF2,RPS6KB1,ACVR2A

miR-195 + miR-584	
Pathways in cancer	FGFR1,BIRC5,CCNE1,GRB2,TPM3,BCL2,RARB,MAPK9,WNT3A,CHUK,CDC42,CCND1,RBX1,VEGFA,ITGA2,AXIN2,FGF2,CCNE2,COL4A1,CRK,CRKL,E2F3,AKT3
Small cell lung cancer	COL4A1,CHUK,CCNE1,CCND1,BCL2,ITGA2,CCNE2,E2F3,AKT3,RARB
Protein processing in endoplasmic reticulum	UBQLN1,SEC63,PDIA6,DNAJA2,CANX,PDIA3,YOD1,RAD23B,DNAJC5,RBX1,BCL2,SEC61A1,MAPK9,NFE2L2
Circadian rhythm - mammal	CLOCK,FBXL3,RBX1,BTRC,BHLHE40
Cell cycle	BUB3,CDC27,YWHAH,CCND2,CCNE1,CCND1,RBX1,CCNE2,E2F3,WEE1,CDC25A
TGF-beta signalling pathway	ACVR2B,SMAD7,RBX1,ACVR1,SMAD5,SMURF2,PPP2CA,RPS6KB1,ACVR2A
Prostate cancer	FGFR1,CHUK,CCNE1,CCND1,GRB2,BCL2,CCNE2,E2F3,AKT3